

**RHODES UNIVERSITY**  
*Where leaders learn*

**Exploring Quinolinyl-Thiazolidinedione Hybrid Compounds as  
Potential Anti-Tubercular Agents**

A dissertation submitted to Rhodes University

by

Thanduxolo Elihle Mtshare, BSc (Hons) (RU)

in fulfilment of the requirements for the degree

of

**Master of Science**

**In Chemistry**

**2019**

## ACKNOWLEDGEMENTS

*“<sup>17</sup>Every good and perfect gift is from above, coming down from the Father of the heavenly lights, who does not change like shifting shadows.”- James 1:17*

I would like to acknowledge God the Lord Almighty for giving me strength and holding me at the palm of his hand to soldier on and complete this work. My family for always believing in me and all the support you have provided me.

To my supervisor, Dr Khanye for the mentorship and wisdom you have counselled me with has really shaped my personal and career growth. I will forever be grateful to your selfless support and guidance towards shaping my professional growth as an aspiring chemist.

I am also grateful to my co-supervisor, Dr Richard Beteck for your all your assistance in this work. Without your valuable input, this work would have taken ages to be completed, I greatly appreciate your promptly assistance.

I am also thankful to Prof Klein for always opening your door for me for my unannounced random consultation.

I am also thankful to the past and present fellow labmates for making the lab F22 awesome. A special thanks to Ogunyemi “Yemist” Oderinlo for being like a mentor and sharing your wisdom with me. To Sinobomi Marwarwa a special utmost gratitude for all your support you’ve given me throughout, I’ll forever be grateful.

My gratitude also goes to the chemistry support staff for always being in my corner and providing me with coffee/tea. To the office of the secretariat, Benita Tarr, Barbara Ah Yui,

Alyssa Williams for always making sure my chemicals were ordered timely and just making the administration smooth.

“This work is based on the research supported wholly/in part by the National Research Foundation of South Africa (Grant Numbers: 113175)”; and Sandisa Imbewu grant.

## ABSTRACT

Tuberculosis (TB) is an infectious disease caused by the pathogen, *Mycobacterium tuberculosis*. According to the World Health Organization, TB is the ninth leading cause of death worldwide ranking above HIV/AIDS. This high mortality rate of TB begs the questions about the efficiency of the current therapy and raises an urgent need to create novel anti-tuberculosis agents which will aid in curbing this burden.

Quinoline containing compounds have remarkable biological activities across a wide spectrum of diseases including anti-tuberculosis. On the other hand, thiazolidinedione containing compounds possess a broad spectrum of biological properties. In this study, we rationally designed compounds containing these pharmacophoric units and investigated them for their potential biological activity against *Mycobacterium tuberculosis*. Considering antimalarial activity of quinoline-based compounds, the compounds achieved were also cross-screened for their activity against the *Plasmodium falciparum* parasite, a causative agent of malaria.

In all the synthesized compounds, compound **2.6a**, **2.6b** and **2.7b** emerged as most active compounds against the H37Rv strain with MIC<sub>90</sub> values ranging in between of 1.08 – 17.1  $\mu$ M. In addition, none of the compounds showed any inhibitory activities against the 3D7 strain of *P. falciparum* parasite. All the compounds prepared in this study showed no significant human cytotoxic effects as measured by HeLa cell line.

## Table of Contents

ACKNOWLEDGEMENTS .....	I
ABSTRACT.....	III
LIST OF SYMBOLS AND ABBREVIATIONS .....	VI
PUBLICATION AND CONFERENCES PARTICIPATION.....	IX
CHAPTER ONE.....	1
1.1 INTRODUCTION .....	1
1.2 PATHOGENESIS OF PULMONARY TUBERCULOSIS.....	2
1.3 STRUCTURE OF TUBERCULOSIS .....	3
1.4 CURRENT CHEMOTHERAPY AND THEIR TARGETS.....	3
1.5 QUINOLINE AND THE CORRESPONDING CHEMISTRY .....	7
1.5.1 Skraup reaction .....	8
1.5.2 Knorr synthesis of quinolines .....	9
1.5.3 Conrad-Limpach quinoline synthesis.....	9
1.5.4 Combes quinoline synthesis.....	10
1.5.5 Pfitzinger reaction.....	10
1.5.6 Meth-Cohn synthesis of quinolines.....	11
1.6 MEDICINIAL CHEMISTRY OF QUINOLINE BASED COMPOUNDS .....	11
1.6.1 Anti-TB activity .....	11
1.6.2 Anti-malarial activity .....	12
1.7 THIAZOLIDINEDIONE.....	13
1.7.1 Chemistry: Synthesis for 2,4-thiazolidinedione ring and related compounds.....	14
1.8 MEDICINIAL CHEMISTRY OF 2,4-THIAZOLIDINEDIONE BASED COMPOUNDS . .....	16
1.8.1 Anti-diabetic activity.....	16
1.8.2 Anti-tuberculosis activity.....	17
1.8.3 Anti-malarial activity .....	18
1.8.4 Anti-inflammatory activity .....	19
1.8.5 Antimicrobial activity .....	20
1.8.6 Antioxidant activity.....	21
1.9 AIMS AND OBJECTIVES OF THE STUDY .....	22
1.9.1 Specific aims.....	22
1.10 REFERENCES .....	23
CHAPTER TWO .....	29
2.1 INTRODUCTION .....	29
2.1.1 Rationale: Hybridization of quinoline and thiazolidinedione .....	29
2.2 RESULTS AND DISCUSSION.....	30

2.2.1 Overall synthetic route .....	30
2.2.2 Synthesis of acetanilides (2.2a–f) .....	31
2.2.3 Synthesis of 2-chloroquinoline-3-carbaldehydes (2.3a-e) .....	33
2.2.4 Synthesis of 6-substituted-2-methoxyquinoline-3-carbaldehydes .....	36
2.2.5 Synthesis of 2,4-thiazolidinedione-carboxylic acid via the ester intermediate .....	39
2.2.6 Synthesis of 2,4-thiazolidinedione-phenyl piperazine .....	41
2.2.7 Hybridization of quinoline-aldehydes and 2,4-THIAZOLIDINEDIONE via Knoevenagel condensation .....	44
2.3 CONCLUSIONS.....	55
2.4 REFERENCES .....	56
CHAPTER THREE .....	58
3.1 Introduction.....	58
3.2 Biological results and discussion .....	58
3.2.1 Anti-plasmodial activity of the target compounds .....	59
3.2.2 Anti-tubercular activity of the target compounds .....	61
3.2.3 <i>In vitro</i> cytotoxicity of synthesized compounds .....	63
3.3 CONCLUSIONS.....	64
3.4 REFERENCES .....	65
CHAPTER FOUR.....	66
4.1 General procedures .....	66
4.2 General synthesis of acetanilides (2.2a-f).....	67
4.3 General synthesis of 2-chloroquinoline-3-carbaldehydes (2.3a-e) .....	69
4.4 General Synthesis of 6-substitued 2-methoxyquinoline-3-carbaldehydes (2.4a-e) .....	71
4.5 Synthesis of methyl 2-(2,4-dioxothiazolidin-3-yl)acetate, 2.10 <sup>12</sup> .....	73
4.6 Synthesis of 2-(2,4-dioxothiazolidin-3-yl)acetic acid <sup>12</sup> (2.11) .....	74
4.7 Synthesis of 2-chloro-1-(4-phenylpiperazin-1-yl)ethan-1-one <sup>12</sup> (2.13).....	74
4.8 Synthesis of 3-(2-oxo-2-(4-phenylpiperazin-1-yl)ethyl)thiazolidine-2,4-dione <sup>12</sup> (2.14)...	75
4.9 General synthesis of quinoline-thiozolidinedione derivatives (2.6a-d) .....	76
4.10 General synthesis of quinoline-thiazolidinedione acid derivatives (2.7a-d).....	78
4.11 General synthesis of thiazolidinedione-phenyl piperazine derivatives (2.8a-e) .....	81
4.12 Biological procedures .....	84
4.12.1 <i>In vitro</i> anti- <i>Plasmodium falciparum</i> (procedure adapted from <sup>18</sup> ).....	84
4.12.2 <i>In vitro</i> anti-tubercular activity (procedure adapted from <sup>19</sup> ) .....	85
4.12.3 <i>In vitro</i> cytotoxicity (procedure adapted from <sup>18</sup> ). .....	86
4.13 REFERENCES .....	87

## LIST OF SYMBOLS AND ABBREVIATIONS

TZD	2,4-thiazolidinedione
EC <sub>50</sub>	Half maximal effective concentration
MIC <sub>50</sub>	Half Minimum inhibitory concentration
MIC <sub>90</sub>	90% Minimum inhibitory concentration
NMR	Nuclear Magnetic Resonance
<sup>1</sup> H NMR	Proton Nuclear Magnetic Resonance
<sup>13</sup> C NMR	Carbon-13 Nuclear Magnetic Resonance
CDCl <sub>3</sub>	Deuterated Chloroform
DMSO- <i>d</i> 6	Deuterated Dimethyl sulfoxide
δ <sub>H</sub>	Proton chemical shift
δ <sub>C</sub>	Carbon chemical shift
ppm	Parts per million
°C	Degree Celsius
<i>J</i>	Spin-spin coupling constant
MHz	Megahertz
Hz	Hertz
HRMS	High Resolution Mass Spectroscopy
ESI	Electrospray Ionisation

Calcd	Calculated
<i>m/z</i>	<i>mass per charge</i>
DMF	Dimethyl formamide
EtOAc	Ethyl acetate
EtOH	Ethanol
MeOH	Methanol
HCl	Hydrochloric acid
K <sub>2</sub> CO <sub>3</sub>	Potassium carbonate
Eq	Equivalence
g	grams
mg	Milligram
mL	Millilitre
μg	Microgram
μM	Micromolar
M	Molar
mmol	Millimoles
mp	Melting point
r.t.	Room temperature
SAR	Structure Activity Relationship
TLC	Thin Layer Chromatography

WHO

World Health Organisation

## PUBLICATION AND CONFERENCES PARTICIPATION

Part of this work has been published and orally presented as detailed below.

### Publication

O.T. Darell, S.T. Hulushe, **T.E. Mtshare**, R.M. Beteck, M. Isaacs, D. Laming, H.C. Hoppe, R.W.M. Krause and S.D. Khanye. Synthesis, Antiplasmodial and Antitrypanosomal Evaluation of a Series of Novel 2-Oxoquinoline-based Thiosemicarbazone Derivatives. *S. Afr. J. Chem.*, **2018**, 71, 174-181. <https://hdl.handle.net/10520/EJC-127eaaf237>

### Conference Participation

Given Oral Presentation titled, “Design and synthesis of quinolinyl-thiazolidinedione hybrids as potential antitubercular agents.” at 43<sup>rd</sup> SACI National Convention 2018 (2-7 December, 2018), located at CSIR-ICC in Pretoria.

<http://www.saci.co.za/SACI2018/2018%20SACI%20Conference%20Book.pdf> (p 97).

## CHAPTER ONE

### INTRODUCTION AND LITERATURE REVIEW

#### 1.1 INTRODUCTION

**T**uberculosis is an infectious disease that is caused by the members of species *Mycobacterium tuberculosis* complex (MTBC)<sup>1</sup>. *Mycobacterium tuberculosis* (*Mtb*) is the causative agent of tuberculosis (TB) in humans. Other important species include *M. bovis*, *M. caprae* and *M. pinnipedii* and these are believed to be causative agents of the wild and domestic mammals<sup>1-3</sup>; *M. microti*, that causes TB only in voles<sup>1,4</sup>, and the one that is the etiologic agent in humans is *M. tuberculosis* (*Mtb*)<sup>1,5</sup>. In this chapter, the focus is on the *M. tuberculosis* which poses as a serious threat to humans. This disease is believed to have claimed its victims' lives for more than 150 million years ago<sup>1</sup>. Despite the earlier investigations into understanding the prevalence of TB, it is still claiming a large number of victims to date and is ranked at the top amongst infectious disease which causes fatality around the globe. In 2018, the World Health Organization (WHO)<sup>6</sup> released a report estimating that 10 million people were infected with tuberculosis, and 1.6 million people died from the disease, and this figure includes 0.3 million who were living with HIV. Even though WHO reported that the incidence rate has fallen to below 2% per annum, the alarming figures of people falling ill and ultimately die from the disease signal the fact there is still a lot to be done to curb this deadly disease.

## 1.2 PATHOGENESIS OF PULMONARY TUBERCULOSIS

In order to better design novel therapeutics to treat this disease, it is crucial to know its pathogenesis and structure. TB affects different organs in the body such as the bone<sup>7</sup>, central nervous system (CNS)<sup>8</sup> and other organelles, but is primarily a pulmonary disease that is initiated by admission of *M. tuberculosis* onto lung alveolar surfaces<sup>9</sup>. According to Zuñiga and co-workers,<sup>10</sup> the pathogenesis of pulmonary TB can be defined into four events. The first event is the inhalation of *M. tuberculosis*, which is usually contained in aerosol droplet and then reside in macrophages which immediately attempts to kill the *Mycobacterium*<sup>10,11</sup>. The second event is the inflammation cell recruitment where the survived *Mycobacteria* in macrophages multiply thus causing the production of pro-inflammatory cytokines<sup>10,12</sup>.

The local inflammatory environment thus produces necessary reagents to fight off the infection. In this process, high levels of tumor necrosis factor alpha (TNF- $\alpha$ ) is produced, which deals with the control of *M. tuberculosis* growth and thus leading to granuloma formation<sup>10,13</sup>. The third event is the control of *Mycobacteria* growth where the immune cells including T cells fights off the infection by containing the *Mycobacterium* within the cell walls of the granulomas<sup>10</sup>. In this process, the *Mycobacterium* is prevented from multiplying and spreading and thus remain in the dormant stage which is usually termed latent infection. The fourth event is the post-primary TB which normally occurs when there is a failure of the immune surveillance resulting in the “contained” *M. tuberculosis* escaping, thus growing rapidly into a disease that is known as TB<sup>10</sup>.

### 1.3 STRUCTURE OF TUBERCULOSIS

The structure of *Mtb* is unique compared to other prokaryotes cells. Most of the prokaryotic cells are characterized by the cell wall mostly made up of peptidoglycan. On the other hand, the cell wall of *Mtb* is composed of 60% lipids, peptidoglycan and arabinogalactan<sup>14</sup>. The abundance of lipids in the *Mtb* has significance in spreading TB. This lipid fraction of the bacteria is made of three major, namely: components mycolic acids, cord factor and wax-D which protect and assist the bacteria in the host<sup>15</sup>. The advantages of having high concentrations of lipid in its structure are that mycolic acid helps the bacteria escape most of the host's defence mechanisms, it also helps the bacteria not to be stained by dyes that are usually used for other bacteria. *M. tuberculosis* cell membranes are impermeable to certain dyes that are used to stain other bacteria. The TB drug resistance to antibiotics is also increased by the lipid layer because they cannot penetrate through the lipid layer. Other advantages of lipid bilayer include resistance to killing by acidic and alkaline compounds, osmotic lysis by complement deposition and lethal oxidations. The lipid layer also improves chances of survival inside the macrophages.

### 1.4 CURRENT CHEMOTHERAPY AND THEIR TARGETS

Within the complex structure of *M. tuberculosis* there is a rich and diverse drug targets that are embedded in each compartment (cell wall/ ribosome/ DNA/RNA). The cell wall alone is regarded as a “fountain” of drug targets because of its uniqueness<sup>16</sup>. Mycolic acid aids the *Mycobacterium* to withstand the chemical damage thus making it difficult for drugs to penetrate the cell wall to get to the target site. There are inhibitors of mycolic acid and these include isonicotinic acid hydrazine, nitroimidazole, and thiamides<sup>16,17</sup>. All the mycolic acid inhibitors (**Figure 1.1**) are prodrugs which are activated in specific sites of the mycolic acid pathway. Isoniazid (**1.1**) which is a first line drug is activated by *M. tuberculosis* catalase-peroxidase to generate reactive oxygen species and other radicals that primarily attack nicotinamide adenine dinucleotide (NAD) to form covalent adduct<sup>18</sup>. The adduct in turn inhibits enoyl-(acyl carrier

protein) reductase that plays a crucial role in the synthesis of a very long chain fatty acid that make up the *M. tuberculosis* cell wall<sup>19</sup>. Ethionamide (**1.3**) on the other hand is activated by an enzyme ethA to form oxide metabolite which disrupts the formation of the cell wall in a similar manner as isoniazid<sup>19</sup>. Delamanid (**1.2**) is a clinical candidate currently in phase III, but the mechanism of action has not been fully elucidated. However, the anti-TB activity of delamanid (**1.2**) is believed to be a result of reductive activation by F420 coenzyme system. This activation leads to inhibition of methoxy-mycolic and keto-mycolic acid which are necessary for mycolic acid biosynthesis<sup>20</sup>. Pretomanid (**1.4**) is activated by nitroreductase thus releasing toxic nitric oxide (NO) that interferes with the electron flow and ATP homeostasis under hypoxic non-replicating condition<sup>21</sup>.

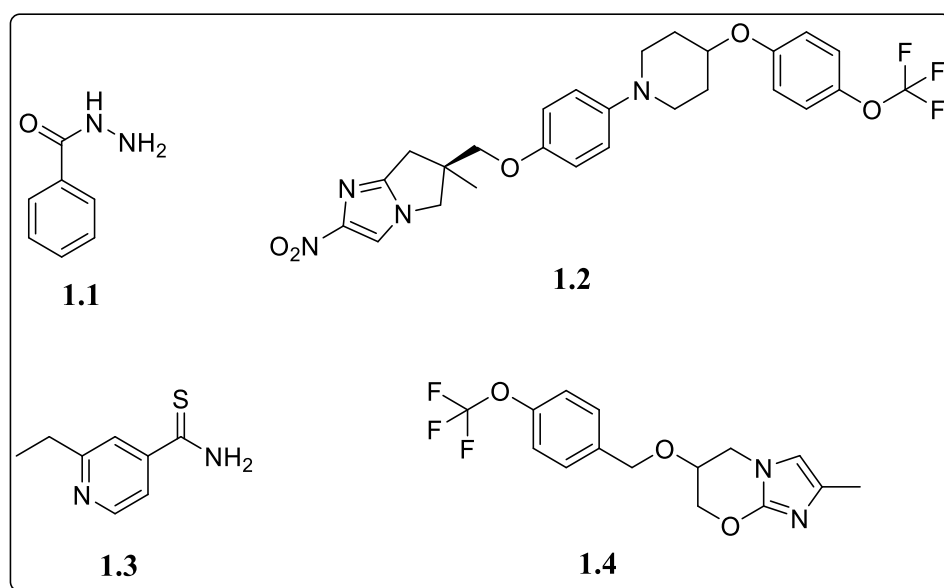


**Figure 1.1:** Mycolic acid inhibitors<sup>16</sup>: Isoniazid (**1.1**), Delamanid (**1.2**), Ethionamide (**1.3**), and Pretomanid (**1.4**).

The sugar components such as, arabinogalactan and peptidoglycan also have their own inhibitors. Ethambutol (**1.5**) and SQ609 (**1.6**), **Figure 1.2**, are the inhibitors of the arabinogalactan, whereas capuramycin (**1.7**) and cycloserine (**1.8**), **Figure 1.3**, are known inhibitors of peptidoglycan synthesis<sup>16</sup>. Ethambutol (**1.5**) is currently part of the first line drugs for treatment of TB. It acts by preventing the interaction of 5'-hydroxyl groups of *D*-arabinose residues of arabinogalactan with mycolic acids that form mycolyl-arabinogalactan-peptidoglycan thereby disrupting the arabinogalactan synthesis<sup>22</sup>. SQ609 (**1.6**) is in pre-clinical development stages and its mechanism of action is incompletely understood but it is believed to inhibit the *Mycobacterial* cell wall synthesis by interfering with the polymerization of arabinogalactan<sup>23</sup>.

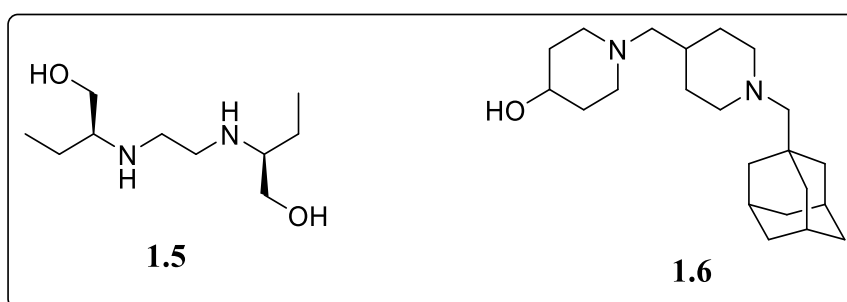


**Figure 1.2:** Arabinogalactan inhibitors. Ethambutol (**1.5**) and SQ609 (**1.6**).

Capuramycin (**1.7**) is reported to inhibit phospho-MurNAc-pentapeptide translocase (translocase I) which is an integral membrane protein that catalyses the first step of the intramembrane cycle of reactions involved in peptidoglycan assembly<sup>24</sup>. Disruption of peptidoglycan synthesis increase the permeability of the cell membrane. Cycloserine (**1.8**) works by interfering with the normal functioning of two crucial enzymes that play a major role in the cytosolic stages of the peptidoglycan synthesis<sup>25</sup>.

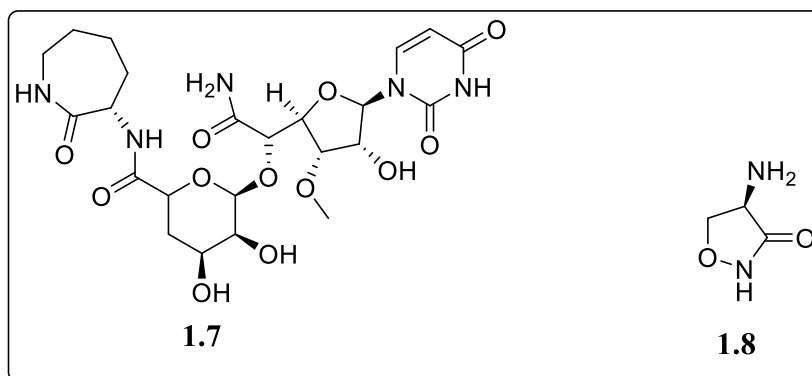


**Figure 1.3:** Peptidoglycan inhibitors. Capuramycin (**1.7**) and Cycloserine (**1.8**).

Pyrazinamide (**1.9**) is another first line drug that is normally employed to treat TB (**Figure 1.4**). It is a prodrug that is activated by an enzyme, pyrazinamidase to yield pyrazinoic acid (**1.10**) which is believed to be the promiscuous active species<sup>26</sup>. Due to its promiscuity, the mechanism of action is still unresolved, but is mainly thought that it acts by inhibiting multiple targets such as energy production, translation and coenzyme A required for persisters survival<sup>27</sup>.

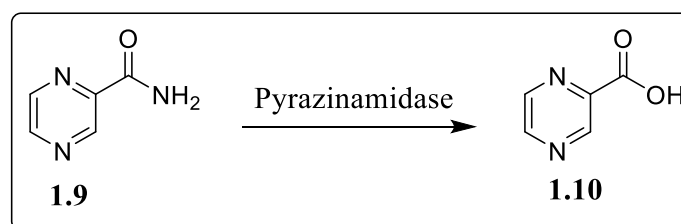


**Figure 1.4:** Conversion of pyrazinamide (**1.9**) to pyrazinoic acid (**1.10**) by *Mtb* enzyme, amidase.

Rifampicin (**1.11**) belong to the first line drugs for treatment of TB. Its mechanism of action gives an insight about a *M. tuberculosis* inhibitor that kills the *Mycobacterium* other than disrupting the cell wall. Rifampicin (**1.11**) is reported to act by binding in to a pocket of ribonucleic acid polymerase (RNAP)  $\beta$ -subunit resulting in the inhibiting of ribonucleic acid (RNA) polymerase<sup>28,29</sup>. This process then disrupts deoxyribonucleic acid (DNA) transcription, ultimately preventing the *Mtb* growth and division.

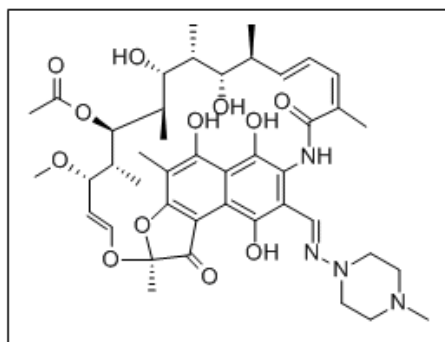


**Figure 1.5:** Chemical structure of rifampicin (**1.11**).

Bedaquiline (**1.12**, TMC207) is another example of TB drug that has been recently approved by Food and Drug Administration (FDA) that acts by a unique mechanism of action. TMC207 acts by binding to the subunit *c* of the ATP synthase thus inhibiting the production of ATP<sup>30</sup>. This process leads to less energy being produced thus resulting in *Mtb* cell death. Bedaquiline (**1.12**) is active against drug susceptible and multi-drug resistant strains of *Mtb*.<sup>30</sup>

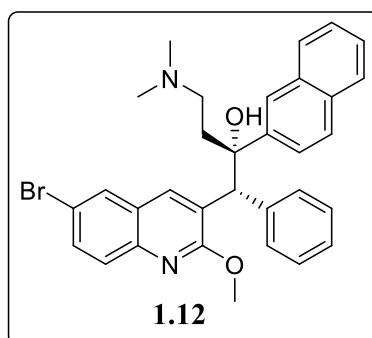


**Figure 1.6:** Chemical structure of bedaquiline (**1.12**).

## 1.5 QUINOLINE AND THE CORRESPONDING CHEMISTRY

Quinoline (**1.13**) is a heterocyclic ring system that has a chemical structure of a pyridine ring fused together with a benzene ring (**Figure 1.7**). Runge was the first to isolate it from the distillation of coal tar in 1834 and called it *leukol*. Subsequently, Gerhardt identified the quinoline following a decomposition of quinine and cinchonine<sup>31</sup>. Physically, it appears as a “white-oil (*leukol* in Germany)”, which turns to yellow if exposed to air and later to brown

color if also exposed to light. The chemical structure of the quinoline (**Figure 1.7**) shows the IUPAC numbering of this heterocyclic compound.

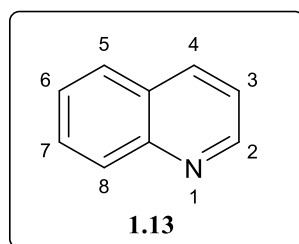
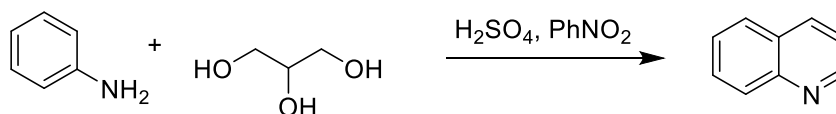


**Figure 1.7:** Chemical structure and numbering of quinoline<sup>32</sup>.

Since its discovery, many researchers have found different approaches to synthesize quinoline. The first synthesis of quinoline was reported by Czech chemist, Zdenko Hans Skraup, in 1880 and later named Skraup reaction. Thereafter several alternative synthetic routes unfolded such as Knorr synthesis of quinolines, Conrad-Limpach synthesis, Combes quinoline synthesis, Pfitzinger reaction, and Meth-Cohn synthesis of quinolones, and these synthetic approaches are briefly discussed below.

### 1.5.1 Skraup reaction

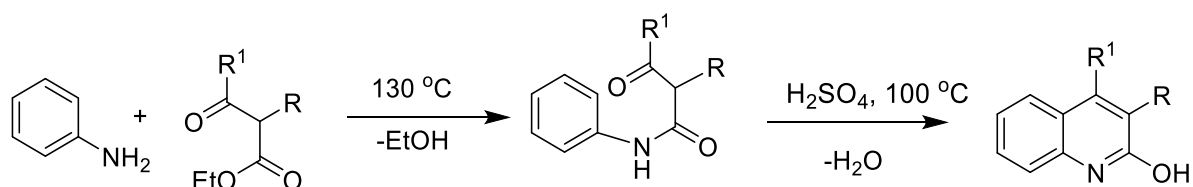
A typical Skraup reaction involve the treatment of glycerol with sulfuric acid to obtain acrolein which in turn reacts with aniline in the presence of oxidizing agent to yield quinoline. Arsenic acid and nitrobenzene have been used as oxidizing agents to which the latter has been proved to react violent, thus the former is usually preferred as it is less violent<sup>33,34</sup>.



**Scheme 1.1:** Skraup reaction for synthesis of quinoline<sup>34</sup>.

### 1.5.2 Knorr synthesis of quinolines

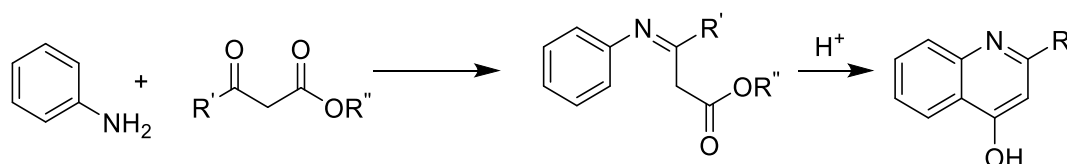
The reaction involves cyclization and dehydration with sulfuric acid of an anilide intermediate that is formed from the condensation of  $\beta$ -ketoesters and anilines at high temperatures to form  $\alpha$ -hydroxyquinolines<sup>35</sup>. Different regioisomeric products formed are controlled by the temperature and reaction conditions. For high temperatures, usually 2-hydroxyquinolines are favored and at low temperatures 4-hydroxyquinolines are formed<sup>36</sup>. The latter is known as Conrad-Limpach reaction.



**Scheme 1.2:** Knorr synthesis of 2-Hydroxyquinoline<sup>35</sup>.

### 1.5.3 Conrad-Limpach quinoline synthesis

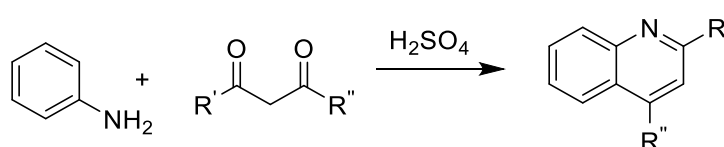
The reaction was first published in 1887 by Conrad and Limpach and it is similar to Knorr reaction of quinoline synthesis with main the difference being that it yields 4-hydroxyquinoline instead of 2-hydroxyquinoline reported by Knorr in 1886. In addition, Conrad-Limpach always proceeds in the presence of an iodine or acidic catalyst<sup>37</sup>.



**Scheme 1.3:** Conrad-Limpach reaction for 4-hydroxyquinoline synthesis<sup>37</sup>.

### 1.5.4 Combes quinoline synthesis

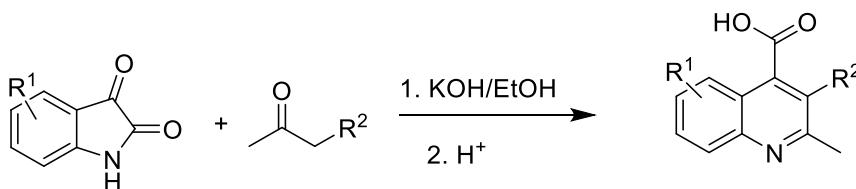
This is an acid-catalyzed condensation reaction of anilines and  $\beta$ -diketones to synthesize 2,4-substituted quinoline skeleton<sup>38</sup>. The reaction suffers from low regioselectivity, however, Sloop<sup>39</sup> has shown that the steric and electronic effects play a major role in the regioselectivity of the quinoline by incorporating the bulky groups on the  $\alpha$ -position of the diketone.



**Scheme 1.4:** Combes reaction of 2,4-substituted quinoline synthesis<sup>38</sup>.

### 1.5.5 Pfitzinger reaction

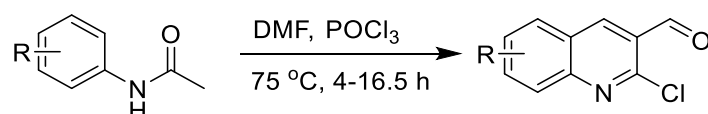
The reaction was reported by Pfitzinger in 1886, where he reported his work on the synthesis of 2-methyl-4-quinolinecarboxylic acid as the result of reaction of isatin with acetone in basic aqueous solution<sup>40</sup>. The reaction is a two-step process using a strong base, and thereafter acidify with strong acids<sup>40,41</sup>. To date this reaction is still being employed to synthesize novel bioactive compounds. For example, Ivachtchenko and co-workers<sup>42</sup> prepared a series of compounds via Pfitzinger synthetic approach to obtain the desired compounds as potent caspase-3 inhibitors.



**Scheme 1.5:** Pfitzinger reaction for 4-quinolinecarboxylic acid<sup>41</sup>.

### 1.5.6 Meth-Cohn synthesis of quinolines

The reaction was first reported in 1979 by Otto Meth-Cohn and co-workers<sup>43</sup> where they were working on the conversion of acetanilides to 2-chloroquinoline-3-carbaldehydes under the Vilsmeier-Haack reaction conditions. The reaction has been utilized over the years to synthesize bioactive compounds, such as quinoline moiety of bedaquiline (**1.12**) which is a highly potent anti-TB drug<sup>30</sup>.



**Scheme 1.6:** Synthesis of 2-chloro-3-quinolinecarbaldehyde via Meth-Cohn reaction<sup>44</sup>.

## 1.6 MEDICINIAL CHEMISTRY OF QUINOLINE BASED COMPOUNDS

Quinolines are privileged versatile class of compounds that bear important pharmacological activity across many biological systems such as anti-cancer<sup>45</sup>, anti-TB<sup>30,32,46</sup>, anti-malaria<sup>47,48</sup>, and anti-trypanosomal<sup>49,50</sup>. However, only anti-TB and anti-Malaria activities reviews will be further discussed below.

### 1.6.1 Anti-TB activity

The discovery of TMC207 (**1.12**) by Johnson and Johnson (J&J) is regarded as the one of the major developments towards the treatment regime of TB. This quinoline containing drug was discovered via a screening program of more than 70,000 compounds with activity against *M. smegmatis*<sup>51</sup>. Bedaquiline is reported to be highly potent against drug susceptible and MDR *M. tuberculosis* and act via a novel mechanism of action through the inhibition of subunit *c* of ATP synthase<sup>30,52</sup>. More importantly, this quinoline based compound is highly selective > 20,000:1 towards mycobacterial ATP synthase as compared to human mitochondrial ATP

synthase<sup>30</sup>. This selectivity is desired considering the fact that toxicity tends to be an issue in drug discovery and development. The low minimum inhibitory concentration (MIC) of less than 0.06 µg/mL across a panel of mycobacterial species make this compound attractive in the search for anti-mycobacterial agents<sup>53</sup>.

### 1.6.2 Anti-malarial activity

There are a variety of anti-malarial drugs containing quinoline moiety such as chloroquine (1.14), quinine (1.15) and mefloquine (1.16)<sup>54</sup>. Although the mode of action of these quinoline based antimalarial is not completely known, it is widely accepted that these compounds act by interfering with the digestion of haemoglobin in the blood stages of the malarial life cycle<sup>47</sup>. Quinine (1.14) is the first antimalarial drug that was extracted from the bark of the cinchona tree found in South America. Thereafter, chloroquine (1.15) was amongst the first synthetic drugs to be used for the treatment of malaria. Considering the heavy use of chloroquine in the late 1940s, drug resistance to chloroquine slowly developed, and quinine became the drug of choice to treat malaria. In the 1970s, mefloquine (1.16) was discovered and it exhibited enhanced potency against malaria. What was even more interesting about mefloquine was the activity against chloroquine-resistant malaria strains.

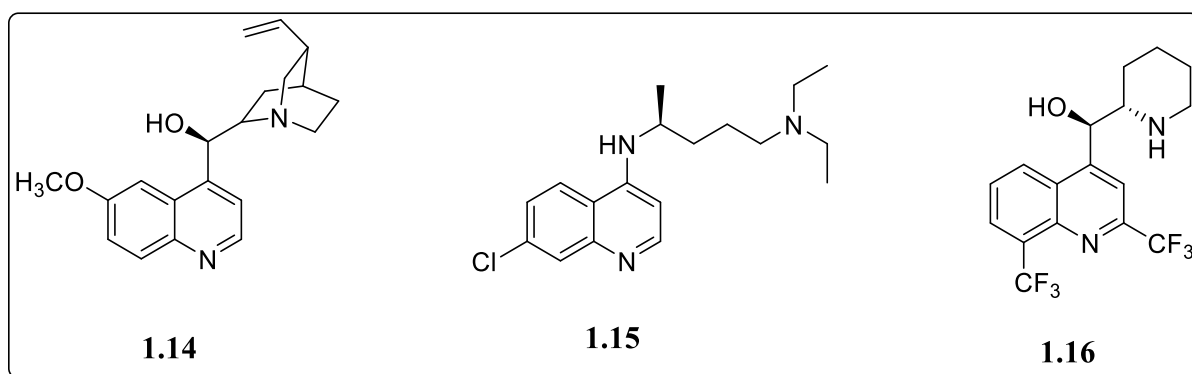


**Figure 1.8:** Chemical structures of clinical approved antimalarial drugs.

Recently, Khanye and co-workers<sup>48</sup> reported the synthesis of 2-oxoquinoline derived thiosemicarbazones represented by compound **1.17** showing potential in vitro antimalarial activity ( $IC_{50} = 1.79 \mu M$ ) against chloroquine-sensitive 3D7 strain of *P. falciparum* parasite.

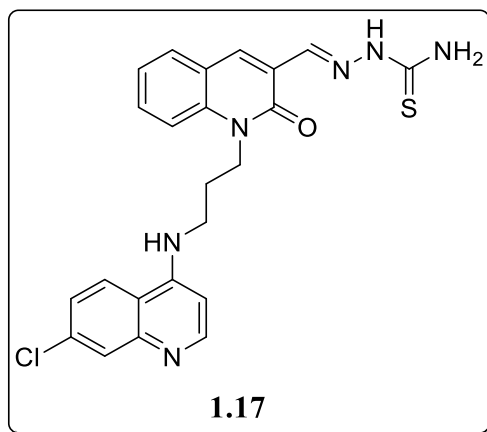


**Figure 1.9:** Quinoline-thiosemicarbazone **1.17** showing anti-malarial activity<sup>48</sup>.

## 1.7 THIAZOLIDINEDIONE

Thiazolidine-2,4-dione (TZD, **Figure 1.10**) is a heterocyclic ring system that has two carbonyl moieties at positions 2 and 4 of the thiazolidione ring. It appears as a white crystalline solid with pKa value of 6.82. The positions 3 and 5 are considered points for further structural modifications in the search for potent novel bioactive compounds that are based on TZD pharmacophoric unit<sup>16</sup>. The presence of the two carbonyl groups at positions 2 and 4 and an  $\alpha$ -hydrogen at the 5<sup>th</sup> position allows the 2,4-thiazolidinedione ring to form different tautomeric structures such as amide/imidol and/or keto-enol.<sup>16</sup>

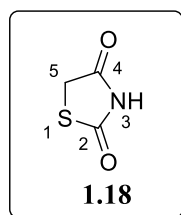


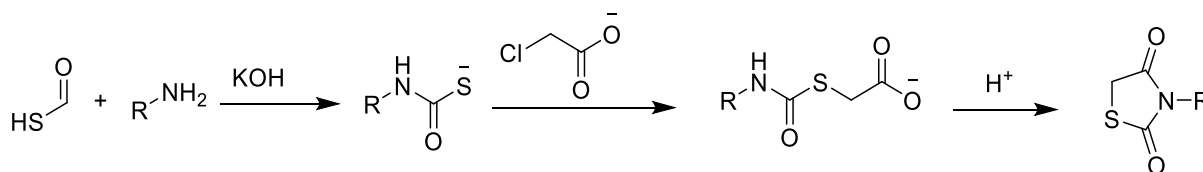
**Figure 1.10:** Chemical structure of 2,4-thiazolidinedione.

### 1.7.1 Chemistry: Synthesis for 2,4-thiazolidinedione ring and related compounds

There are different synthetic routes for accessing the 2,4-thiazolidinedione ring system which have been reported in literature<sup>55,56</sup>. The most commonly employed synthetic route involves refluxing  $\alpha$ -chloroacetic acid with thiourea under acidic conditions. The following brief sections will focus on selected synthetic routes for 2,4-thiazolidinedione framework.

#### 1.7.1.1 Synthesis of 2,4-thiazolidinedione from thiocarbamates

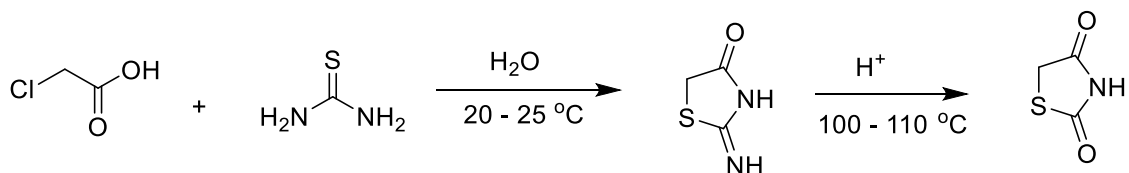
The synthesis of 2,4-thiazolidinedione from thiocarbamates involved the reaction of alkyl thiocarbamates with  $\alpha$ -haloalkanoic acids in the basic reaction conditions<sup>56</sup> (**Scheme 1.7**). In this reaction, the sulphur of the thione group displaces the halogen of the  $\alpha$ -haloalkanoic acid resulting in the loss of the alkyl group as a carbonium ion. Subsequent *S*-carboxymethyl thiocarbamate cyclization resultant in the formation of 2,4-thiazolidinedione structure.



**Scheme 1.7:** Reaction of  $\alpha$ -haloalkanoic acid with alkyl thioncarbamates to yield 2,4-thiazolidinedione<sup>56</sup>.

#### 1.7.1.2 Synthesis of 2,4-thiazolidinedione from thioureas

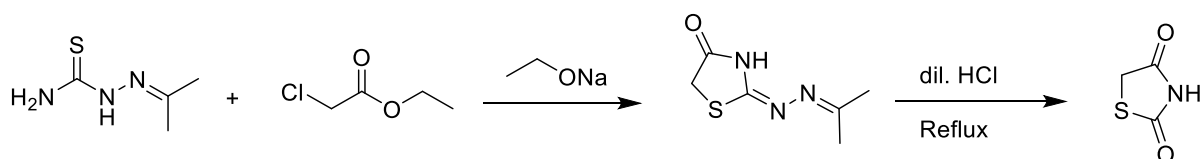
Alternatively, the synthesis of 2,4-thiazolidinedione and related compounds can be achieved from thioureas. In this reaction  $\alpha$ -chloroacetic acid reacts with thiourea to produce 2-imino-4-thiazolidinone, which is refluxed under acidic conditions to obtain 2,4-thiazolidinedione.<sup>57</sup> (**Scheme 1.8**).



**Scheme 1.8:** Reaction of chloroacetic acid and thiourea under acidic conditions to yield 2,4-thiazolidinedione.

#### 1.7.1.3 Synthesis of 2,4-thiazolidinedione from thiosemicarbazone

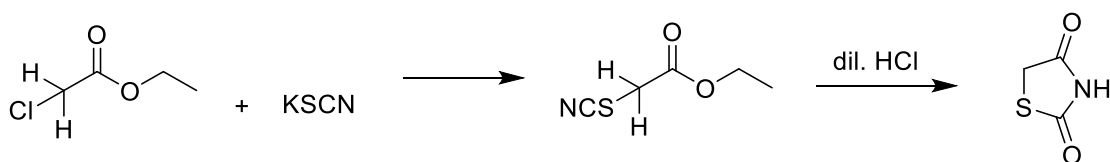
In this reaction, thiosemicarbazone is converted to sodium salt by sodium ethoxide, and then reacted with the ester of the chloroacetic acid to produce 2-hydrazino-4-thiazolidinone. Refluxing this intermediate with dilute hydrochloric acid produces the title compound<sup>16</sup> (**Scheme 1.9**).



**Scheme 1.9:** 2,4-Thiazolidinedione generated from thiosemicarbazone in the presence of a base.

#### 1.7.1.4 Synthesis of 2,4-thiazolidinedione from thiocyanates

In this reaction, ethyl chloroacetate reacts with potassium thiocyanate to give rise to ethyl thiocyanateacetate intermediate (**Scheme 1.10**), which is further treated with dilute hydrochloric acid to produce the target 2,4-thiazolidinedione motif<sup>16</sup>.



**Scheme 1.10:** Synthesis of 2,4-thiazolidinedione from reaction of ethyl chloroacetate with potassium thiocyanate.

## 1.8 MEDICINAL CHEMISTRY OF 2,4-THIAZOLIDINEDIONE BASED COMPOUNDS

A significant number of 2,4-thiazolidinedione containing compounds that exhibit a broad spectrum of pharmacological activities have been synthesized and characterized over the past years<sup>58-60</sup>. **Figure 1.11** shows these pharmacological activities, which are anti-hyperglycemic, anti-cancer, anti-oxidant, anti-inflammatory and anti-microbial.

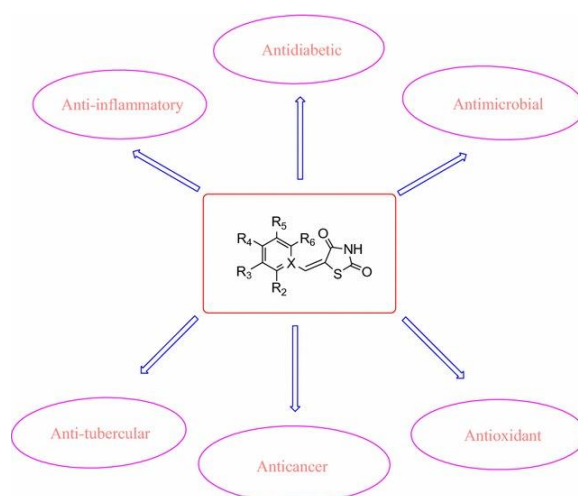


**Figure 1.11:** Biological activities of 2,4-thiazolidinedione derivatives (adapted from<sup>61</sup>).

### 1.8.1 Anti-diabetic activity

In the early 1980s, a number of compounds containing the TZD scaffold were intensively explored for their anti-hyperglycaemic activity<sup>62</sup>. The first representative of this class was ciglitazone (**1.19**), whereas other derivatives such as englitazone (**1.20**), pioglitazone (**1.21**) and troglitazone (**1.22**) were subsequently discovered. In all these compounds, the thiazolidine-2,4-dione framework has been found to be responsible for majority of their pharmacological actions. Thiazolidinedione were first recognised to improve the lipid-lowering and weaker glucose-lowering properties of the fibrates<sup>63</sup>.

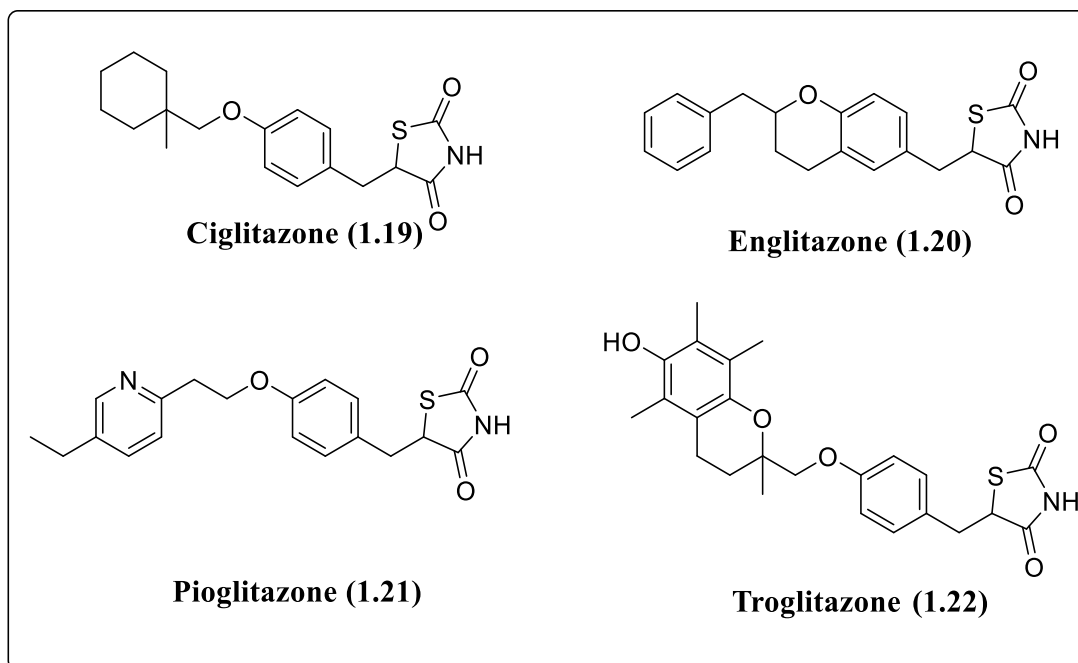


**Figure 1.12:** Anti-diabetic compounds bearing TZD ring.

### 1.8.2 Anti-tuberculosis activity

The first compound to be pharmacologically evaluated for anti-TB activity containing the thiazolidinedione unit was reported by an Italian scientist, Vistentini, in 1954<sup>16</sup>. The recent work by Shaik and co-workers<sup>64</sup> reported compound **1.23**, which featured the TZD, to show great anti-TB activity with MIC of 25  $\mu\text{g/mL}$  against *Mtb* H37Rv. Despite the promising activity of **1.23**, the mechanism of action of this class of compounds remains unclear. On the other hand, Chilamakuru and co-workers<sup>60</sup> prepared a series of thiazolidinedione-based compounds which showed anti-tubercular activity when evaluated *in vitro* against the *M. tuberculosis* strain H37Rv. They identified a series of compounds with compound **1.24** (**Figure 1.13**) showing anti-tubercular activity with MIC value of 12.5  $\mu\text{g/mL}$ .

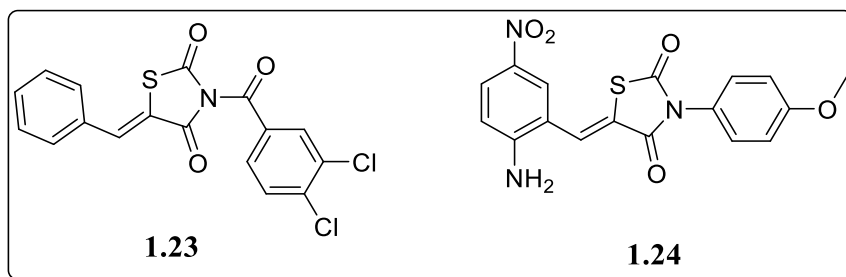


**Figure 1.13:** Anti-tuberculosis compounds bearing TZD ring.

### 1.8.3 Anti-malarial activity

Mital and co-workers<sup>65</sup> reported a series of TZD compounds, which were screened against the K1 resistant strain of *P. falciparum* and L-6 cell line for antimalarial activity and human cytotoxic effect, respectively. Compound **1.25** and **1.26** emerged as the most active compounds with  $EC_{50}$  values in the range of 0.09 and 0.061  $\mu$ M, and mammalian cell line, L6 toxicity of  $EC_{50}$  > 100 and 71  $\mu$ M, respectively.

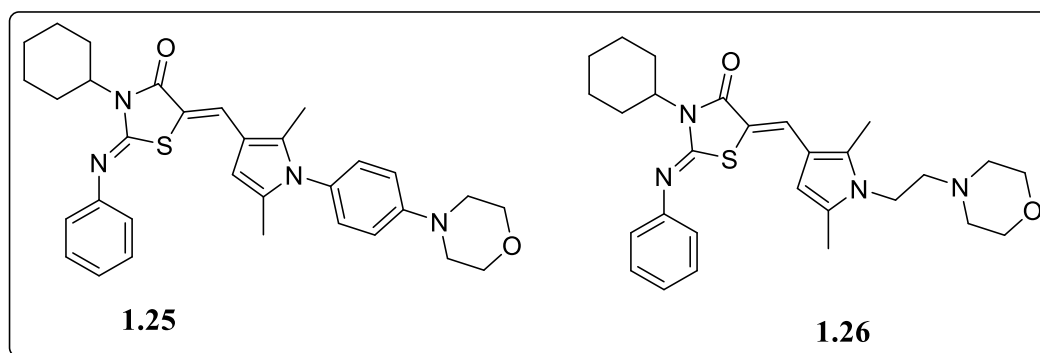


**Figure 1.14:** Anti-malarial compounds bearing TZD ring.

Sharma and co-workers<sup>66</sup> with the help of structure-based virtual screening successfully synthesized compound **1.27** which showed activity against the W2 resistant strain *P. falciparum* through the inhibition of cysteine protease falcipain (FP-2), an essential enzyme in haemoglobin hydrolysis.

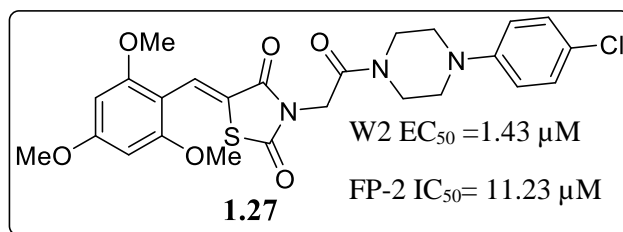


**Figure 1.15:** Compound **1.27** with anti-plasmodial activity.

Oderinlo and co-workers<sup>59</sup> also reported anti-malarial TZD based compounds bearing a ferrocene group, which were evaluated *in vitro* against *P. falciparum*, Dd2 strain. From the series of compounds reported, they obtained compounds **1.28** and **1.29** which had IC<sub>50</sub> values in the range of 14.6 and 18.6 μM, respectively. All the synthesized compounds exhibited no significant cytotoxicity effects on the HeLa cell line.

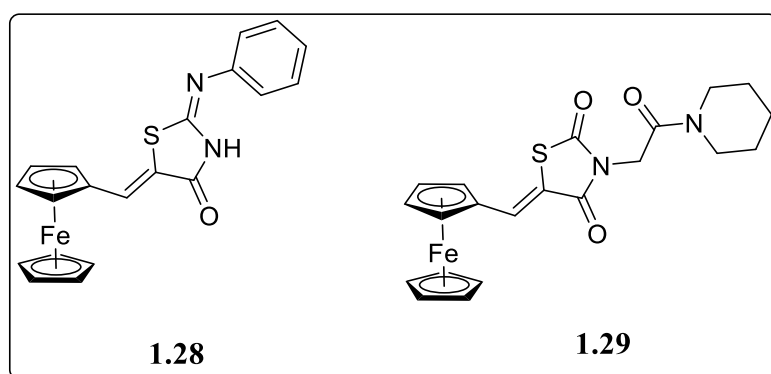


**Figure 1.16:** Ferrocenyl-TZD based compounds with anti-plasmodial activity.

#### 1.8.4 Anti-inflammatory activity

Phagocyte NADPH oxidase is an enzyme that is responsible for the respiratory burst and generates high concentration of reactive oxygen species (ROS), such as superoxide anion<sup>67</sup>. These highly reactive species are believed to be directly toxic to different cell types and amplify the inflammatory processes<sup>67,68</sup>. Youssef and co-workers<sup>69</sup> synthesized novel pyrazolyl-2,4-thiazolidinedione derivatives and biologically evaluated *in vitro* these compounds for their

inflammatory and neuroprotective properties. Compounds **1.30**, **1.31** and **1.32** inhibited mononuclear phagocyte respiratory burst at IC<sub>50</sub> values of 8.08 and 1 μM, respectively.

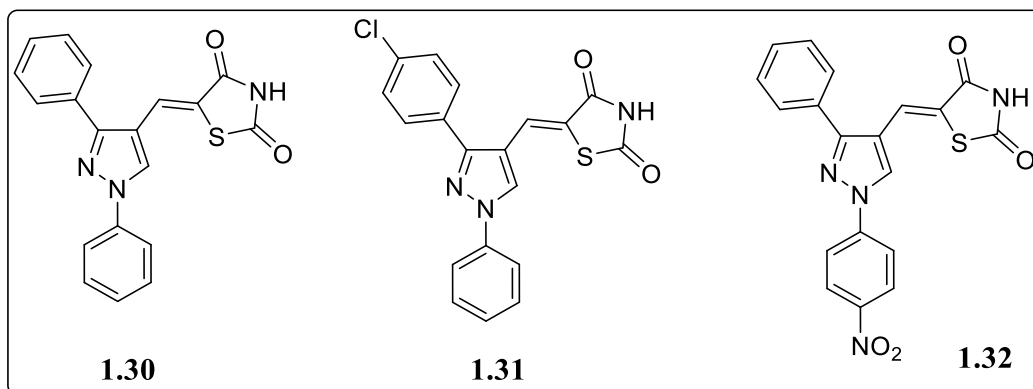


**Figure 1.17:** Anti-inflammatory compounds bearing TZD ring.

### 1.8.5 Antimicrobial activity

A microbe is a pathogenic species that if left untreated could cause severe illness<sup>70</sup>. Microbes exist as bacteria, viruses, fungi, algae, and protozoa<sup>71</sup>. Microbes pose as a worldwide public health problem. The most common cases includes pathogens such as such as Salmonella, and enterohaemorrhagic *Escherichia coli* (causes of bloody diarrhea)<sup>72</sup>. Alagawadi and Alegaon<sup>55</sup> reported a series of compounds which they screened for anti-microbial activity across different microorganism strains. These microorganisms include both Gram positive and negative bacterial strains, and the fungal strains. Compounds **1.33** – **1.35** emerged as moderate to good anti-microbial agents. Compounds **1.33** and **1.35** showed activity against both bacterial and fungal strains while compound **1.34** appears to be selective towards fungal strains.

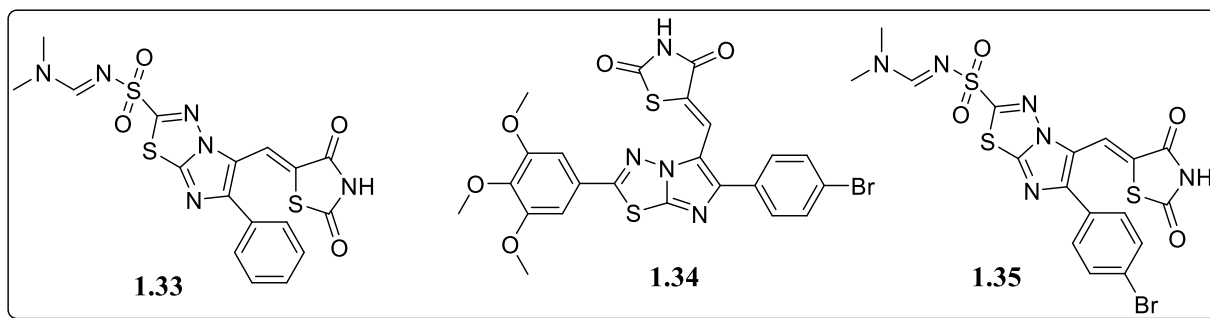


**Figure 1.18:** Anti-microbial compounds bearing TZD ring.

### 1.8.6 Antioxidant activity

The anti-oxidant effects of TZD depend on peroxisome proliferator-activated receptor- $\gamma$  PPAR $\gamma$ . A work done by Chung and co-workers<sup>73</sup> showed how the synthetic TZDs **1.19**, **1.20** and **1.36** displayed anti-oxidative effects in pancreatic  $\beta$ -cells. They exposed pancreatic  $\beta$ -cells,  $\beta$ TC3 and INS-1 cells in a high level of H<sub>2</sub>O<sub>2</sub>, which was generated by glucose, and glucose oxidase in the media. Thereafter, treatment of the cells with compounds **1.19**, **1.20** and **1.36** resulted in the reduction of H<sub>2</sub>O<sub>2</sub> levels. In addition to H<sub>2</sub>O<sub>2</sub> levels, reactive oxygen species (ROS) was also measured, and it was observed that these TZD has effectively reduced the ROS levels close to basal levels.

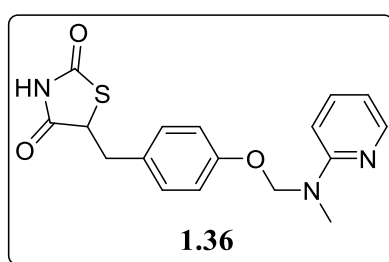


**Figure 1.19:** Antioxidant compound bearing TZD ring.

## 1.9 AIMS AND OBJECTIVES OF THE STUDY

The primary objective of this work was to identify a series of quinolinyl-thiazolidinedione derivatives with *in vitro* activity against *M. tuberculosis*, a causative agent of TB. However, the presence of the quinoline moiety and thiazolidinedione ring in malarial therapy prompted us to also cross-screen the identified series against *P. falciparum* as part of broad screening approach of novel bioactive compounds employed by our laboratory. Despite recent gains, the current available therapy against TB and malaria remain inadequate and drugs targeting these diseases are characterized by poor efficacy, toxicity and emergence of drug resistant. Therefore, there is an urgent need to develop new improved drugs with specific or multiple targets against *M. tuberculosis* and *P. falciparum* strains.

### 1.9.1 Specific aims

The specific aims to realise the overall goal of this project include:

- Design, synthesis and fully characterization of quinolinyl-thiazolidinedione series derivatives as antitubercular compounds for treatment of TB.
- *In vitro* pharmacological evaluation of achieved compounds against the H37Rv strain of *M. tuberculosis*.
- Cross-pollination screening of achieved against the *P. falciparum* strain with the intention to find alternative use of these compounds.

## 1.10 REFERENCES

1. Delogu, G., Sali, M. & Fadda, G. *Mediterr., J. Hematol. Infect. Dis.*, **2013**, 5, e2013070.
2. Palmer, M. V. Mycobacterium bovis Infection in Animals and Humans, 2nd Edition. *Emerg. Infect. Dis.* **2006**, 12, 1306.
3. Michel, A. L., Müller, B. & van Helden, P. D. *Vet. Microbiol.*, **2010**, 140, 371–381.
4. Smith, N. H., Crawshaw, T., Parry, J. & Birtles, R. J., *J. Clin. Microbiol.*, **2009**, 47, 2551–2559.
5. de Keijzer, J., Mulder, A., de Haas, P. E. W., de Ru, A. H., Heerkens, E. M., Amaral, L., van Soolingen, D., van Veelen, P. A., *J. Proteome Res.*, **2016**, 15, 1776–1786.
6. WHO | Global tuberculosis report 2018. WHO Available at: [http://www.who.int/tb/publications/global\\_report/en/](http://www.who.int/tb/publications/global_report/en/). (Accessed: 20th February 2019)
7. Pigrau-Serrallach, C. & Rodríguez-Pardo, D., *Eur. Spine J.*, **2013**, 22, 556–566.
8. Rock, R. B., Olin, M., Baker, C. A., Molitor, T. W. & Peterson, P. K., *Clin. Microbiol. Rev.*, **2008**, 21, 243–261.
9. Smith, I., *Clin. Microbiol. Rev.*, **2003**, 16, 463–496.
10. Zuñiga, J., Torres-García, D., Santos-Mendoza, T., Rodriguez-Reyna, T. S., Granados, J., Yunis, E. J., *Clin. Dev. Immunol.*, **2012**, 2012, 1–18.
11. Pieters, J., *Cell Host Microbe*, **2008**, 3, 399–407.
12. Ahmad, S., *Clin. Dev. Immunol.*, **2011**, 1–17.
13. Sasindran, S. J., and Torrelles, J. B., *Front. Microbiol.*, **2011**, 2, 1-16.
14. Rajni, Rao, N., and Meena, L. S., *Biotechnol. Res. Int.*, **2011**, 2011, 1–7.
15. Marrakchi, H., Lanéelle, M. A., and Daffé, M., *Chem. Biol.*, **2014**, 21, 67–85.
16. Chadha, N., Bahia, M.S., Kaur, M., and Silakari, O., *Bioorg. Med. Chem.*, **2015**, 23, 2953–2974.

17. Quémard, A., Lacave, C., and Lanéelle, G., *Antimicrob. Agents Chemother.*, **1991**, 35, 1035–1039.
18. Timmins, G. S., and Deretic, V., *Mol. Microbiol.*, **2006**, 62, 1220–1227.
19. Johnsson, K., King, D. S., and Schultz, P. G., *J. Am. Chem. Soc.*, **1995**, 117, 5009–5010.
20. Xavier, A. S., and Lakshmanan, M., *J. Pharmacol. Pharmacother.*, **2014**, 5, 222–224.
21. Manjunatha, U., Boshoff, H. I., and Barry, C. E., *Commun. Integr. Biol.*, **2009**, 2, 215–218.
22. Goude, R., Amin, A. G., Chatterjee, D., and Parish, T., *Antimicrob. Agents Chemother.*, **2009**, 53, 4138–4146.
23. Sacksteder, K. A., Protopopova, M., Barry, C. E., Andries, K., and Nacy, C. A., *Future Microbiol.*, **2012**, 7, 823–837.
24. Koga, T., Fukuoka, T., Doi, N., Harasaki, T., Inoue, H., Hotoda, H., Kakuta, M., Muramatsu, Y., Yamamura, N., Hoshi, M., and Hirota, T., *J. Antimicrob. Chemother.*, **2004**, 54, 755–760.
25. Bhat, Z. S., Rather, M. A., Maqbool, M., Lah, H. U., Yousuf, S. K., and Ahmad, Z., *Biomed. Pharmacother.*, **2017**, 95, 1520–1534.
26. Ma, Z., Ginsberg, A. M., and Spigelman, M., Antimycobacterium Agents. in *Comprehensive Medicinal Chemistry II* (eds. Taylor, J. B. & Triggle, D. J.), Elsevier, **2007**, Ch. 7.24, 699–730. doi:10.1016/B0-08-045044-X/00224-8
27. Zhang, Y., Shi, W., Zhang, W., and Mitchison, D., *Microbiol. Spectr.*, **2013**, 2, 1–12.
28. Wehrli, W., *Rev. Infect. Dis.*, **1983**, 5 Suppl 3, S407-411.
29. Pang, Y., Lu, J., Wang, Y., Song, Y., Wang, S., Zhao, Y., *Antimicrob. Agents Chemother.*, **2013**, 57, 893–900.
30. Jain, P. P., Degani, M. S., Raju, A., Ray, M., and Rajan, M. G. R., *Bioorg. Med. Chem. Lett.*, **2013**, 23, 6097–6105.
31. Manske, R. H., *Chem. Rev.*, **1942**, 30, 113–144.

32. Keri, R. S., and Patil, S. A., *Biomed. Pharmacother.*, **2014**, 68, 1161–1175.
33. Yale, H. L., *J. Am. Chem. Soc.*, **1947**, 69, 1230–1230.
34. Skraup's Synthesis. *Vive Chemistry* (2012), Available at: <https://vivechemistry.wordpress.com/2012/11/03/skraups-synthesis/>. (Accessed: 22<sup>nd</sup> February 2019).
35. Knorr quinoline synthesis. Available at: <http://www.rsc.org/publishing/journals/prospect/ontology.asp?id=RXNO:0000394>. (Accessed: 22<sup>nd</sup> February 2019)
36. Wang, Z. (2010). Knorr Quinoline Synthesis. In *Comprehensive Organic Name Reactions and Reagents* (abstract), Z. Wang (Ed.). doi:10.1002/9780470638859.conrr365
37. Makelane, H. R. Regioselectivity of palladium-catalyzed sonogashira cross-coupling of 2-aryl-4-chloro-3-iodoquinoline- derivatives with terminal alkynes., **2010**, University of South Africa.
38. Wang, Z. (2010). Combes Quinoline Synthesis. In *Comprehensive Organic Name Reactions and Reagents* (abstract), Z. Wang (Ed.). doi:10.1002/9780470638859.conrr151
39. Sloop, J. C., *J. Phys. Org. Chem.*, **2009**, 22, 110–117.
40. Shvekhgeimer, M. G. A., *Chem. Heterocycl. Compd.*, **2004**, 40, 257–294.
41. Lu, L., Zhou, P., Hu, B., Li, X., Huang, R., and Yu, F., *Tetrahedron Lett.*, **2017**, 58, 3658–3661.
42. Kravchenko, D. V., Kysil, V. V., Ilyn, A. P., Tkachenko, S. E., Maliarchouk, S., Okun, I. M., and Ivachtchenko, A. V., *Bioorg. Med. Chem. Lett.*, **2005**, 15, 1841–1845.
43. Meth-Cohn, O., Narine, B., and Tarnowski, B. *Tetrahedron Lett.*, **1979**, 20, 3111–3114.
44. Li, J. J. *Name Reactions in Heterocyclic Chemistry*. (John Wiley & Sons, 2004).

45. Jain, S., Chandra, V., Kumar Jain, P., Pathak, K., Pathak, D., and Vaidya, A., Comprehensive review on current developments of quinoline-based anticancer agents (In press). *Arab. J. Chem.* (2016). doi:10.1016/j.arabjc.2016.10.009
46. Jain, P. P., Degani, M. S., Raju, A., Anantram, A., Seervi, M., Sathaye, S., Ray, M., and Rajan, M. G. R., *Bioorg. Med. Chem. Lett.*, **2016**, 26, 645–649.
47. Foley, M., and Tilley, L., *Int. J. Parasitol.*, **1997**, 27, 231–240.
48. Darrell, O. T., Hulushe, S. T., Mtshare, T. E., Beteck, R. M., Isaacs, M., Laming, D., Hoppe, H. C., Krause, R. W. M., Khanye, S. D., *South Afr. J. Chem.*, **2018**, 71, 174–181.
49. Cretton, S., Breant, L., Pourrez, L., Ambuehl, C., Marcourt, L., Ebrahimi, S. N., Hamburger, M., Perozzo, R., Karimou, S., Kaiser, M., Cuendet, M., and Christen, P., *J. Nat. Prod.*, **2014**, 77, 2304–2311.
50. Chanquia, S. N., Larregui, F., Puente, V., Labriola, C., Lombardo, E., and García Liñares, G., *Bioorganic Chem.*, **2019**, 83, 526–534.
51. Matteelli, A., Carvalho, A. C., Dooley, K. E., and Kritski, A., *Future Microbiol.*, **2010**, 5, 849–858.
52. Chetty, S., Ramesh, M., Singh-Pillay, A., and Soliman, M. E. S., *Bioorg. Med. Chem. Lett.*, **2017**, 27, 370–386.
53. Andries, K., Verhasselt, P., Guillemont, J., Göhlmann, H. W. H., Neefs, J., Winkler, H., Gestel, J. V., Timmerman, P., Zhu, M., Lee, E., Williams, P., Chaffoy, D., Huitric, E., Hoffner, S., Cambau, E., Truffot-Pernot, C., Lounis, N., and Jarlier, V., *Science*, **2005**, 307, 223–227.
54. Achan, J., Talisuna, A. O., Erhart, A., Yeka, A., Tibenderana, J. K., Baliraine, F. N., Rosenthal, P. J., and D'Alessandro, U., *Malar. J.*, **2011**, 10, 144.
55. Alagawadi, K. R., and Alegaon, S. G., *Arab. J. Chem.*, **2011**, 4, 465–472.

56. Chadha, N., and Silakari, O., Key Heterocycle Cores for Designing Multitargeting Molecules: *Thiazolidine-2,4-Dione: A Potential Weapon for Targeting Multiple Pathological Conditions*, Elsevier, **2018**, Ch. 5, p 175-209.
57. Kaur Manjal, S., Kaur, R., Bhatia, R., Kumar, K., Singh, V., Shankar, R., Kaur, R., Rawal, R. K., *Bioorganic Chem.*, **2017**, 75, 406–423.
58. Nanjan, M. J., Mohammed, M., Prashantha Kumar, B. R., and Chandrasekar, M. J. N. *Bioorganic Chem.*, **2018**, 77, 548–567.
59. Oderinlo, O. O., Tukulula, M., Isaacs, M., Hoppe, H. C., Taylor, D., Smith, V. J., Khanye, S. D., *Appl. Organomet. Chem.*, **2018**, 32, e4385.
60. Chilamakuru, N. B., Shankarananth, V., Rajasekhar, K. K., and Singirisetty, T., *Asian J. Pharm. Clin. Res.*, **2013**, 6, 29–33.
61. Sucheta, Tahlan, S., and Verma, P. K., *Chem. Cent. J.*, **2017**, 11, 130.
62. Jain, V. S., Vora, D. K., and Ramaa, C. S., *Bioorg. Med. Chem.*, **2013**, 21, 1599–1620.
63. Lalloyer, F., and Staels, B., *Arterioscler. Thromb. Vasc. Biol.*, **2010**, 30, 894–899.
64. Shaikh, F. M., Patel, N. B., and Rajani, D., *Indian J. Biotech. Pharm. Res.*, 2013, **1**, 496–503.
65. Mital, A., Murugesan, D., Kaiser, M., Yeates, C., and Gilbert, I. H., *Eur. J. Med. Chem.*, **2015**, 103, 530–538.
66. Sharma, R. K., Younis, Y., Mugumbate, G., Njoroge, M., Gut, J., Rosenthal, P. J., and Chibale, K., *Eur. J. Med. Chem.*, **2015**, 90, 507–518.
67. El-Benna, J., Dang, P. M.-C., Gougerot-Pocidallo, M. A., and Elbim, C., *Arch. Immunol. Ther. Exp. (Warsz.)*, **2005**, 53, 199–206.
68. Yang, P., Huang, S., and Xu, A., The Oxidative Burst System in *Amphioxus*. in *Amphioxus Immunity* (ed. Xu, A.), Academic Press, **2016**, Ch. 8, p 153-165.

69. Youssef, A. M., Sydney White, M., Villanueva, E. B., El-Ashmawy, I. M., and Klegeris, A., *Bioorg. Med. Chem.*, **2010**, 18, 2019–2028.
70. Casadevall, A., and Pirofski, L., *Trends Microbiol.*, **2004**, 12, 259–263.
71. Wegley, L., Edwards, R., Rodriguez-Brito, B., Liu, H. & Rohwer, F., *Environ. Microbiol.*, **2007**, 9, 2707–2719.
72. E. coli. Available at: <https://www.who.int/news-room/fact-sheets/detail/e-coli>. (Accessed: 18th March 2019)
73. Chung, S. S., Kim, M., Lee, J. S., Ahn, B. Y., Jung, H. S., Lee, H. M., Park, K. S., *Am. J. Physiol.-Endocrinol. Metab.*, **2011**, 301, E912–E921.

**CHAPTER TWO**  
**SYNTHESIS AND CHARACTERIZATION OF QUINOLINYL-**  
**THIAZOLIDINEDIONE HYBRID DERIVATIVES**

**2.1 INTRODUCTION**

**T**his chapter is providing details of the synthesis and characterization of target quinolinyl thiazolidinedione derivatives. The synthesis of these compounds was achieved through multistep conventional synthetic methods. The characterization of each compound was achieved using the common spectroscopic techniques.

**2.1.1 Rationale: Hybridization of quinoline and thiazolidinedione**

In view of wide spread of multi-drug resistant (MDR) TB, there is an urgent need to discover bioactive compounds with unique structures and novel mode of actions. The new anti-TB agents should be able to shorten treatment duration, target MDR or extreme-drug resistance (XDR) strains, simplify the treatment by reducing the daily pill burden and can be co-administered with HIV medications. Quinoline-based compounds such as bedaquiline have been discussed in the previous sections. More importantly, quinoline-based compounds are endowed with remarkable pharmacological activities against TB. The remarkable activity of bedaquiline includes good selectivity towards mycobacterial ATP synthase compared to human mitochondrial ATP synthase<sup>1</sup> with good potency, MIC = 0.1  $\mu$ M, against TB<sup>2</sup>. Many research groups around the world have explored key structural modification of quinoline motif towards the design of promising anti-TB agents.

On the other hand, thiazolidinedione based compounds reported by Shaikh and co-workers<sup>3</sup> showed good activity with percent inhibition of 99% against H37Rv *M. tuberculosis* strain. These results presented the TZD as a desirable and attractive structural framework for further manipulation in an effort to develop novel anti-TB agents for global control and eradication of this epidemic. Similarly, Alegeon and co-workers<sup>4</sup> also reported compounds carrying thiazolidinedione moiety and from this work compound **1.34** showed promising anti-TB activity with MIC value of 3.12  $\mu\text{g/mL}$ . This literature precedence prompted us to design through molecular hybridization approach compounds represented in (**Figure 2.1**) containing quinoline and thiazolidinedione core structures in a single molecule and investigate their potential activity against H37Rv strain.

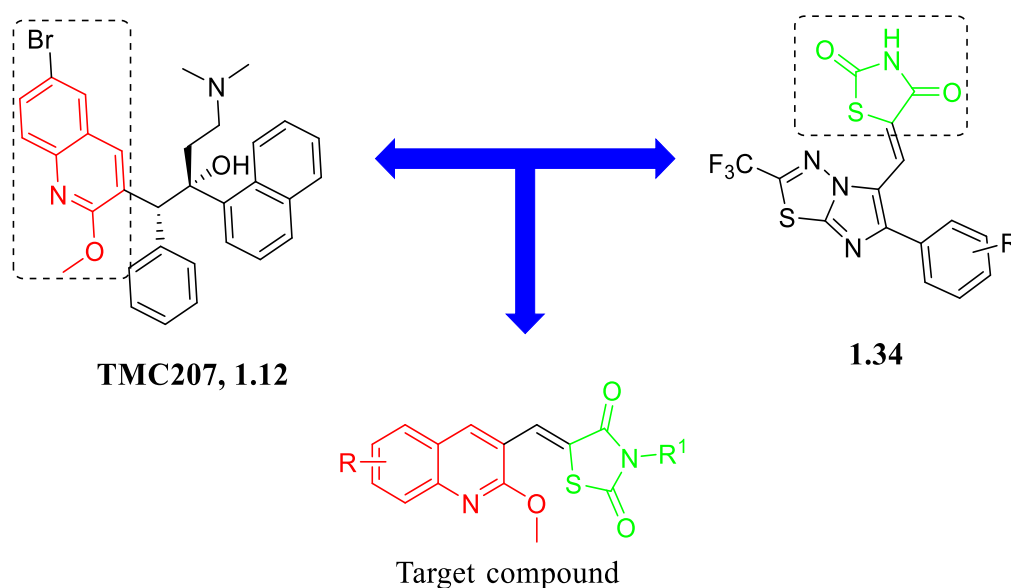


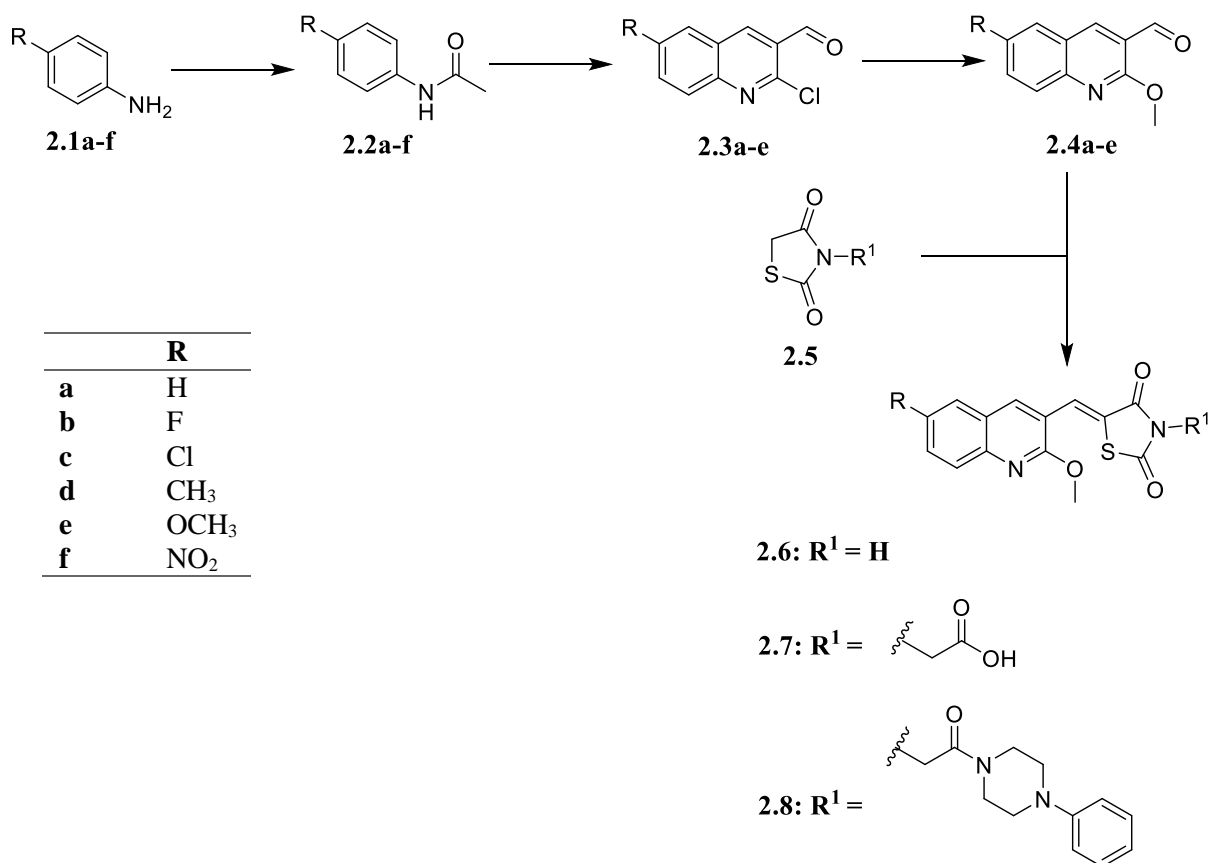
**Figure 2.1:** Rationale and design of hybrid quinoline thiazolidinedione derivatives.

## 2.2 RESULTS AND DISCUSSION

### 2.2.1 Overall synthetic route

The synthesis of the target compounds commenced with the synthesis of key intermediates that will be discussed in this chapter. The first step begins with acetylation of *p*-substituted anilines (**2.1**) to obtain key acetanilide (**2.2a-e**), to which under Vilsmeier-Haack conditions were

cyclized to obtain 2-chloroquinoline-3-carbaldehyde (**2.3a-e**). Compounds **2.3a-e** were then methoxylated on the 2<sup>nd</sup> position to obtain the desired quinoline moiety, 2-methoxyquinoline-3-carbaldehyde (**2.4a-e**). Thereafter, hybridization of compounds **2.4a-e** with 2,4-thiazolidinedione derivatives (**2.5**) via Knoevenagel condensation allowed us to achieve our desired quinolinyl-thiazolidinedione molecular hybrids as seen in **Scheme 2.1**.

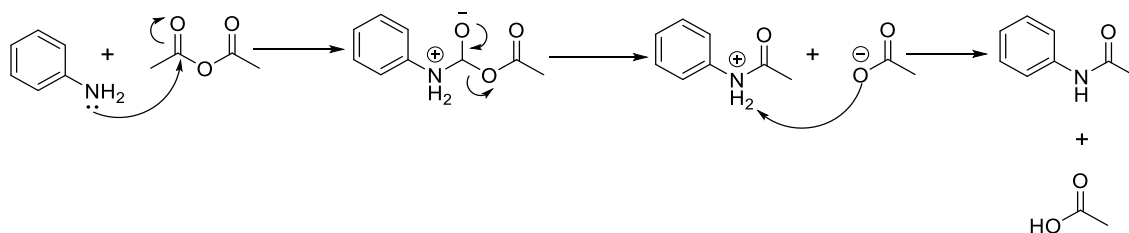


**Scheme 2.1: Reagents and reaction conditions.** (a) AcO<sub>2</sub>/AcOH, Reflux at 120 °C, 30 min. (b) DMF/POCl<sub>3</sub>; Reflux at 75 °C, 8-18hrs. (c) KOH/MeOH, Reflux at 70 °C, 3-4 hrs.; (d) i. Piperidine/Ethanol reflux at 85 °C for 4-6hrs, ii. Piperidine, acetic acid (2-3 drops)/ toluene reflux at 100 °C for 4-6hrs.

### 2.2.2 Synthesis of acetanilides (2.2a-f)

Briefly, acetanilides (**2.2a-f**) were synthesized from anilines (**2.1a-f**) by treating the anilines with acetic anhydride and acetic acid generated as a side product. After stirring, the precipitate

was washed with water, dried and recrystallized using either water or ethanol to obtain acetanilides **2.2a–f** with percentage yields in the range of 50 – 92%. In this reaction, the NH<sub>2</sub> group of aniline acts as a nucleophile and an acetyl group (CH<sub>3</sub>CO) of the acetic anhydride acts as an electrophile. **Scheme 2.2** below represents the reaction mechanism of how aniline reacts with acetic anhydride to yield acetanilide and acetic acid as a by-product.



**Scheme 2.2:** Reaction mechanism of aniline and acetic anhydride transforming into acetanilide, having acetic acid as a by-product.

All the achieved compounds portrayed similar characteristics to confirm their formation. Spectroscopic techniques such as <sup>1</sup>H and <sup>13</sup>C NMR were used to confirm the successful formation and identity of acetanilides. For example, the <sup>1</sup>H-NMR spectrum (**Figure 2.2**) of acetanilide **2.2a** showed a singlet chemical shift at 2.15 ppm integrating with three protons, which was attributed to the acetyl group. Furthermore, a broad signal at δ 7.72 ppm integrating for one proton confirms the presence of the CONH group. <sup>13</sup>C-NMR spectrum (**Figure 2.3**) of compound **2.2a** showed the expected 6 carbon signals which are consistent with acetyl group resonating at δ 24.8 ppm and carbonyl signal at δ 168.8 ppm confirming the proposed structure.

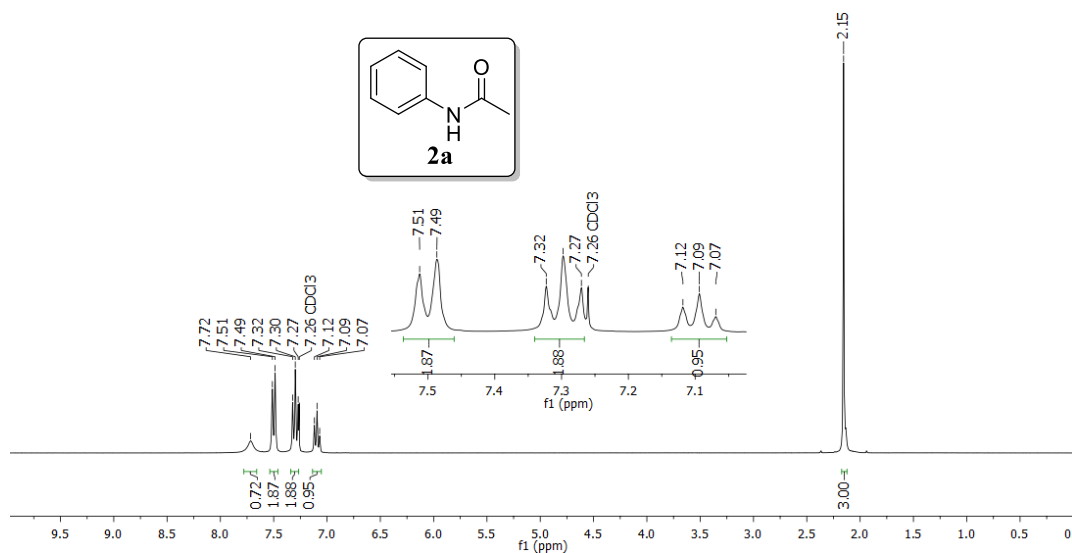


**Figure 2.2:** 300 MHz <sup>1</sup>H-NMR spectrum of compound **2.2a** in CDCl<sub>3</sub>.

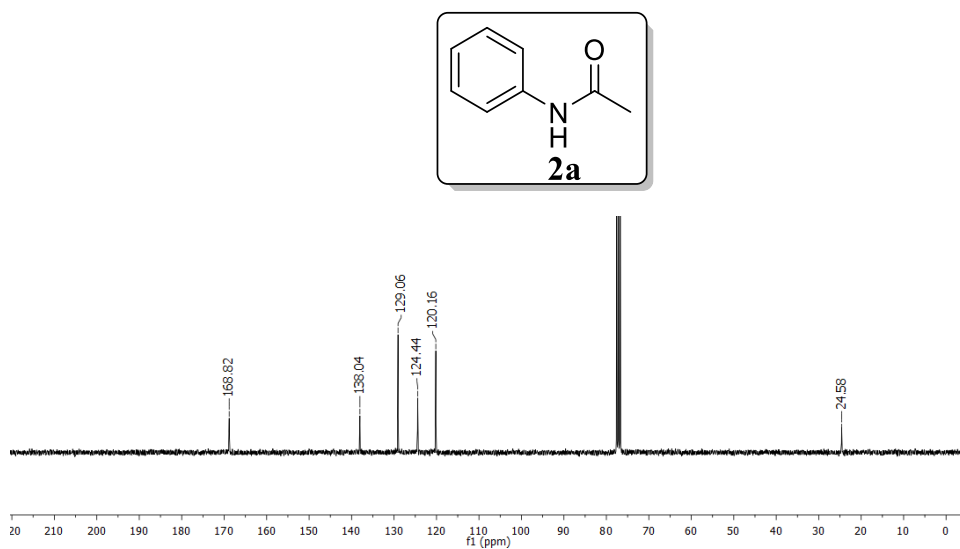
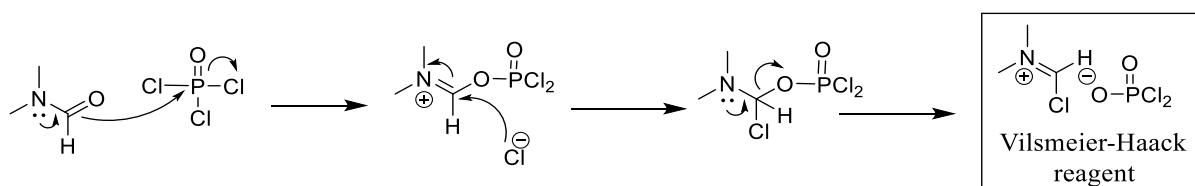


**Figure 2.3:** 75 MHz <sup>13</sup>C-NMR spectrum of compound **2.2a** in CDCl<sub>3</sub>.

### 2.2.3 Synthesis of 2-chloroquinoline-3-carbaldehydes (**2.3a-e**)

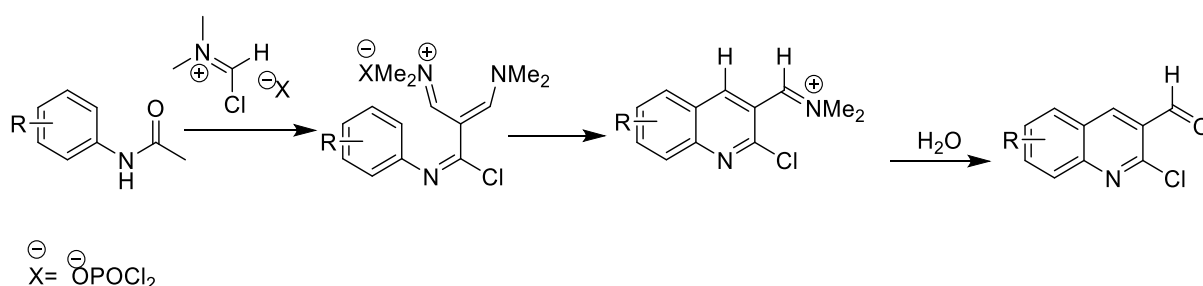
In the second step, the cyclization of acetanilides **2.2a-f** was achieved under Vilsmeier-Haack reaction conditions to form 6-substituted-2-chloroquinoline-3-carbaldehydes derivatives in 31 – 88% yields (**2.3a-e**). The Vilsmeier-Haack reaction is a versatile reaction often employed for a large variety of synthetic transformations to introduce formyl group in electron-rich carbocyclic aromatic compounds<sup>5</sup>. The reaction starts with the synthesis of Vilsmeier-Haack

reagent (**Scheme 2.3**), which is a halomethyleneiminium salt formed from the Lewis acids ( $\text{POCl}_3$ ) and  $N,N'$ -dimethylformamide (DMF)<sup>6</sup>.



**Scheme 2.3:** Synthesis of Vilsmeier-Haack reagent<sup>7</sup>.

The halomethyleneiminium salt then reacts with electron-rich aromatic compounds to yield, after loss of hydrogen chloride, iminium salts, which is hydrolysed to afford aldehyde derivatives (**Scheme 2.4**).



**Scheme 2.4:** Cyclization mechanism of acetanilide under Vilsmeier-Haack conditions to yield 6-substituted-2-chloroquinoline-3-carbaldehyde<sup>5</sup>.

In this work, the Vilsmeier-Haack reagent was prepared each time, where anhydrous DMF (3 eq) was cooled into 0–10 °C was treated with phosphoryl chloride (7 eq) followed by acetanilide (1 eq) and the reaction mixture was heated to reflux, and upon completion as guided by TLC, the reaction content was poured into ice water and stirred for additional 30 minutes to give the target cyclized products. The compounds **2.3a–e** synthesized were obtained in yields of 31–88%. The electron withdrawing substituent group reduces the nucleophilicity of the ring resulting in low yields and prolonged reaction time, and this was evident in this work as *p*-fluoro and *p*-chloro substituted acetanilide gave yields between 31% and 45%, respectively.

Despite numerous attempts which involved changing of reaction conditions, adjusting molar ratios of DMF/ $\text{POCl}_3$  from 3:7 to 5:12, 4-nitroacetanilide did not yield the cyclized product. However, electron-donating substituent group such as methyl and methoxy gave good yields between 63% and 88%, respectively, whilst the unsubstituted acetanilide yielded 52%.

All the products were characterized using  $^1\text{H}$  and  $^{13}\text{C}$ -NMR and full spectral data are summarized reported in the experimental section. Using compound **2.3a** to illustrate the characterization of compounds **2.3a–f**, it can be noted on  $^1\text{H}$ -NMR spectrum (**Figure 2.4**) that the signal at  $\delta_{\text{H}}$  10.53 ppm resonating with 1H as a singlet confirms the aldehydic proton which attest that formylation was successful. The singlet peak at  $\delta$  8.73 ppm was attributed the double bond hydrogen ( $\text{H}_4$ ) and this signal confirmed the electrophilic substitution during cyclization of acetanilide (**Scheme 2.4**) to form the desired quinoline moiety.

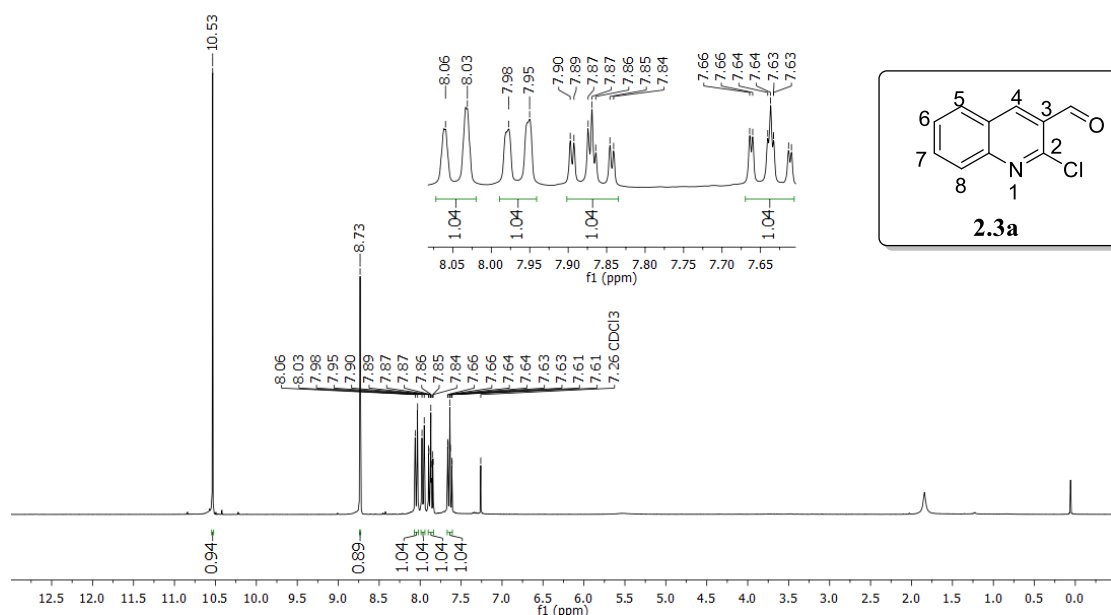


**Figure 2.4:** 300 MHz  $^1\text{H}$ -NMR spectrum of compound **2.3a** in  $\text{CDCl}_3$ .

Furthermore,  $^{13}\text{C}$ -NMR (**Figure 2.5**) was employed to confirm the skeletal structure of compound **2.3a** with all the carbons of the achieved product accounted for. The spectrum

showed 10 expected carbon signals which are consistent with the structure of compound **2.3a**. The aromatic carbons showed carbon signals in the region  $\delta$  126.3–150.1 ppm and the aldehyde carbon resonated at  $\delta$  189.2 ppm.

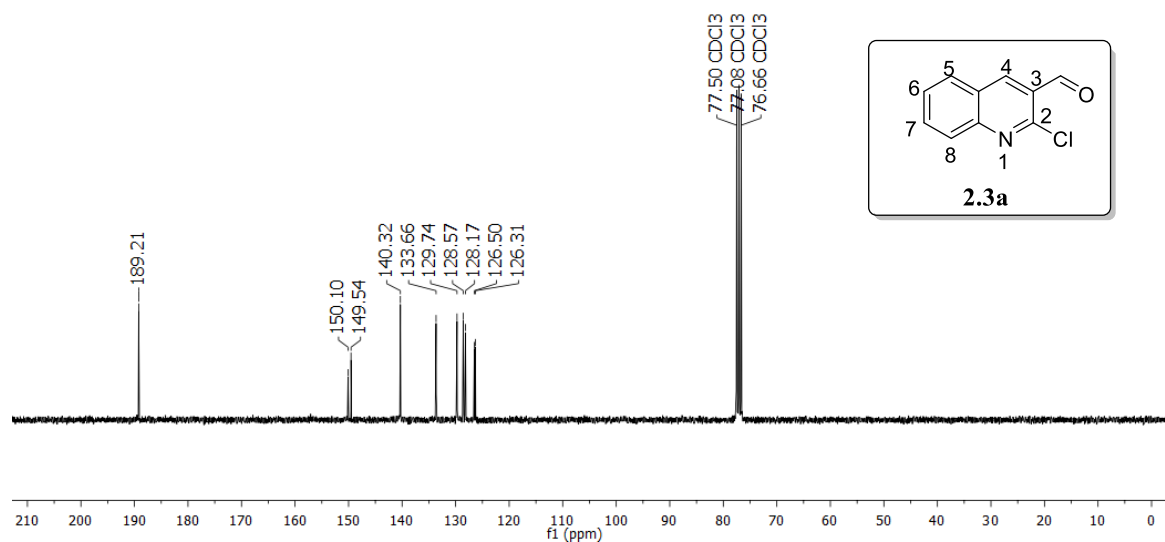
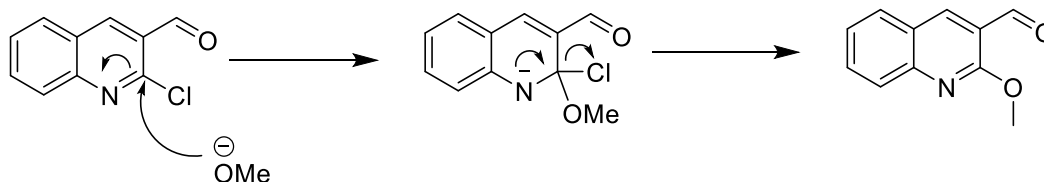


**Figure 2.5:** 75 MHz <sup>13</sup>C-NMR spectrum of compound **2.3a** in CDCl<sub>3</sub>.

#### 2.2.4 Synthesis of 6-substituted-2-methoxyquinoline-3-carbaldehydes

Subsequently, the quinoline intermediates **2.3a–e** were methoxylated at C-2 of quinoline scaffold to obtain the desired quinoline aldehydes **2.4a–e** in the yields ranging from 22% to 60%. A work done by Joshi and co-workers<sup>8</sup> involving the synthesis of quinoline derived compounds demonstrated that the resultant compounds showed moderate to good inhibitory activity against the *M. tuberculosis* strains. The study revealed that the replacement of the chlorine atom with methoxy group led to compounds with enhanced antibacterial and anti-tubercular activities<sup>8</sup>, further emphasizing the relevance of methoxy group for biological activity. In quinolines, the nucleophilic substitution occurs at the pyrido- rather than benzo- ring due to the nitrogen in the pyridine part of the quinoline acting as an electron sink. Herein,

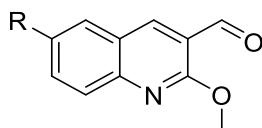
potassium hydroxide was treated with methanol and the reaction was left to stir for approximately 5 minutes at room temperature. The generated methoxide anion undergoes aromatic nucleophilic substitution to replace the chlorine atom at reflux temperature as shown in **Scheme 2.5**.



**Scheme 2.5:** Proposed reaction mechanism of nucleophilic substitution of chlorine by a methoxy group<sup>10</sup>.

When the reaction had completed, it was cooled down to room temperature and then precipitated it out by pouring it in ice-cold water to which the precipitate was collected using Buchner funnel. **Table 2.1** is showing the isolated yields for compounds **2.4a-e**.

**Table 2.1:** Isolated yields of compound **2.4a-e**.



Compound	R	Yield (%)
<b>2.4a</b>	H	40
<b>2.4b</b>	F	22
<b>2.4c</b>	Cl	34
<b>2.4d</b>	CH <sub>3</sub>	54
<b>2.4e</b>	OCH <sub>3</sub>	60

<sup>1</sup>H-NMR and <sup>13</sup>C-NMR was used to characterize compounds **2.4a-e**. For example, the <sup>1</sup>H-NMR spectrum of compound **2.4a** (**Figure 2.6**) shows a new singlet chemical shift at 4.18 ppm integrating for three protons and this confirmed the attachment of the methoxy group at C-2 of

the quinoline to form the desired compounds. Furthermore,  $^{13}\text{C}$ -NMR (**Figure 2.7**) shows 11 carbon signals with the methoxy carbon appearing at  $\delta$  53.9 ppm.

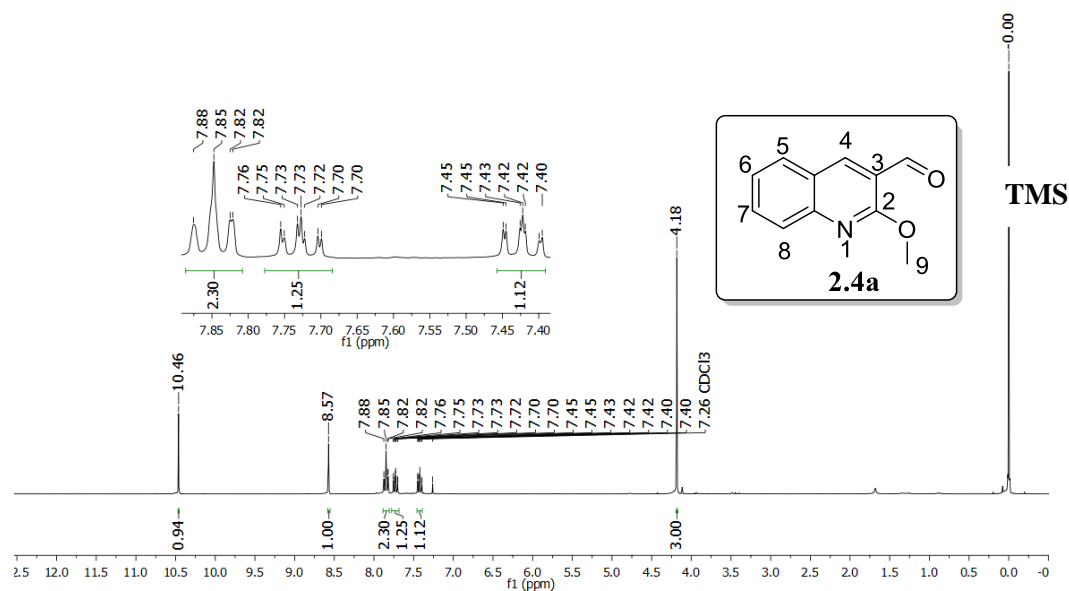


**Figure 2.6:** 300 MHz  $^1\text{H}$ -NMR spectrum of compound **2.4a** in  $\text{CDCl}_3$ .

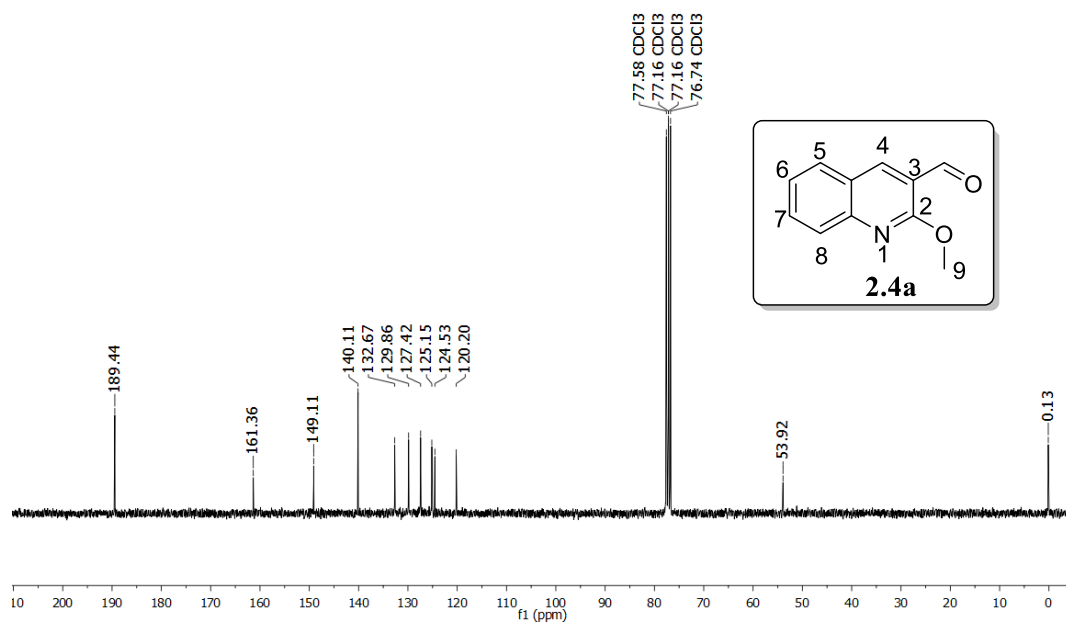
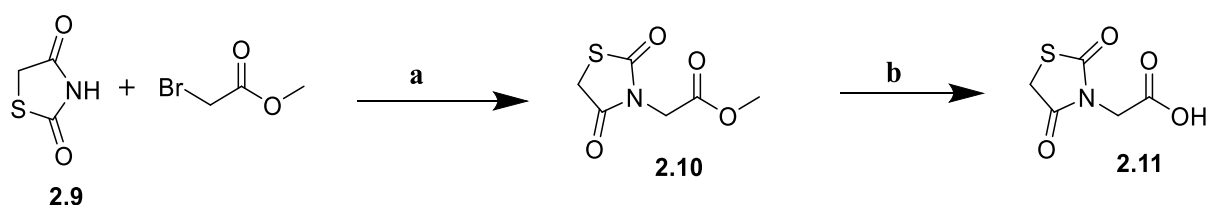


**Figure 2.7:** 75 MHz  $^{13}\text{C}$ -NMR spectrum of compound **2.4a** in  $\text{CDCl}_3$ .

### 2.2.5 Synthesis of 2,4-thiazolidinedione-carboxylic acid via the ester intermediate

Upon successful synthesis of the desired quinoline moiety (**2.4a-e**), the next task was to synthesize the 2,4-thiazolidinedione derivatives comprising of carboxylic acid (**2.11**). The synthesis of TZD-carboxylic (**2.11**) acid began with the reaction of commercially available TZD (**2.9**) with bromoacetyl methyl ester under basic reaction conditions to obtain TZD-ester (**2.10**) that was hydrolyzed using 48% HBr to obtain the desired acid (**2.11**) in 52% yield (**Scheme 2.6**).



**Scheme 2.6:** Reagents and conditions: a) NaH, DMF, 0–25 °C, 24 h; b) 48% HBr, 100 °C, 4 h.<sup>11</sup>

The <sup>1</sup>H-NMR (**Figure 2.8**) of compound **2.10** revealed a singlet signal at  $\delta$  4.25 ppm integrating for 2 protons consistent with the methylene adjacent to the carboxylic ester group, and additional singlet at  $\delta$  3.66 ppm with 3 protons confirming the presence of the methyl ester. The singlet signal at 3.93 ppm with 2 protons further confirmed the methylene of the TZD motif.

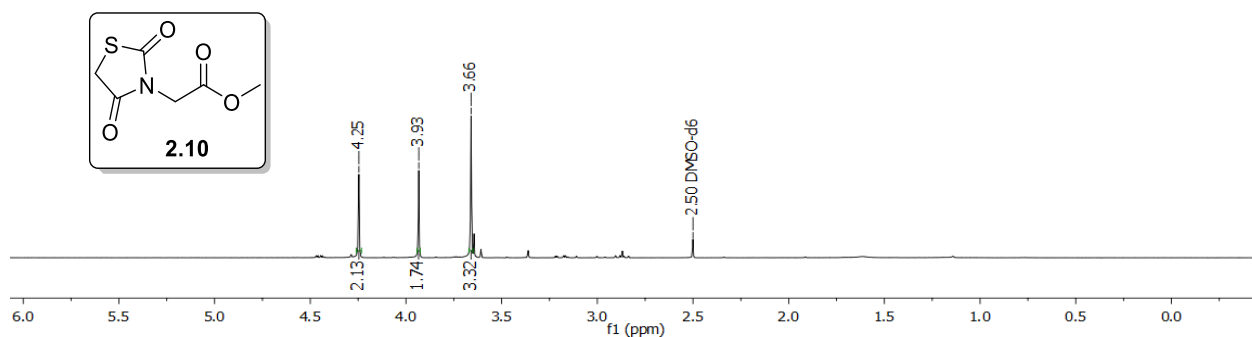


**Figure 2.8:** 300 MHz <sup>1</sup>H-NMR spectrum of compound **2.10** in DMSO-*d*<sub>6</sub>.

The  $^1\text{H-NMR}$  of compound **2.11** (Figure 2.9) shows the disappearance of methyl ester at chemical shift 3.66 ppm, and this confirmed the success of the hydrolysis. According to Abraham and co-workers, the signals due to  $-\text{OH}$  and  $-\text{NH}$  group are often not observed on  $^1\text{H-NMR}$  especially when DMSO is used as a solvent, and this is due to the proton exchange with DMSO<sup>12</sup>.

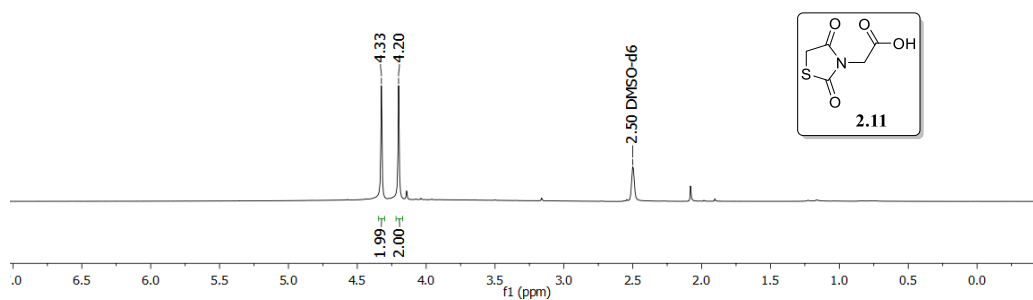


**Figure 2.9:** 300 MHz  $^1\text{H-NMR}$  spectrum of compound **2.11** in DMSO- $d_6$ .

The FT-IR (Figure 2.10) was employed to confirm the presence of  $-\text{OH}$  of the carboxylic acid. The broad band at  $3104\text{ cm}^{-1}$  was observed and attributed to the  $-\text{OH}$  of the carboxylic acid to which its respective carbonyl band was observed at  $1652\text{ cm}^{-1}$ . This further confirmed the success the hydrolysis of the ester (compound **2.10**) to the desired carboxylic acid, compound **2.11**. The bands at 1729 and  $1760\text{ cm}^{-1}$  represent the carbonyls of the TZD ring.

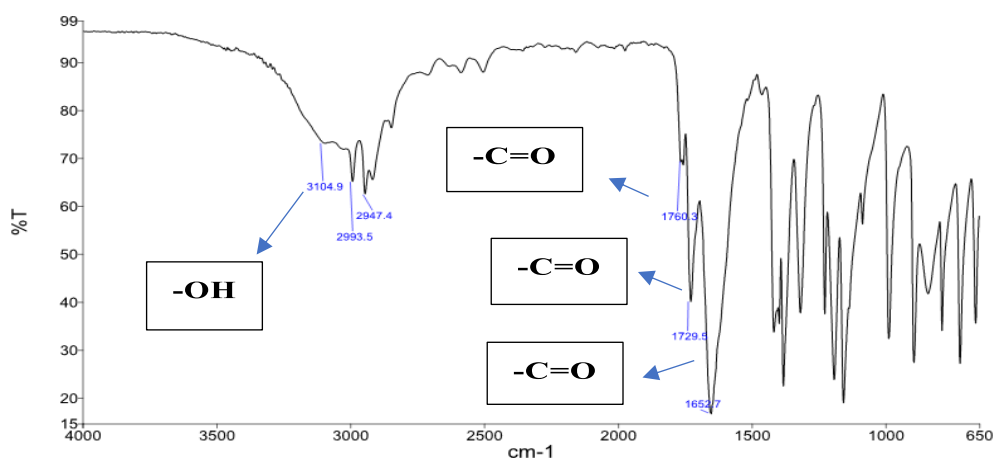


**Figure 2.10:** FT-IR spectrum of compound **7**.

Additionally,  $^{13}\text{C}$ -NMR (**Figure 2.11**) accounts for all 5 carbons of compound **2.11** with chemical shifts at  $\delta$  171.9 and 171.5 ppm attributed to the carbonyls of the TZD ring, and the signal at  $\delta$  168.1 ppm accounts for the carbonyl of the carboxylic acid. The carbon signal at  $\delta$  42.1 ppm is for the methylene attached to the electronegative nitrogen, hence is deshielded and appears downfield, whereas the signal at  $\delta$  34.1 ppm is attributed to methylene of the TZD core structure.

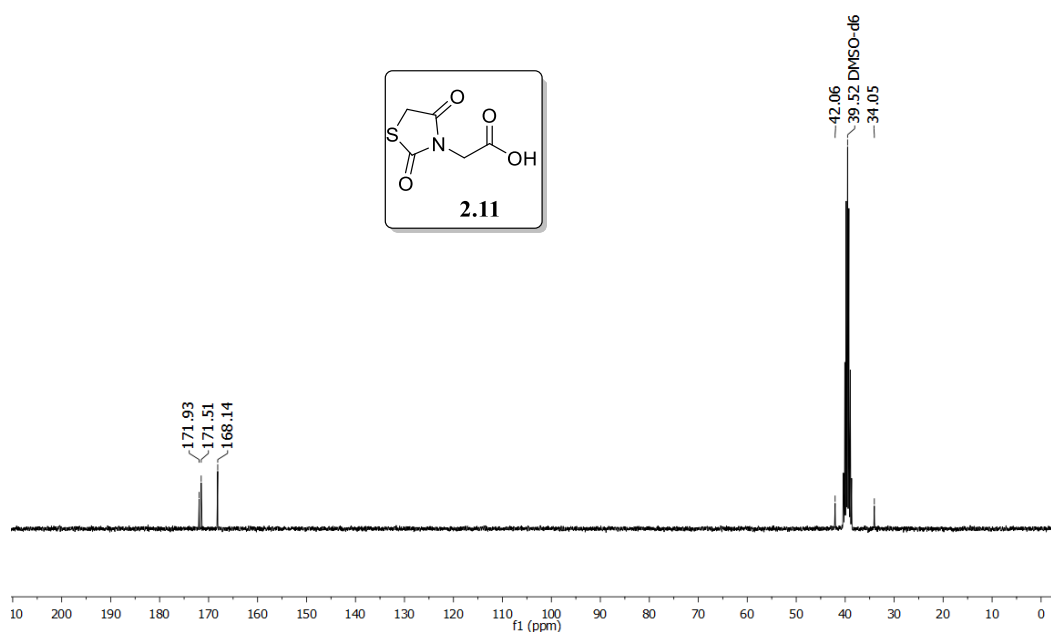
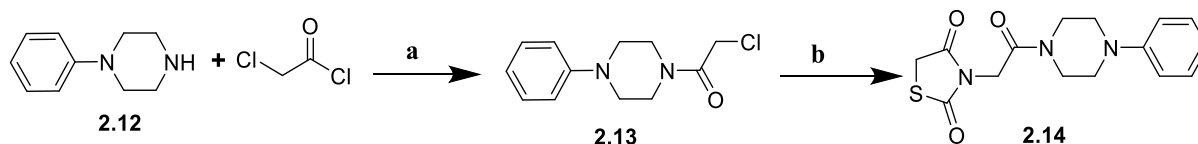


**Figure 2.11:** 75 MHz  $^{13}\text{C}$ -NMR spectrum of compound **2.11** in  $\text{DMSO-}d_6$ .

### 2.2.6 Synthesis of 2,4-thiazolidinedione-phenyl piperazine

The TZD-phenylpiperazine **2.14** was synthesized in two steps (**Scheme 2.7**), where step 1 involved nucleophilic acyl substitution of chloro-acetyl chloride with 1-phenylpiperazine to form intermediate **2.13**, which was treated with commercial 2,4-thiazolidinedione in step 2 to form compound **2.14**.



**Scheme 2.7:** Reagents and conditions: a) chloroacetyl chloride, Et<sub>3</sub>N, DCM, 0 °C, 1 h; b) 2,4 thiazolidinedione, K<sub>2</sub>CO<sub>3</sub>, acetone, 60–70 °C, 24 h.<sup>11</sup>

Likewise, spectroscopic analysis aided to confirm that compound **2.14** was successfully synthesized. The <sup>1</sup>H-NMR (**Figure 2.12**) of the intermediate (**2.13**) was obtained and the signals observed in the region δ 6.84 – 7.24 ppm confirmed the presence of the aromatic ring, and the singlet signal resonating at δ 4.05 ppm confirmed the presence of the methylene protons adjacent to the carbonyl group. Lastly the presence of the piperazine ring is observed with methylene signals resonating at δ 3.68 and 3.16 ppm.

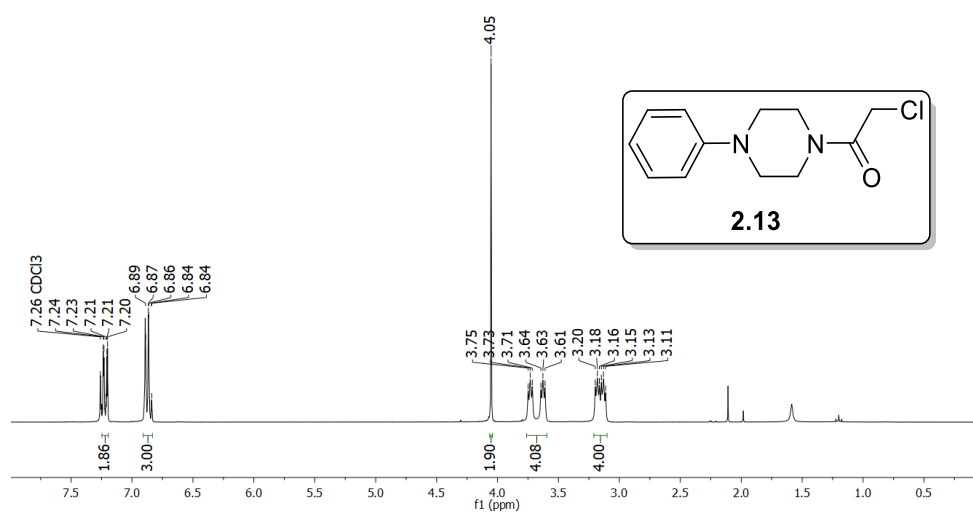


**Figure 2.12:** <sup>1</sup>H-NMR spectrum of compound **2.13** in CDCl<sub>3</sub>.

Compound **2.14** was characterized using <sup>1</sup>H and <sup>13</sup>C NMR as well as DEPT135. From the <sup>1</sup>H-NMR (**Figure 2.13**), the new singlet signal at δ 4.45 ppm confirmed the presence of the methylene protons of the TZD ring, whereas all the other signals remain relatively in the same region.

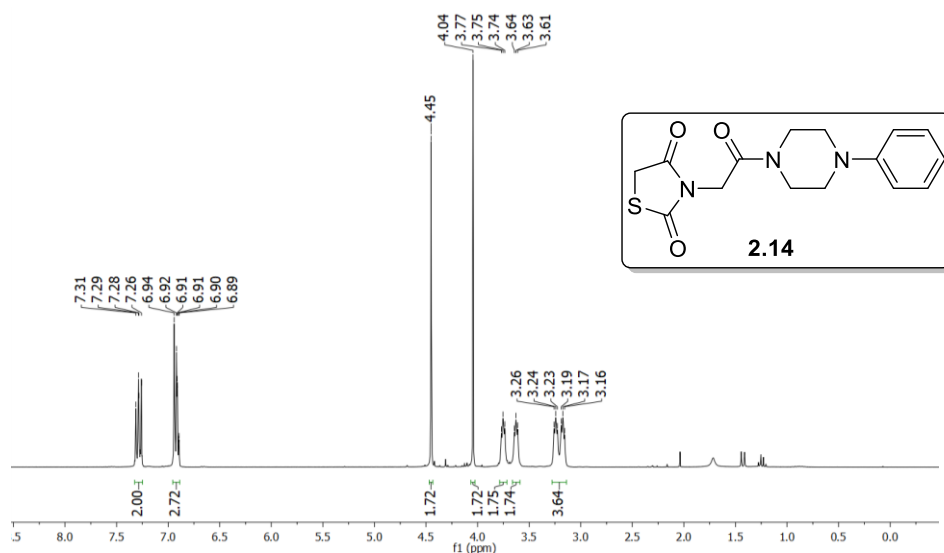


**Figure 2.13:** 300 MHz  $^1\text{H}$ -NMR of compound **2.14** in  $\text{CDCl}_3$ .

Furthermore, the  $^{13}\text{C}$ -NMR (**Figure 2.14**) showed the 3 characteristic signals of the TZD ring which are 2 carbonyl signals appearing at  $\delta$  171.7 and 171.3 ppm and the methylene signal at  $\delta$  34.0 ppm, whereas the amide carbonyl adjacent to the piperazine ring was observed at  $\delta$  162.9 ppm with its methylene appearing at  $\delta$  34.1 ppm. Lastly, the aromatic ring signals was observed in the expected region of  $\delta$  116.9 – 150.9 ppm, and the signals at  $\delta$  42.4 – 49.6 ppm confirmed the methylene carbons of the piperazine ring.

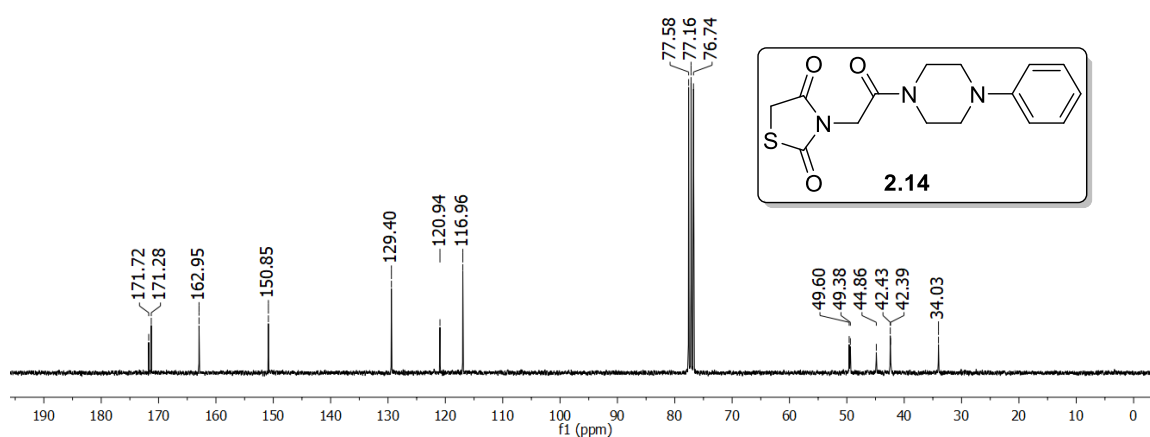


**Figure 2.14:** 75 MHz  $^{13}\text{C}$ -NMR spectrum of compound **2.14** in  $\text{CDCl}_3$ .

Further characterization using DEPT135 NMR experiment (**Figure 2.15**) confirmed the presence of  $6 \times \text{CH}_2$  (negative signals) and the expected  $3 \times \text{CH}$  (positive signals) of the aromatic ring.

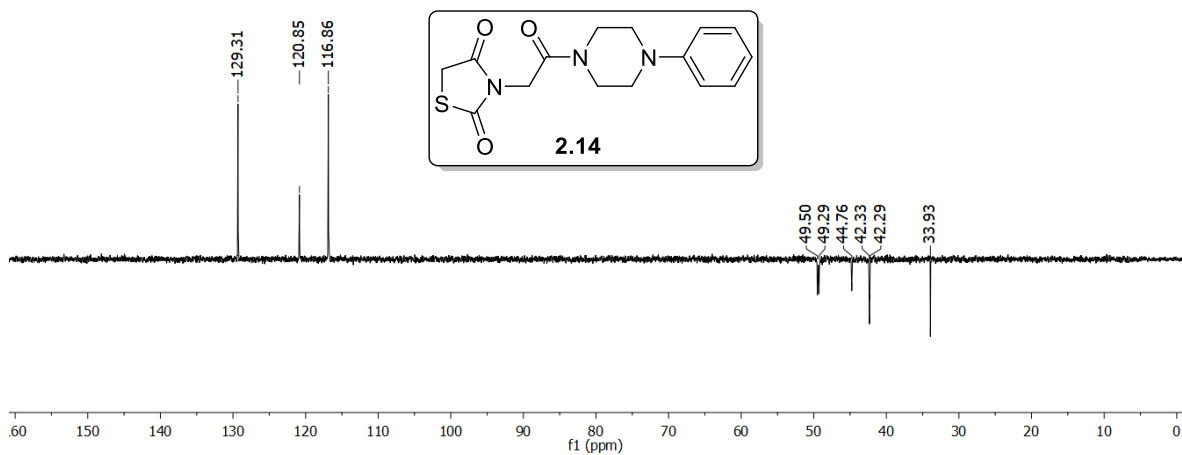
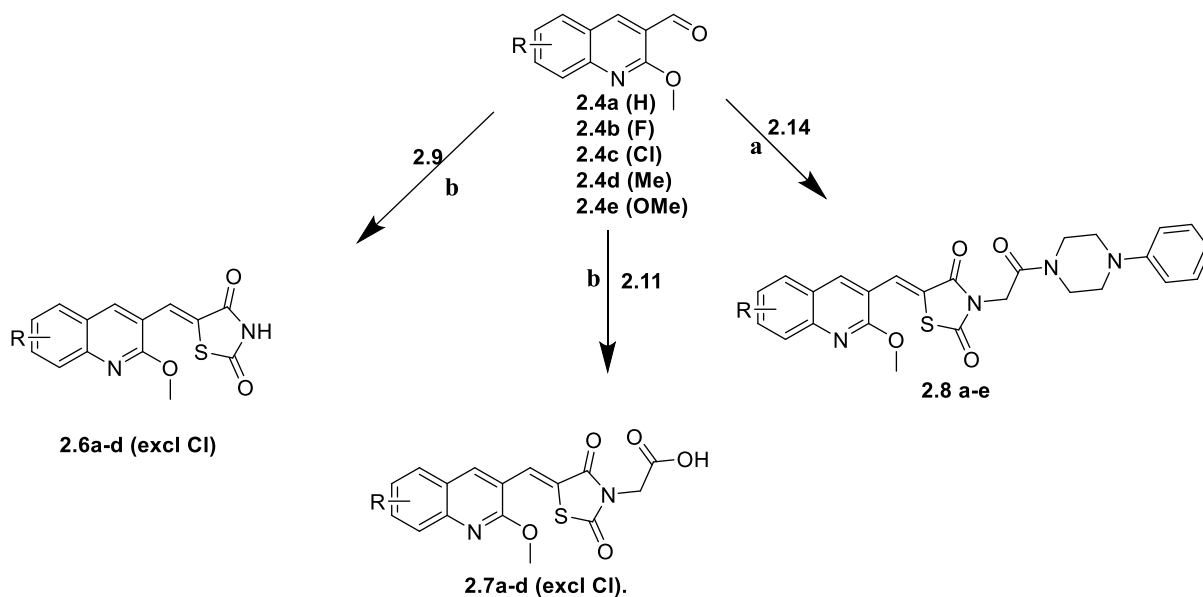


**Figure 2.15:** DEPT135 NMR spectrum of compound **2.14** with unreferenced solvent peak.

### 2.2.7 Hybridization of quinoline-aldehydes and 2,4-Thiazolidinedione via Knoevenagel condensation

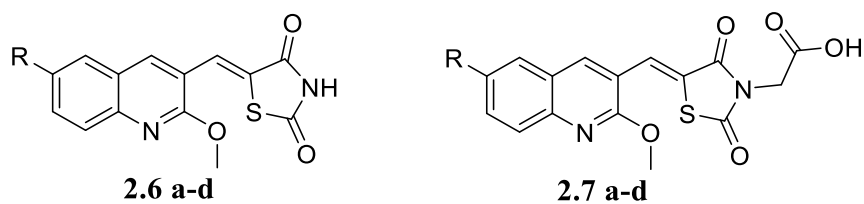
Upon successful synthesis of various 3-quinolinecarbaldehyde derivatives with a methoxy group at the position C-2 of the quinoline (**2.4a-e**), the next step was to couple these 3-quinolinecarbaldehyde derivatives **2.4a-e** with a set of 2,4-thiazolidinedione derivatives **2.9**, **2.11** and **2.14** via Knoevenagel condensation (**Scheme 2.8**).



**Scheme 2.8:** *Reagents and conditions:* a) Anhydrous ethanol, piperidine catalyst (1.5 eq), 80 °C, 6 h. b) Anhydrous toluene, 2-3 drops of glacial acetic acid, piperidine catalyst (1.5 eq), 105 °C, 6h.

The hybridization of the quinoline-carbaldehydes with TZD derivatives was performed in two separate solvent media. This was done to induce the precipitation of our target compounds. From just mere trial run reactions under weak basic conditions, it was observed that polar solvents favored the precipitation of non-polar compounds whilst non-polar solvent favored the precipitation of polar compound. Therefore, for the synthesis of compounds **2.6** and **2.7** derivatives, dry toluene was used as the solvent of choice considering that these compounds are relatively polar, thus using a non-polar solvent medium greatly induced the precipitation. In ethanol, precipitation of these compounds was not achieved and isolation by liquid-liquid extraction using ethyl acetate yielded crude products which were difficult to purify on silica gel chromatography.

**Table 2.2:** Isolated yields of compounds **2.6** and **2.7**.



Compound	R	Yield (%)
<b>2.6a</b>	H	41
<b>2.6b</b>	F	52
<b>2.6c</b>	CH <sub>3</sub>	49
<b>2.6d</b>	OCH <sub>3</sub>	20
<b>2.7a</b>	H	29
<b>2.7b</b>	F	36
<b>2.7c</b>	CH <sub>3</sub>	39
<b>2.7d</b>	OCH <sub>3</sub>	46

Spectroscopic tools were used to characterize these achieved compounds. As an illustration of compounds **2.6** derivatives, the <sup>1</sup>H-NMR spectrum (**Figure 2.16**) of compound **2.6a** was used as a representative, and it showed the disappearance of the aldehydic proton signal observed for **2.4a** and the methylene signal of the TZD ring and the appearance of the new singlet signal (H<sub>1</sub>) at δ 7.87 ppm consistent with vinylic proton attesting the success of Knoevenagel condensation. Furthermore, the broad signal with one proton at δ 12.69 ppm confirmed the presence of –NH of the TZD. The other signals of the quinoline moiety remained relatively unchanged.

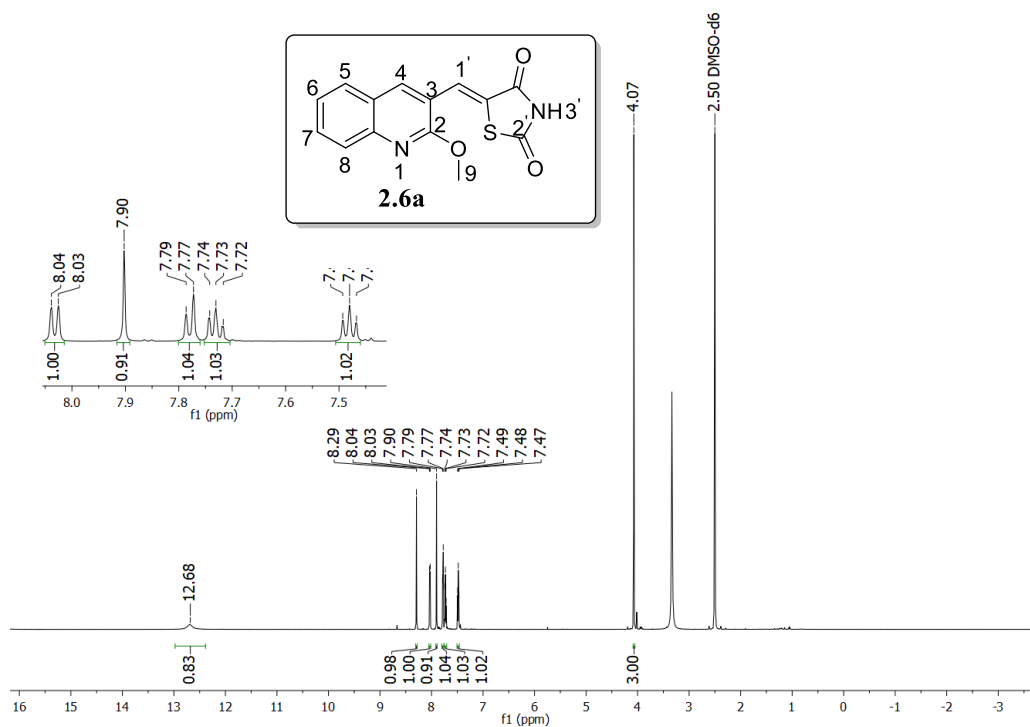


**Figure 2.16:** 600 MHz <sup>1</sup>H-NMR spectrum of compound **2.6a** in DMSO-*d*<sub>6</sub>.

<sup>13</sup>C-NMR spectrum (**Figure 2.17**) of compound **2.6a** further confirmed the presence of all the expected 14 carbons with carbonyl groups of the TZD ring resonating at  $\delta$  167.8 and 167.2 ppm and aromatic signals at the region  $\delta$  118.1-145.9 ppm. The methoxy signal was still observed at  $\delta$  4.07 ppm.

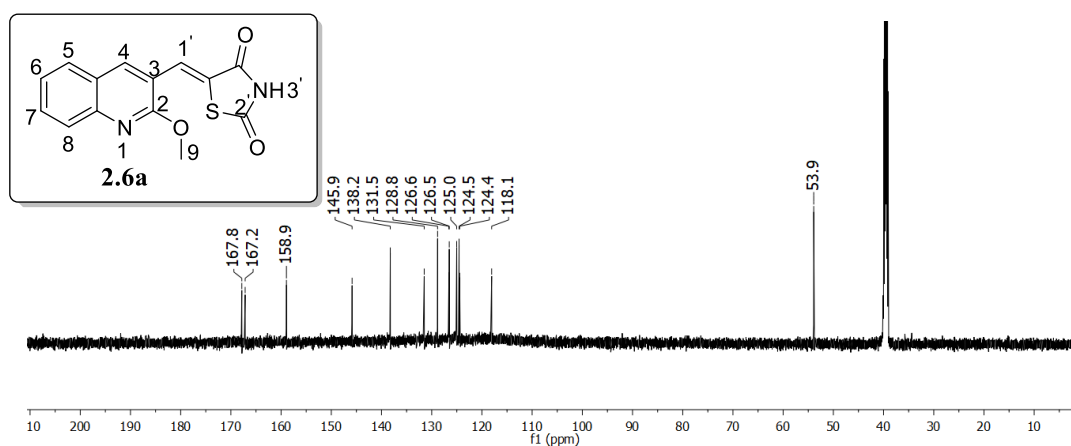


**Figure 2.17:** 150 MHz <sup>13</sup>C-NMR of compound **2.6a** in DMSO-*d*<sub>6</sub>.

The FT-IR spectrum (**Figure 2.18**) of compound **2.6a** confirmed the presence of the C-H stretch of the methoxy group at the 2993 cm<sup>-1</sup>. The bands at 1742 and 1688 cm<sup>-1</sup> were due to

the two carbonyls of the TZD ring, and the key band at  $2796\text{ cm}^{-1}$  confirmed the  $\text{CH}_3$  of the methoxy group.

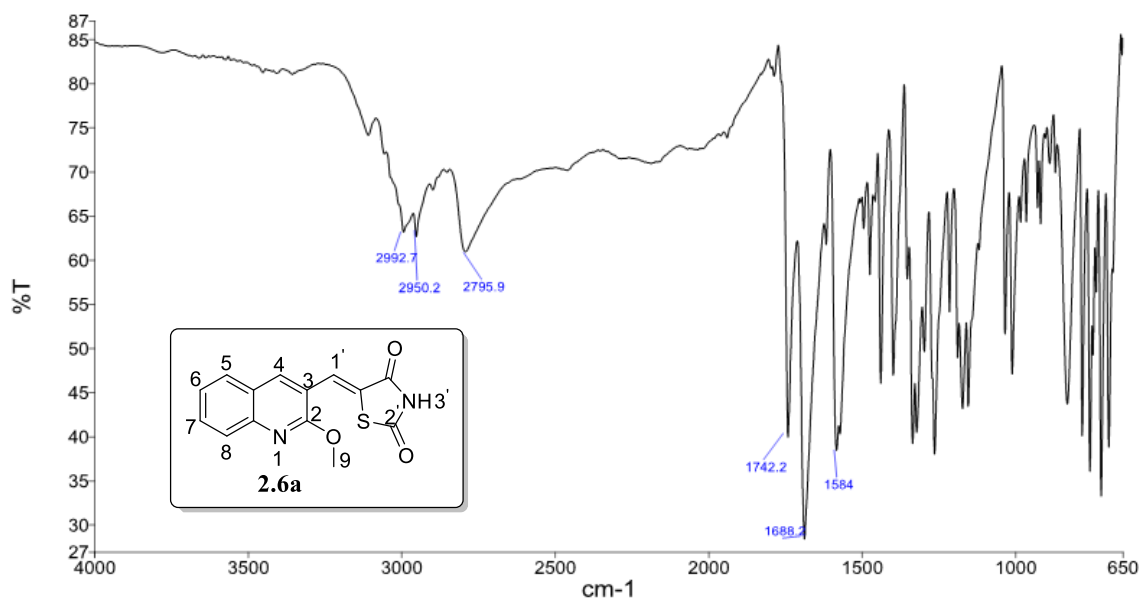


**Figure 2.18:** FT-IR spectrum of compound 2.6a.

Additionally, the high-resolution mass spectroscopy also confirmed the successful synthesis of compound 2.6a with the pseudo molecular ion peak observed at  $m/z$  287.0488 (Figure 2.19).

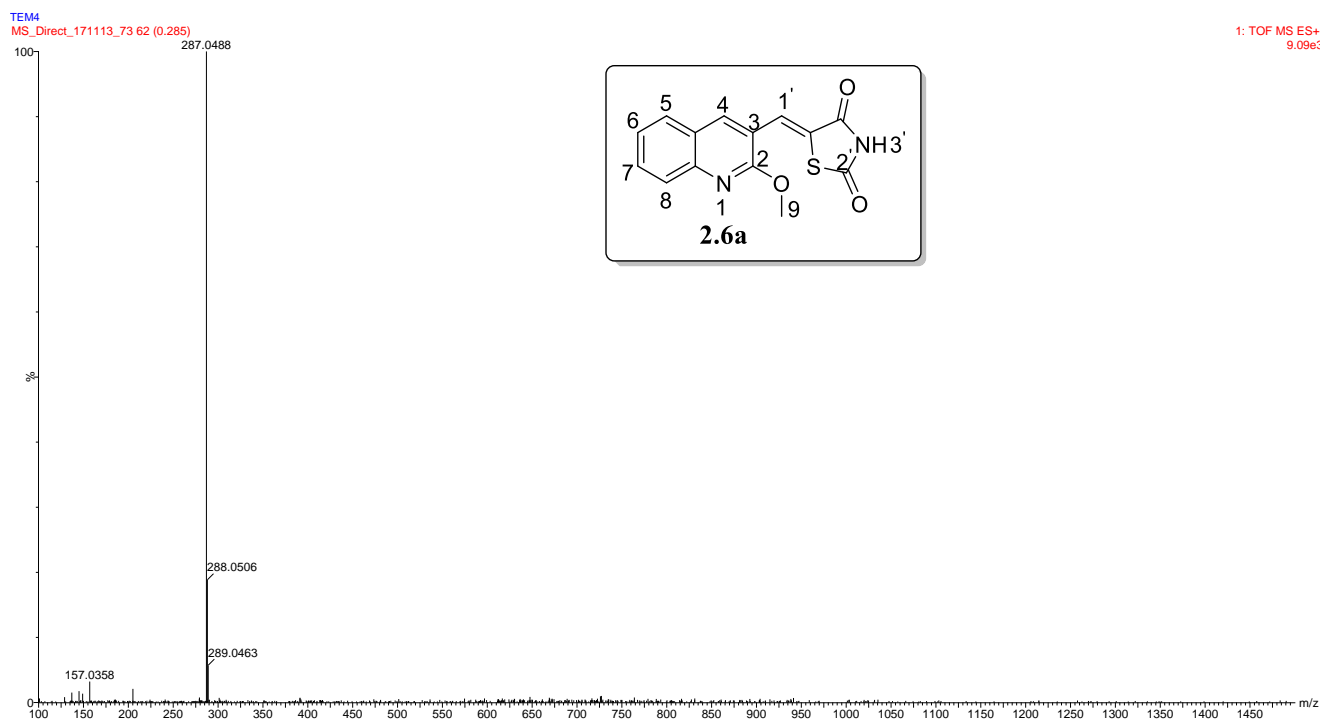


**Figure 2.19:** HRMS spectrum of compound 2.6a

Similarly, compounds **2.7** were characterized with common spectroscopic techniques. Using compound **2.7a** as an example, it was observed from the  $^1\text{H-NMR}$  spectrum (**Figure 2.20**) that the hybridization of compound **2.4a** and compound **2.11** via Knoevenagel condensation was successful with the appearance of the characteristic signal ( $\text{H}_{1'}$ ) at  $\delta$  8.01 ppm confirming the newly formed vinylic proton while the activated methylene group of the TZD ring, compound **2.11**, is no longer observed.

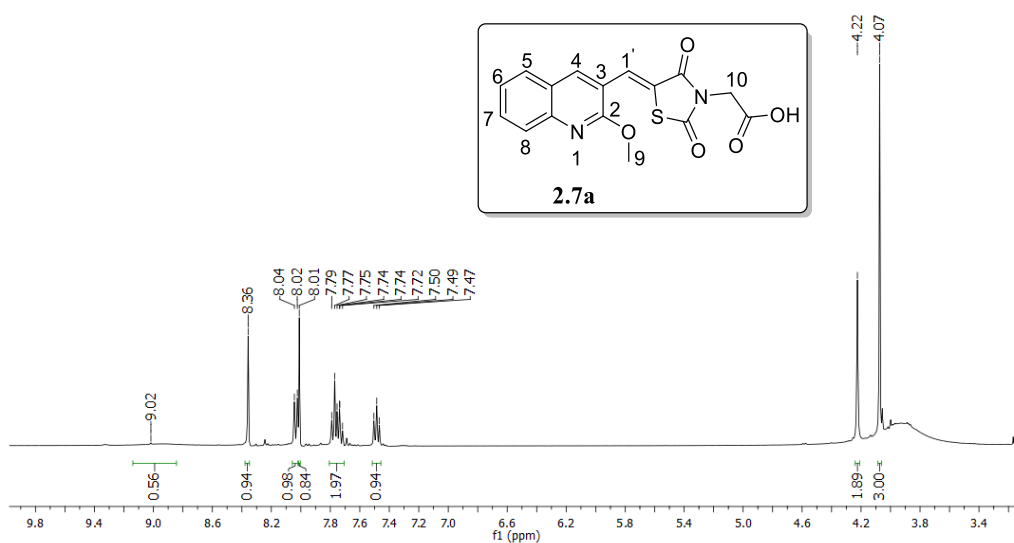


**Figure 2.20:** The 400 MHz  $^1\text{H-NMR}$  spectrum of compound **2.7a** in  $\text{DMSO-}d_6$ .

Due to proton exchange of the carboxylic acid  $-\text{OH}$  with  $\text{DMSO-}d_6$ , the  $-\text{OH}$  signal is hardly observed as it is too broad. Therefore, the FT-IR was employed to confirm  $-\text{OH}$  functionality. FT-IR spectrum (**Figure 2.21**) of compound **2.7a** shows the broad  $-\text{OH}$  band at  $3409\text{ cm}^{-1}$  confirming the presence of the carboxylic acid with its respective carbonyl band appearing at  $1588\text{ cm}^{-1}$ . The bands at  $1731$  and  $1681\text{ cm}^{-1}$  were attributed to the carbonyls of the TZD ring. Lastly the band at  $2950\text{ cm}^{-1}$  is assigned to the  $\text{CH}_3$  of the methoxy group on the quinoline moiety.

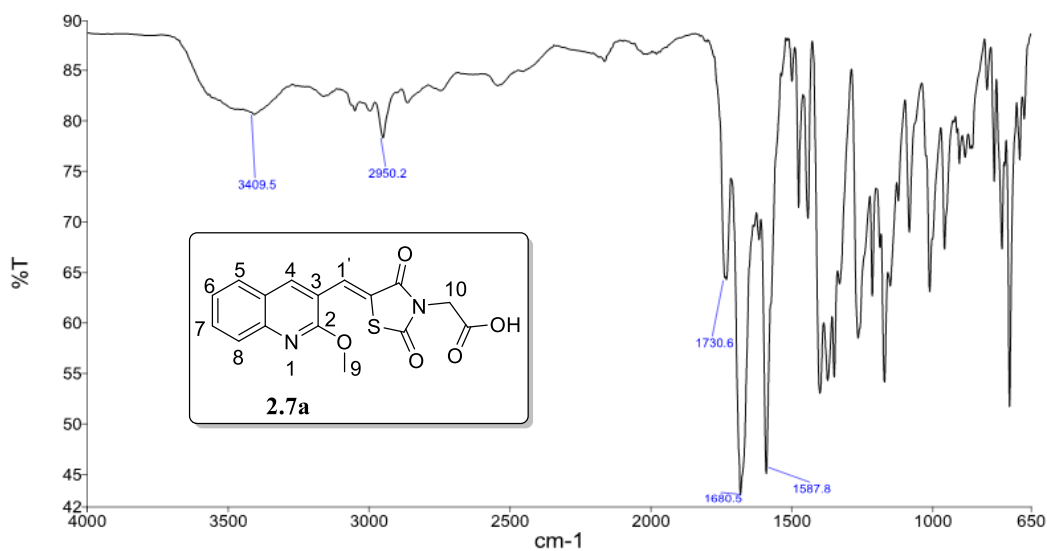


**Figure 2.21:** FT-IR spectrum of compound **2.7a**.

In addition,  $^{13}\text{C}$ -NMR experiment accounted for all the expected 16 carbon signals. **Figure 2.22** shows the  $^{13}\text{C}$ -NMR of compound **2.7a** with carbonyls of the TZD ring resonating at  $\delta$  168.4 and 167.5 ppm, and the carbonyl signal for the carboxylic acid resonating at  $\delta$  165.5 ppm. All the other signals remained unchanged and accounted for all the expected signals.

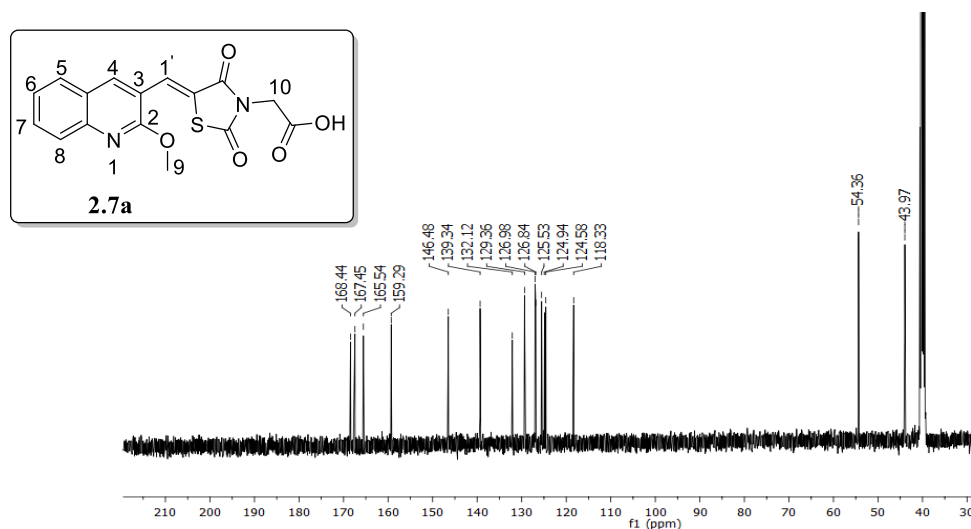


**Figure 2.22:** 100 MHz  $^{13}\text{C}$ -NMR spectrum of compound **2.7a** in  $\text{DMSO-d}_6$ .

After confirming the skeletal structure of compound **2.7a** using  $^1\text{H}$ - and  $^{13}\text{C}$ -NMR, and the expected key functional groups using FT-IR, the exact mass observed (**Figure 2.23**) further confirmed the structure of compound **2.7a** with the pseudo molecular ion peak at  $m/z$  345.0547.

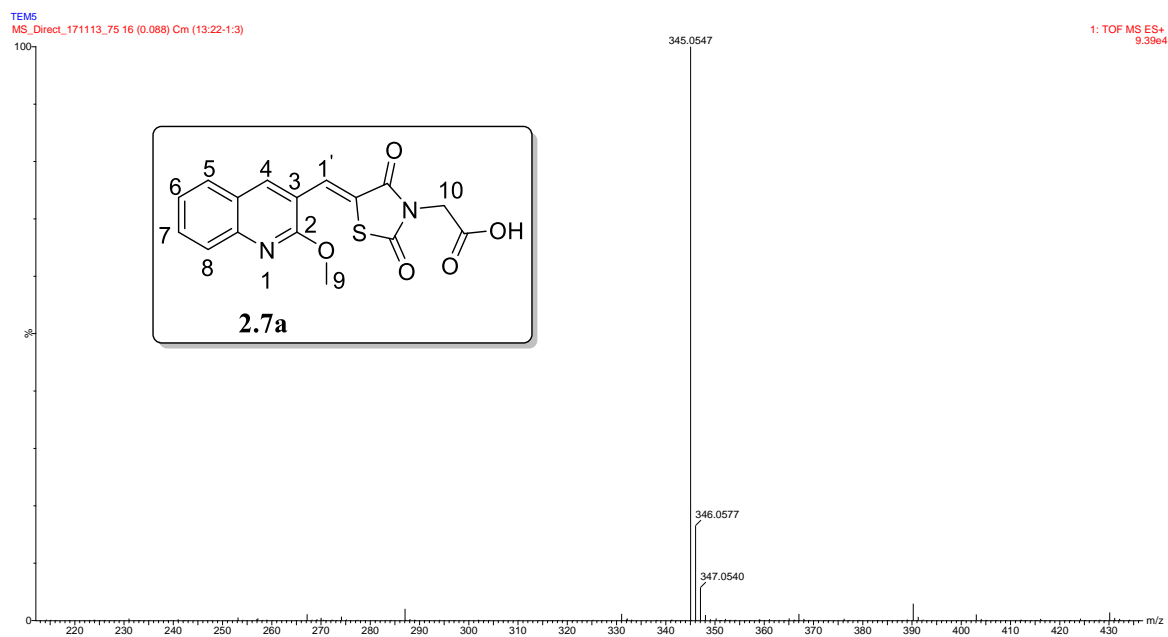
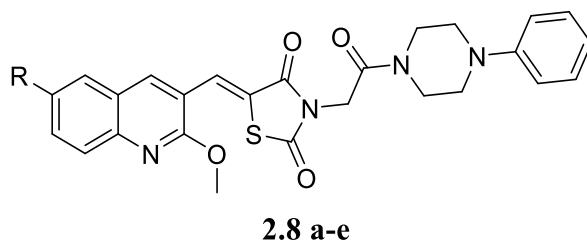


**Figure 2.23:** HRMS spectrum of compound **2.7a**.

For the synthesis of compound **2.8** derivatives (**Scheme 2.8**), anhydrous ethanol was used as the solvent medium under weak basic conditions. The reaction of compound **2.14** with **2.4** derivatives in the presence of piperidine as a base in anhydrous ethanol yielded compounds **2.8** as yellow precipitate. The resulting compounds were isolated in yields in the range of 16–40% (**Table 2.3**).

**Table 2.3:** Isolated yields of compounds **2.8**.



Compound	R	Yield (%)
<b>2.8a</b>	H	40
<b>2.8b</b>	F	27
<b>2.8c</b>	Cl	16
<b>2.8d</b>	CH <sub>3</sub>	22
<b>2.8e</b>	OCH <sub>3</sub>	34

All the synthesized compounds **2.8a–e** were characterized using the common spectroscopic techniques. With compound **2.8a** as representative example, the <sup>1</sup>H-NMR spectrum (**Figure 2.24**) showed the absence of the aldehydic proton signal which was observed in the spectrum of **2.4a**. Furthermore, the disappearance of the methylene protons signal of compound **2.14** confirmed the successful hybridization of these molecules via Knoevenagel condensation to form **2.8a–e**. The aromatic signals in the region  $\delta$  6.81–8.42 ppm accounted for all aromatic protons, and the characteristic signal at  $\delta$  8.06 ppm integrating for 1H was attributed to vinylic proton. The methylene protons adjacent to nitrogen were observed at  $\delta$  4.70 ppm. The methoxy group remained unchanged at  $\delta$  4.10 ppm, the presence of the piperazine ring is observed with methylene signals resonating at  $\delta$  3.66 and 3.18 ppm.

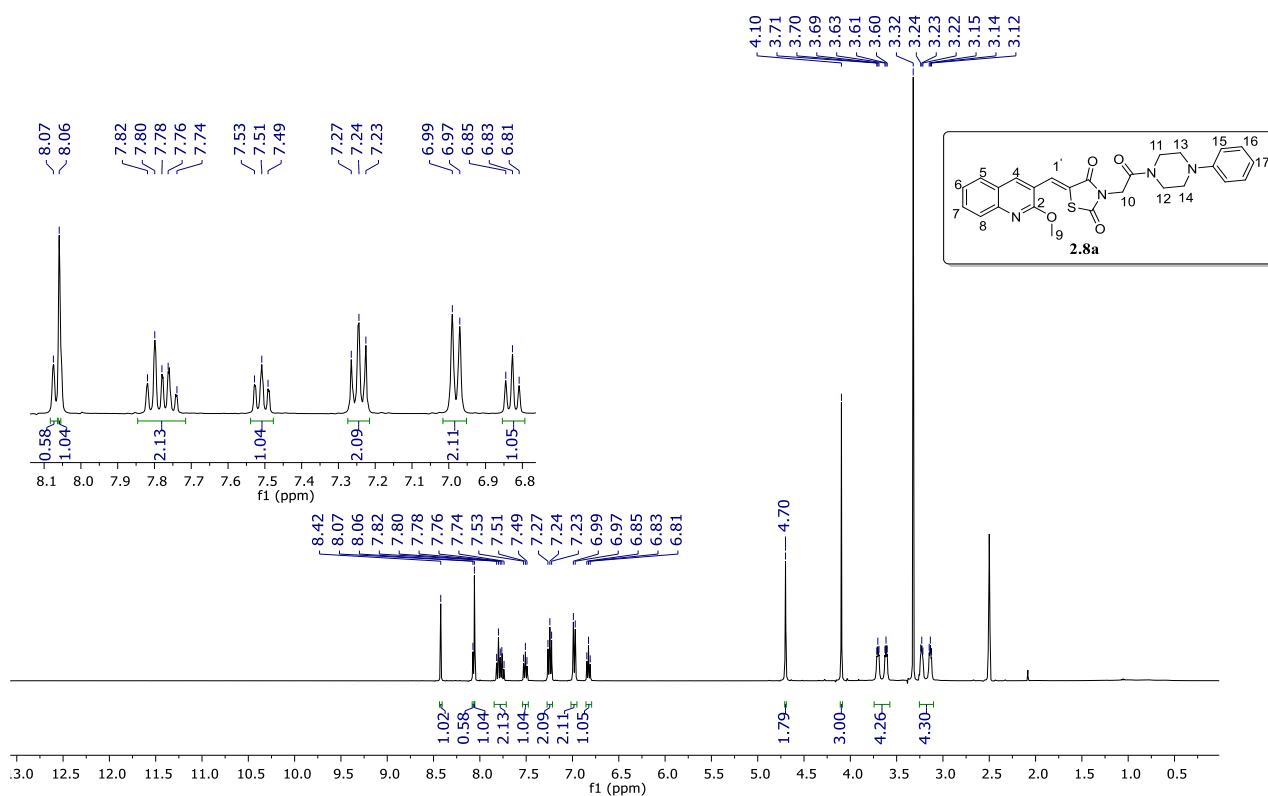


**Figure 2.24:** The 400 MHz <sup>1</sup>H-NMR spectrum of compound **2.8a** in DMSO-*d*<sub>6</sub>.

After confirming all the protons of compound **2.8a** with <sup>1</sup>H-NMR experiment, the <sup>13</sup>C-NMR spectrum (**Figure 2.25**) of compound **2.8a** confirmed its structural identity with all the carbon signals accounted for and the carbonyl signals of the TZD ring were observed at  $\delta_c$  167.6 and 165.6 ppm, and the signal at  $\delta_c$  163.7 ppm attributed to “linker” carbonyl linking 1-(phenyl)piperazine and TZD ring. The carbon signal at  $\delta_c$  54.4 ppm was attributed to the methoxy group. The signals appearing upfield in the range of  $\delta_c$  49.1–42.1 ppm are attributed to the CH<sub>2</sub> of the piperazine unit, which were further verified by DEPT135 (**Figure 2.26**) experiment, and further showed all the 9 positive signals representing the –CH on the aromatic region  $\delta$  139.5 - 116.5 ppm. Lastly, all the 5 negative signals ranging from  $\delta_c$  49.1–42.1 ppm accounted for all 5 methylene protons found in compound **2.8a**.

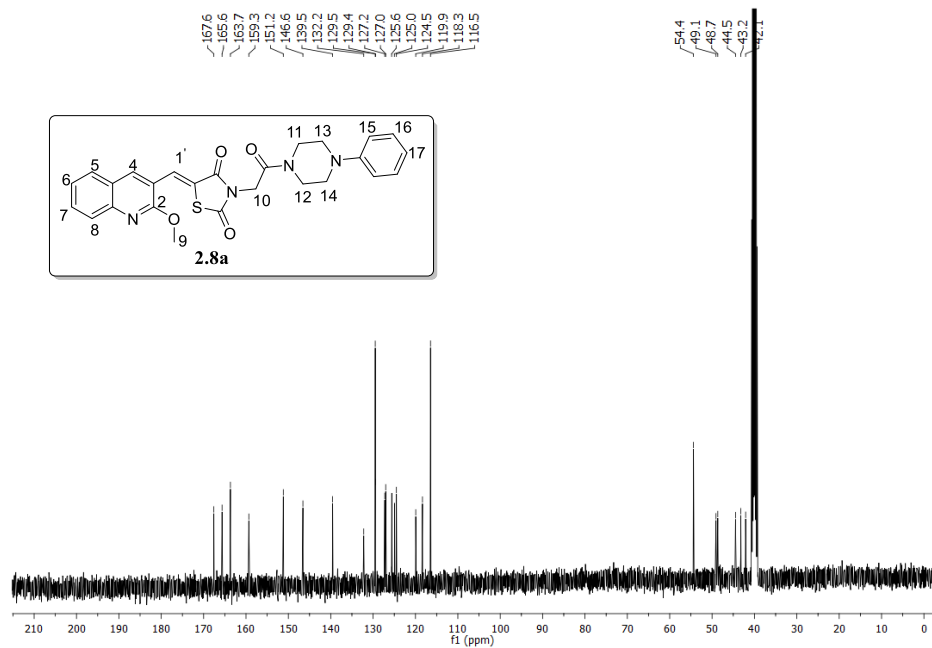


**Figure 2.25:** The 100 MHz  $^{13}\text{C}$ -NMR spectrum of compound **2.8a** in DMSO- $d_6$ .

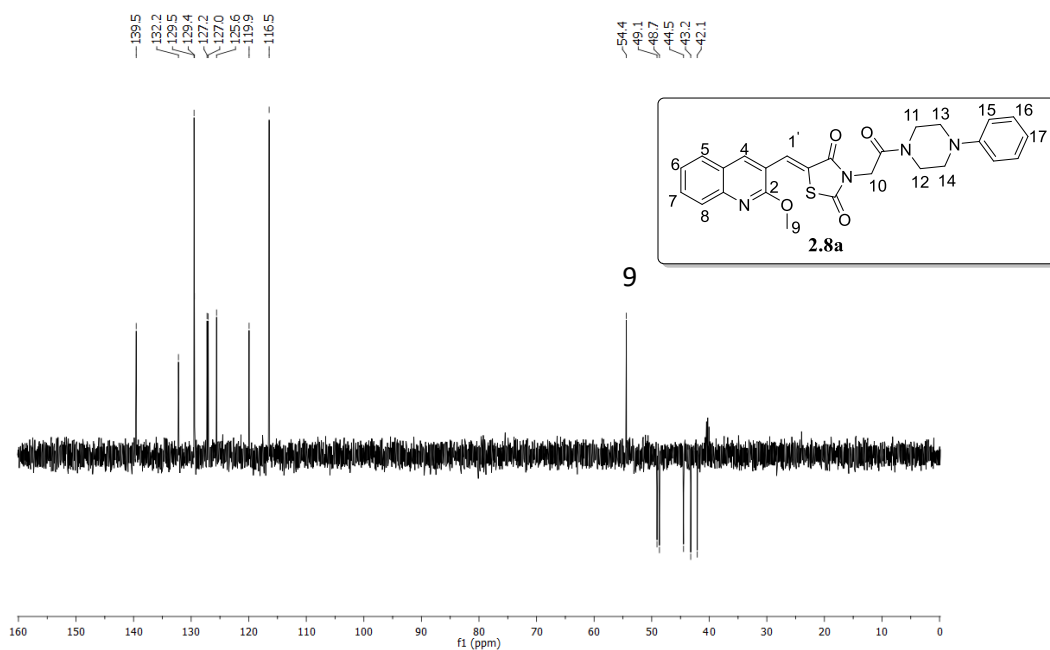


**Figure 2.26:** DEPT135 spectrum of compound **2.8a** in an unreferenced DMSO- $d_6$ .

Additionally, HRMS experiment was conducted to further confirm the identity of compound **2.8a** by obtaining its mass and elemental composition. In **Figure 2.27**, which is a high-resolution mass spectrum, it can be observed that the expected elemental composition of compound **2.8a**, which is  $C_{26}H_{24}N_4O_4S$ , was confirmed using mass spectroscopy, as the obtained elemental composition was  $C_{26}H_{25}N_4O_4S$ , with the extra H being due to the M+H ionization method. Furthermore, the expected molecular ion peak at  $m/z$  489.1596 representing the M+H ionization was also observed.

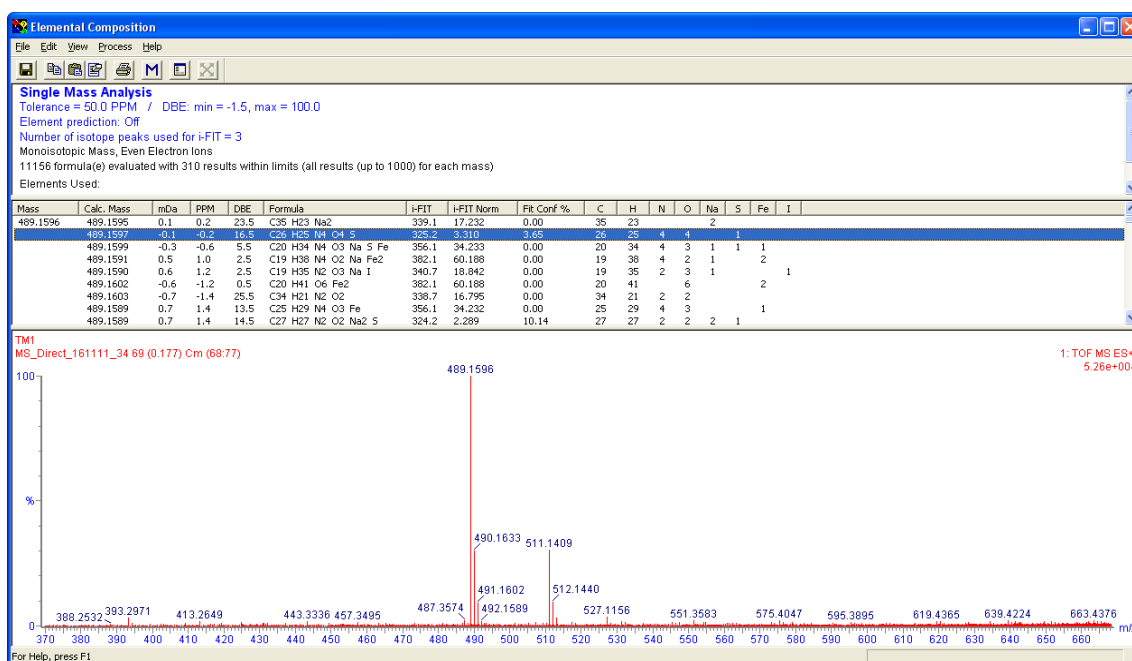


**Figure 2.27:** HRMS spectrum of compound **2.8a**.

## 2.3 CONCLUSIONS

In conclusion, the synthesis of the novel target compounds **2.6**, **2.7**, and **2.8** derivatives were achieved by the multi step reactions that were discussed above. Chromatographic techniques aided us to monitor the reaction progress, whilst the spectroscopic techniques were employed to characterize these achieved compounds. From the spectroscopic evidence presented in this study, conclusion can be drawn that the overall objectives and aims of this project were met as

the synthesis of the desired quinolinyl-thiazolidinedione derivatives hybrids was successful. Thereafter, these compounds were progressed to biological screening against *Mtb*, *P. falciparum*, and HeLa cell line to further satisfy the aims of this study, which will be discussed in Chapter 3.

## 2.4 REFERENCES

1. Jain, P. P., Degani, M. S., Raju, A., Ray, M. & Rajan, M. G. R., *Bioorg. Med. Chem. Lett.*, **2013**, 23, 6097–6105.
2. Jain, P. P., Degani, M. S., Raju, A., Anantram, A., Seervi, M., Sathaye, S., Ray, M., Rajan, M. G. R., *Bioorg. Med. Chem. Lett.*, **2016**, 26, 645–649.
3. Shaikh, F. M., Patel, N. B. & Rajani, D., *Indian J. Biotech. Pharm. Res.*, **2013**, 1, 496–503.
4. Alegaon, S. G., Alagawadi, K. R., Sonkusare, P. V., Chaudhary, S. M., Dadwe, D. H., Shah, A. S., *Bioorg. Med. Chem. Lett.*, **2012**, 22, 1917–1921.
5. Meth-Cohn, O. & Stanforth, S. P., *Compr. Org. Synth.*, **1991**, 2, 777–794.
6. Aneesa, F., Rajanna, K. C., Reddy, K. R., Ali, M. M., and Kumar, Y. A., *Synth. React. Inorg. Met. Org. Nano-Met. Chem.*, **2015**, 45, 651–659.
7. Li, J. J. Vilsmeier–Haack reaction. in *Name Reactions: A Collection of Detailed Mechanisms and Synthetic Applications Fifth Edition*, ed. Li, J. J., Springer International Publishing, **2014**. p 615-616.
8. Joshi, S. D., More, U. A., Parkale, D., Aminabhavi, T. M., Gadad, A. K., Nadagouda, M. N., and Jawarkar, R., *Med. Chem. Res.*, **2015**. 24, 3892–3911.
9. Kwan, E. E., Zeng, Y., Besser, H. A., and Jacobsen, E. N., *Nat. Chem.*, **2018**. 10, 917.
10. Clayden, J., Greeves, N., Warren, S., and Wothers, P. *Organic Chemistry*. Oxford University Press, **2000**, Ch. 23, p 589-590.

11. Sharma, R. K., Younis, Y., Mugumbate, G., Njoroge, M., Gut, J., Rosenthal, P. J., and Chibale, K., *Eur. J. Med. Chem.*, **2015**, 90, 507–518.
12. Abraham, R. J., Byrne, J. J., Griffiths, L., and Perez, M., *Magn. Reson. Chem.*, **2006**, 44, 491–509.

## CHAPTER THREE

### BIOLOGICAL EVALUATION OF THE TARGET COMPOUNDS

#### 3.1 Introduction

This chapter describes the *in vitro* biological evaluation against *Mycobacterium tuberculosis* strain (H37Rv), chloroquine-sensitive strain 3D7 of *Plasmodium falciparum*, and HeLa (human cervix adenocarcinoma) cell line. The susceptible *M. tuberculosis* H37Rv strain is widely used in research community since it can retain its virulence in the laboratory. The publication of the whole genome sequence of H37Rv by Stewart and co-workers in 1998<sup>1</sup> has led into insights into the biology, metabolism and evolution of this infectious pathogen. The *P. falciparum* 3D7 is a widely used strain in malarial research because its genome has been fully sequenced<sup>2</sup>, thus provides new exciting possibilities for designing novel potent anti-malarial drugs which target specific pathways. Despite being cancerous, HeLa cell line has been widely used as cellular model to measure human cytotoxicity of bioactive drug molecules and they are easy to grow in the laboratory. The biological screening assays were conducted in collaboration with following laboratories: 1) Biochemistry and Microbiology Department, Rhodes University – Associate Professor Heinrich Hoppe; 2) SAMRC/NHLS/UCT Molecular Mycobacteriology Research Unit, Department of Pathology, University of Cape Town – Associate Professor Digby Warner.

#### 3.2 Biological results and discussion

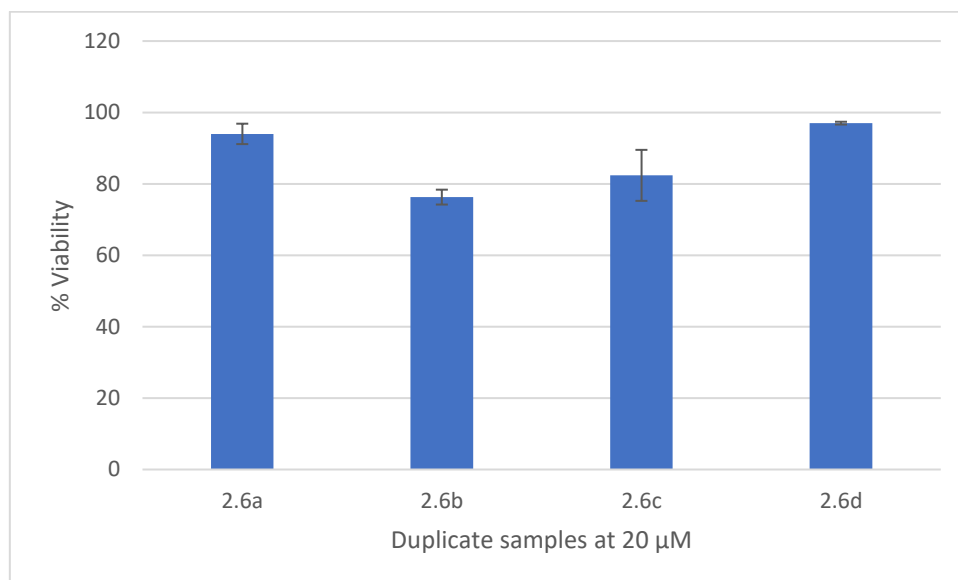
In line with the aims and objectives of this project, the synthesized compounds in this study were biologically evaluated *in vitro* for their inhibitory activities against *M. tuberculosis* (H37Rv), and *P. falciparum* (3D7) strains with rifampicin (RMP) and chloroquine (CQ) were

included as control drugs, respectively. Cytotoxicity effects of these compounds were evaluated on HeLa cell line with emetine which was utilized as a standard.

### 3.2.1 Anti-plasmodial activity of the target compounds

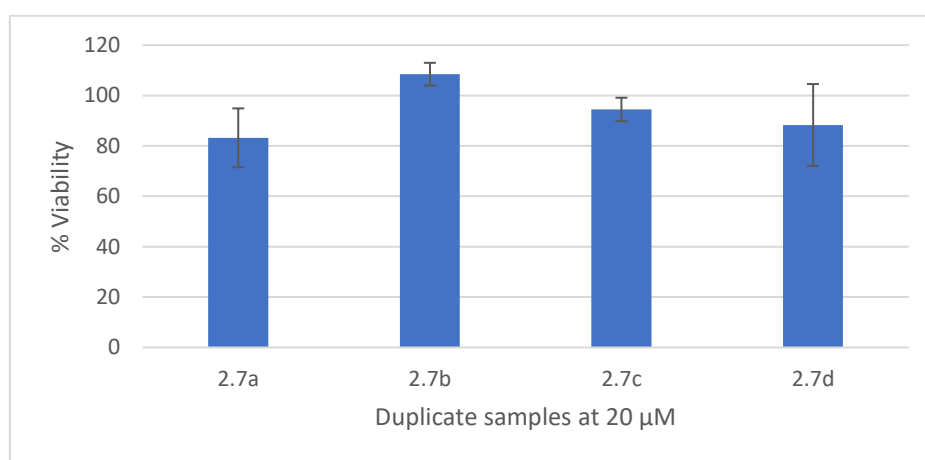
The antiplasmodial activity of the target compounds **2.6a-d**, **2.7a-d**, and **2.8a-e** was evaluated against chloroquine-sensitive 3D7 strain of *P. falciparum* parasite. Considering the importance of quinoline scaffold in compounds showing antimalarial properties, we envisaged that hybridization of quinoline unit with 2,4-thiazolidinedione framework would likely yield new compounds with enhanced antiplasmodium activity. More importantly, compounds containing quinoline<sup>3</sup> and thiazolidinedione<sup>4</sup> scaffolds have been shown to exhibit antiplasmodial activity.

**Figure 3.1** summarized the antiplasmodial activity of the resultant compounds **2.6a-d**. In general, these compounds showed no activity at the initial concentration of 20  $\mu\text{M}$  and none of the compounds showed the desirable parasite percentage viability to below 30%, hence the compounds were not put forward to determine the corresponding  $\text{IC}_{50}$  values.



**Figure 3.1:** *In vitro* antiplasmodial activity data for compounds **2.6a-d**.

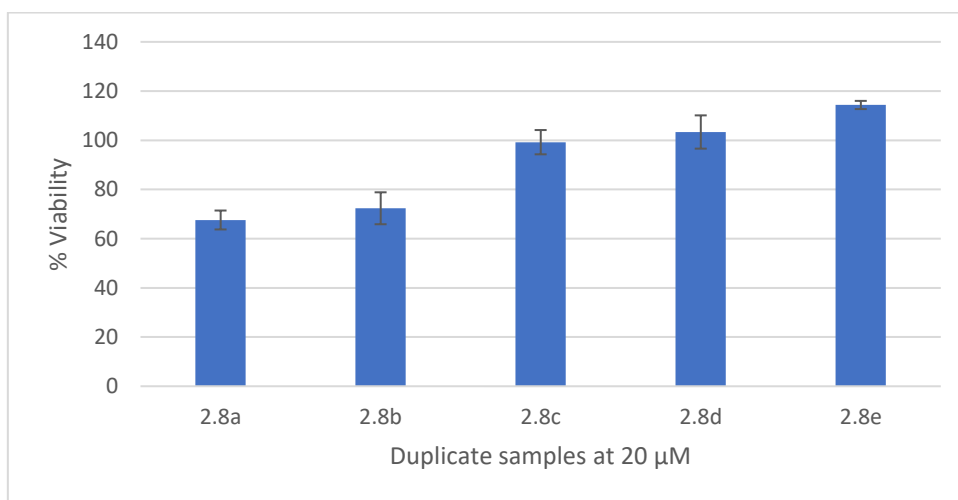
The acidity and the ability of the carboxylic acid group to form strong electrostatic interactions and hydrogen bonding with numerous drug targets<sup>5</sup> prompted us to further modify compounds **2.6a-d** by incorporating the carboxylic acid moiety to achieve compounds **2.7a-d**. Similarly, the incorporation of the acid moiety into **2.6a-d** to obtain **2.7a-d** proved to be futile as none of the compounds showed activity at the initial concentration of 20  $\mu$ M (**Figure 3.2**). These compounds were also not progressed further to determine their corresponding IC<sub>50</sub> values as they failed to reduce parasite viability to below set threshold of 30%.



**Figure 3.2:** The percentage parasite (3D7) viability of growth inhibition of compounds **2.7a-d**.

Recently, Sharma<sup>4</sup> and co-workers developed compounds such as compound **24** (Chapter 1) showing significant antimalarial activity through the inhibition of cysteine protease, falcipain 2 of the *P. falciparum* parasite. The emerged SAR suggested that incorporation of phenyl piperazine unit onto the position 3 of the 2,4-thiazolidinedione core significantly enhanced activity against the chloroquine-resistant W2 strain of *P. falciparum*<sup>4</sup>. Considering this literature evidence, compounds **2.6a-d** were converted to the corresponding derivatives **2.8a-e** (**Figure 3.3**) by incorporation of phenyl piperazine on the 3<sup>rd</sup> position of the 2,4-thiazolidinedione core structure.

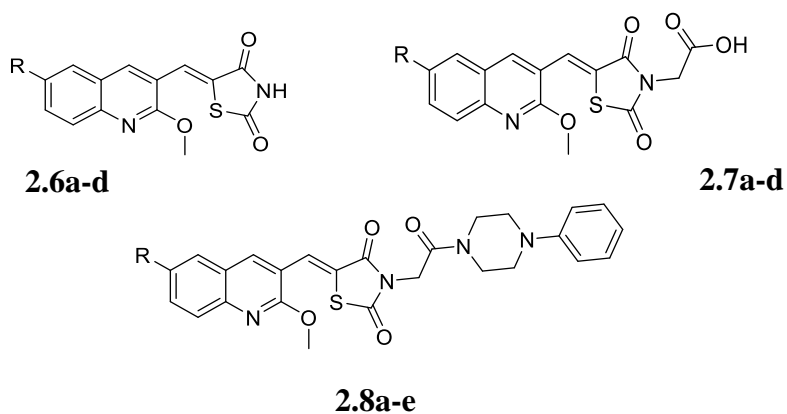
**Figure 3.3** summarised the *in vitro* biological data of resulting compounds **2.8a–e**. It can be observed that the resulting compounds possessed no desirable growth inhibition of the *P. falciparum* 3D7 strain at the concentration of 20  $\mu$ M. All the compounds showed >50% of the parasite percentage viability at this concentration. Once again, these compounds were not progressed further to determine the corresponding IC<sub>50</sub> values.



**Figure 3.3:** The percentage parasite (3D7) viability of growth inhibition of compounds **2.8a–e**.

### 3.2.2 Anti-tubercular activity of the target compounds

The antimycobacterial activity of the compounds **2.6a-d**, **2.7a-d** and **2.8a-e** was evaluated against susceptible strain H37Rv of *M. tuberculosis* and rifampicin was used as a drug control. Previously Alegaon and co-workers<sup>6</sup> reported antibacterial activity of 2,4-thiazolidinedione and rhodanine derivatives bearing imidazole ring at the position 5 of thiazolidinedione structure. The study revealed compounds with inhibitory activity against *M. tuberculosis* H37Rv and compounds containing the 2,4-thiazolidinedione scaffold exhibited less activity compared to rhodanine derivatives. In this work, we replaced the imidazole ring with the quinoline motif to form compounds with enhanced *M. tuberculosis* inhibitory activity (Table 3.1).

**Table 3.1:** *In vitro* anti-Mtb H37Rv activity of quinoline-thiazolidinedione derivatives.

Compound	R	MIC <sub>90</sub> (μM)	ClogP*
2.6a	-H	4.13	2.419
2.6b	-F	1.08	2.585
2.6c	-CH <sub>3</sub>	31.4	2.918
2.6d	-OCH <sub>3</sub>	>125	2.688
2.7a	-H	55.3	2.748
2.7b	-F	17.1	2.914
2.7c	-CH <sub>3</sub>	55.5	3.247
2.7d	-OCH <sub>3</sub>	>125	3.017
2.8a	-H	>125	4.711
2.8b	-Cl	>125	5.447
2.8c	-F	>125	4.877
2.8d	-CH <sub>3</sub>	>125	5.210
2.8e	-OCH <sub>3</sub>	>125	4.981
Rifampicin	-	0.054	

\*Calculated using ChemBioDraw Ultra version 14.0.0117

From **Table 3.1**, compounds **2.6a** and **2.6b** exhibited MIC<sub>90</sub> of <5 μM. While compound **2.6c** showed moderate activity, compound **2.6d** was inactive probably due to its poor aqueous solubility. Further modifications of the TZD core structure at the position 3 by incorporating the carboxylic acid group to form **2.7a–d** led to reduced inhibitory activity with MIC<sub>90</sub> values of 17.1–55.5 μM for acid derivatives **2.7a–c** whereas compound **2.7d** was inactive. On the other hand, the phenyl piperazine derivatives **2.8a–e** showed no activity at the maximum tested concentration of 125 μM.

### 3.2.3 *In vitro* cytotoxicity of synthesized compounds

As with the standard practice in drug design, it is crucial to know if the resulting novel compounds do not possess any adverse cytotoxicity effects on healthy human cells. In this study, HeLa cell line was used to measure the human cytotoxicity because of their ease to grow in the laboratory. As it can be seen in **Figure 3.4**, all the compounds (**2.6a–d**, **2.7a–d** and **2.8a–e**) did not exhibit cytotoxic effect and the percentage viability of the HeLa cells was often above 80% during a 24 h incubation.

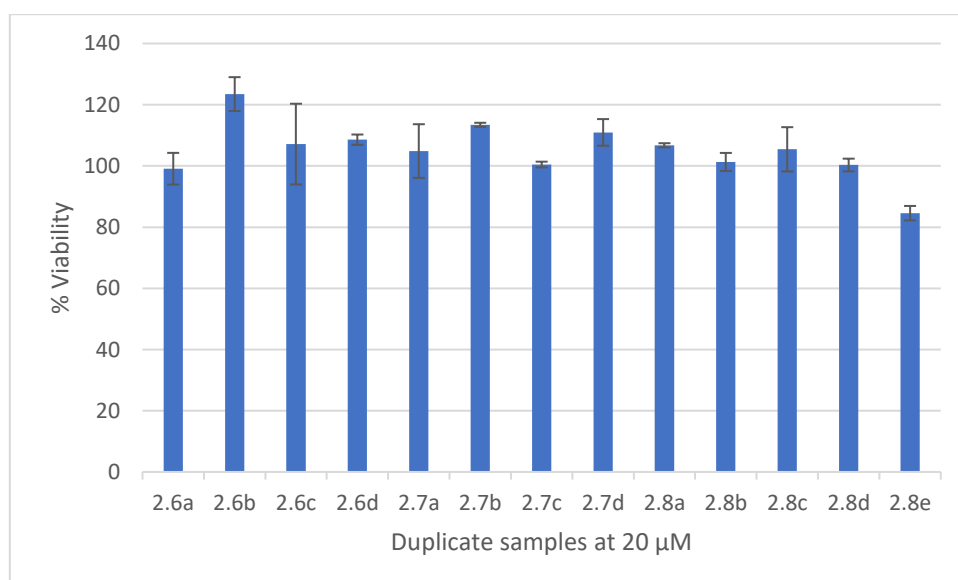


**Figure 3.4:** *In vitro* cytotoxicity (HeLa) data for all the target compounds.

### 3.3 CONCLUSIONS

All the achieved compounds **2.6a-d**, **2.7a-d**, and **2.8a-e** exhibited no antiplasmodial activity against the chloroquine-sensitive 3D7 strain of *P. falciparum*. The lack of activity of these compounds could partly be explained by poor aqueous solubility that majority of these compounds showed in various organic solvents and water. More importantly, the quinoline-based compounds with antiplasmodial activity are substituted with bulky groups on the 4<sup>th</sup> position (Quinine, Chloroquine, and Mefloquine), whereas our quinoline hybrids contain bulky groups on the 3<sup>rd</sup> position of the quinoline moiety.

While compounds **2.6a** and **2.6b** exhibited MIC<sub>90</sub> of 4.13 and 1.08 μM, respectively, the rest of compounds reported in this study showed moderate to weak activity against the H37Rv strain of *M. tuberculosis*. Incorporating bulky groups on the 3<sup>rd</sup> position of the 2,4-thiazolidinedione ring often leads to loss of the anti-TB activity. The success of obtaining compounds with MIC<sub>90</sub> that is less than 60 μM attests to the success of our rational design to specifically prepare compounds targeting *M. tuberculosis* strain. All the compounds prepared in this study showed no significant human cytotoxic effects as measured by HeLa cell line.

### 3.4 REFERENCES

1. Ioerger, T. R., Feng, Y., Ganesula, K., Chen, X., Dobos, K. M., Fortune, S., Jacobs, W. R., Mizrahi, V., Parish, T., Rubin, E., Sasseti, C., Sacchetti, J. C. *J. Bacteriol.* **2010**, 192, 3645–3653.
2. Llinás, M., Bozdech, Z., Wong, E. D., Adai, A. T. and DeRisi, J. L. *Nucleic Acids Res.* **2006**, 34, 1166–1173.
3. Achan, J., Talisuna, A. O., Erhart, A., Yeka, A., Tibenderana, J. K., Baliraine, F. N., Rosenthal, P. J., D'Alessandro, U. *Malar. J.* **2011**, 10, 144.
4. Sharma, R. K. Younis, Y., Mugumbate, G., Njoroge, M., Gut, J., Rosenthal, P. J., and Chibale, K. *Eur. J. Med. Chem.* **2015**, 90, 507–518.
5. Ballatore, C., Hury, D. M. and Smith, A. B. *ChemMedChem.* **2013**, 8, 385–395.
6. Alegaon, S. G., Alagawadi, K. R., Sonkusare, P. V., Chaudhary, D. H., Dadwe, D. H., Shah, A. S. *Bioorg. Med. Chem. Lett.* **2012**, 22, 1917–1921.
7. Patel, R. V. and Park, S. W. *Mini Rev. Med. Chem.* **2013**, 13, 1579–1601.

## CHAPTER FOUR

### EXPERIMENTAL SECTION

#### 4.1 General procedures

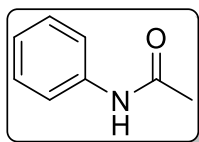
All commercially available chemicals were purchased from either Sigma-Aldrich or Merck and were used without further purification. Merck Silica 60 (particle size 0.063–0.2 mm) mesh was used for column chromatography. Reactions were monitored by thin layer chromatography (TLC) using Merck 60F254 aluminium coated silica gel plates and were visualized by ultraviolet light (254/365 nm) or exposure to iodine. NMR spectra were recorded on both Bruker 300 MHz AVANCE<sup>TM</sup>, 400 MHz AVANCE<sup>TM</sup>, and Biospin 600 MHz spectrometers. Chemical shifts are internally referenced to residual solvent peaks ( $\delta$  H: 7.26 ppm for CDCl<sub>3</sub>, 2.50 ppm for DMSO-d<sub>6</sub>;  $\delta$  C: 77.0 ppm for CDCl<sub>3</sub>, 39.4 ppm for DMSO-d<sub>6</sub>). Coupling constants, *J*, are measured in Hertz (Hz). Peak multiplicities are abbreviated as follows: singlet (s), doublet (d), doublet of doublet (dd), doublet of triplet (dt), multiplet (m), triplet (t), and broad singlet (br). All NMR spectra were analysed using MestReNova software.

High-resolution mass spectrometry was recorded on a Waters Synapt G2, ESI probe injected into a stream of methanol, ESI positive, Cone Voltage 15 V (University of Stellenbosch, South Africa). Infra-red (IR) spectra were recorded on a Perkin-Elmer FT-IR Spectrum 100 spectrometer (neat). Melting points were measured using Gallenkamp melting point apparatus (Registered design no. 889339) on an open capillary tube and are uncorrected.

## 4.2 General synthesis of acetanilides (2.2a-f)

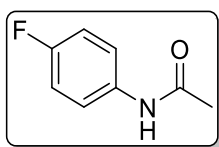
A 50 mL round bottom flask fitted with a reflux condenser was charged with 10 mL of aniline (1.0 eq), 10 mL acetic anhydride (1.1 eq) and 10 mL of acetic acid (1.1 eq). The mixture was then refluxed at 120 °C for 20-30 minutes. Upon reaction completion as indicated by TLC, the hot mixture was poured into a 200 mL beaker containing approximately 100 mL ice cold water and vigorously stirred for 10 minutes to hydrolyze the excess acetic anhydride and to precipitate the acetanilide formed. The precipitate was filtered and washed with cold water. The crude was then recrystallized from the boiling water to afford intermediate **2.2a-f**.

### Acetanilide – (2.2a)



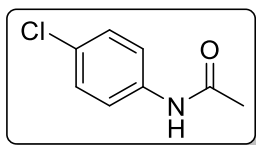
Shiny white solid. Yield (50 %). M.p. 114–116 °C (*lit.*<sup>1</sup> 116 °C). <sup>1</sup>H-NMR (300 MHz, CDCl<sub>3</sub>): δ<sub>H</sub> 7.72 (1H, s, CONH), 7.50 (2H, d, *J* = 6.0 Hz, Ar-H), 7.30 (2H, t, *J* = 7.5 Hz, Ar-H), 7.09 (1H, t, *J* = 7.5 Hz, Ar-H), 2.15 (3H, s, -CH<sub>3</sub>). <sup>13</sup>C-NMR (75 MHz, CDCl<sub>3</sub>): δ<sub>C</sub> 168.8 (C=O), 138.0 (Ar-C), 129.1 (Ar-C×2), 124.4 (Ar-C), 120.2 (Ar-C×2), 24.6 (CH<sub>3</sub>).

### *p*-Fluoroacetanilide – (2.2b)



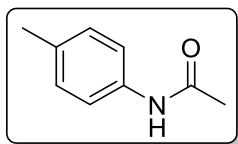
Fluffy white solid. Yield (77 %). M.p. 148–150 °C (*lit.*<sup>2</sup> 151-154 °C). <sup>1</sup>H-NMR (300 MHz, DMSO-*d*<sub>6</sub>): δ<sub>H</sub> 9.97 (1H, s, CONH), 7.58 (2H, m, Ar-H), 7.14 – 7.08 (2H, m, Ar-H), 2.03 (3H, s, CH<sub>3</sub>). <sup>13</sup>C-NMR (75 MHz, DMSO-*d*<sub>6</sub>): δ<sub>C</sub> 168.1 (C=O), 159.0 (Ar-C-F), 156.6 (Ar-C-F), 135.7 (Ar-C), 120.7 (Ar-C×2), 115.3 (Ar-C×2), 23.9 (CH<sub>3</sub>).

### *p*-Chloroacetanilide – (2.2c)



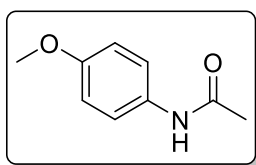
White solid. Yield (88%). M.p. 178–180 °C (*lit.*<sup>2</sup> 175-178 °C). <sup>1</sup>H-NMR (300 MHz, DMSO-*d*<sub>6</sub>): δ<sub>H</sub> 10.04 (1H, s, CONH), 7.63 – 7.58 (2H, m, Ar-H), 7.35 – 7.30 (2H, m, Ar-H), 2.04 (3H, s, CH<sub>3</sub>). <sup>13</sup>C-NMR (75 MHz, DMSO-*d*<sub>6</sub>): δ<sub>C</sub> 168.4 (C=O), 138.3 (Ar-C), 128.5 (Ar-C × 2), 126.5 (Ar-C), 120.5 (Ar-C × 2), 24.0 (CH<sub>3</sub>).

### *p*-Methylacetanilide (2.2d)



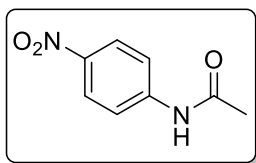
White solid. Yield (75%). M.p. 145–147 °C (*lit.*<sup>3</sup> 146- 148 °C). <sup>1</sup>H-NMR (300 MHz, CDCl<sub>3</sub>): δ<sub>H</sub> 7.59 (1H, s, CONH), 7.36 (2H, d, *J* = 9.0 Hz, Ar-H), 7.10 (2H, d, *J* = 9.0 Hz, Ar-H), 2.30 (3H, s, Ar-CH<sub>3</sub>), 2.14 (3H, s, -CH<sub>3</sub>). <sup>13</sup>C-NMR (75 MHz, CDCl<sub>3</sub>): δ<sub>C</sub> 168.7 (C=O), 135.5 (Ar-C), 134.1 (Ar-C), 126.5 (Ar-C × 2), 120.3 (Ar-C × 2), 24.5 (CH<sub>3</sub>), 21.0 (CH<sub>3</sub>).

### *p*-Methoxyacetanilide (2.2e)



Purple solid. Yield (81%). M.p. 124–126 °C (*lit.*<sup>4</sup> 126-128 °C). <sup>1</sup>H-NMR (300 MHz, CDCl<sub>3</sub>): δ<sub>H</sub> 7.62 (1H, s, CONH), 7.39 – 7.36 (2H, m, Ar-H), 6.84 – 6.81 (2H, m, Ar-H), 3.77 (3H, s, OCH<sub>3</sub>), 2.13 (3H, s, CH<sub>3</sub>). <sup>13</sup>C-NMR (75 MHz, CDCl<sub>3</sub>): δ<sub>C</sub> 168.7 (C=O), 156.5 (Ar-C), 131.1 (Ar-C), 122.2 (Ar-C × 2), 114.2 (Ar-C × 2), 55.6 (OCH<sub>3</sub>), 24.4 (CH<sub>3</sub>).

### ***p*-Nitroacetanilide (2.2f)**

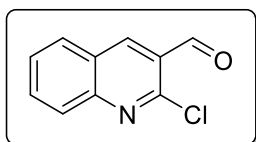


Green solid. Yield (92%). M.p. 212–214 °C (*lit.*<sup>5</sup> 212 – 215 °C). <sup>1</sup>H-NMR (300 MHz, DMSO-*d*<sub>6</sub>): δ 10.53 (1H, s, CONH), 8.22 – 8.16 (2H, m, Ar-H), 7.84 – 7.78 (2H, m, Ar-H), 2.11 (3H, s, CH<sub>3</sub>). <sup>13</sup>C-NMR (75 MHz, DMSO-*d*<sub>6</sub>): δ 169.3 (C=O), 145.4 (Ar-C), 142.0 (Ar-C), 125.0 (Ar-C × 2), 118.5 (Ar-C × 2), 24.2 (CH<sub>3</sub>).

### **4.3 General synthesis of 2-chloroquinoline-3-carbaldehydes (2.3a-e)**

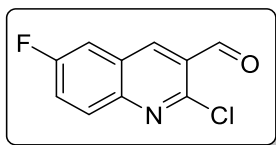
A 50 mL round bottom flask containing DMF (5 mL) was cooled in ice to 0 °C and then phosphoryl chloride (17 mL) was added dropwise and the reaction mixture was stirred for 10-15 minutes. Thereafter, an appropriate acetanilide (15 mmol) was added and the reaction mixture heated at 75 °C for 18 hours. Whilst still hot, the reaction content was poured onto ice water forming a precipitate. The precipitate was filtered and washed with cold water.

### **2-Chloroquinoline-3-carbaldehyde (2.3a)**



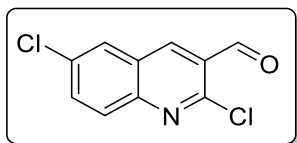
Yellow solid. Yield (52%). M.p. 141–143 °C (*lit.*<sup>6</sup> 142 - 143 °C). <sup>1</sup>H-NMR (300 MHz, CDCl<sub>3</sub>): δ<sub>H</sub> 10.53 (1H, s, CHO), 8.73 (1H, s, Ar-H), 8.05 (1H, d, *J* = 9.0 Hz, Ar-H), 7.96 (1H, d, *J* = 9.0 Hz, Ar-H), 7.90 – 7.84 (1H, m, Ar-H), 7.66 – 7.63 (1H, m, Ar-H). <sup>13</sup>C-NMR (75 MHz, CDCl<sub>3</sub>): δ<sub>C</sub> 189.2 (CHO), 150.1 (Ar-C), 149.6 (Ar-C), 140.3 (Ar-C), 133.7 (Ar-C), 129.8 (Ar-C), 128.6 (Ar-C), 128.2 (Ar-C), 126.5 (Ar-C), 126.3 (Ar-C).

### 2-Chloro-6-fluoroquinoline-3-carbaldehyde (2.3b)



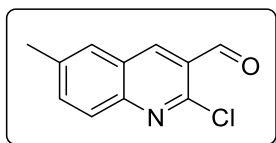
Brown solid. Yield (31%). M.p. 120–122 °C.  $^1\text{H-NMR}$  (300 MHz,  $\text{CDCl}_3$ ):  $\delta_{\text{H}}$  10.56 (1H, s,  $\text{CHO}$ ), 8.71 (1H, s, Ar-H), 8.09 (1H, dd,  $J = 6.9, 3.9$  Hz, Ar-H), 7.68–7.64 (1H, m, Ar-H), 7.62–7.58 (1H, m, Ar-H).  $^{13}\text{C-NMR}$  (75 MHz,  $\text{CDCl}_3$ ):  $\delta_{\text{C}}$  180.1 ( $\text{CHO}$ ), 162.4 (Ar-C-F), 159.9 (Ar-C-F), 146.8 (Ar-C), 139.7 (Ar-C), 131.4 (Ar-C), 131.3 (Ar-C), 127.4 (Ar-C), 127.0 (Ar-C), 124.1 (Ar-C), 112.7 (Ar-C).

### 2,6-Dichloroquinoline-3-carbaldehyde (2.3c)



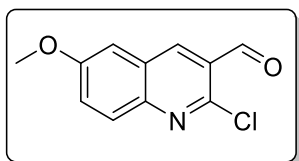
Orange solid. Yield (45%). M.p. 175–177 °C (*lit.*<sup>7</sup> 191–192 °C).  $^1\text{H-NMR}$  (300 MHz,  $\text{CDCl}_3$ ):  $\delta_{\text{H}}$  10.55 (1H, s,  $\text{CHO}$ ), 8.66 (1H, s, Ar-H), 8.03–7.99 (1H, m, Ar-H), 7.95 (1H, d,  $J = 3.0$  Hz, Ar-H), 7.80 (1H, dd,  $J = 6.0, 3.0$  Hz, Ar-H).  $^{13}\text{C-NMR}$  (75 MHz,  $\text{CDCl}_3$ ):  $\delta_{\text{C}}$  188.9 ( $\text{CHO}$ ), 150.5 (Ar-C), 148.1 (Ar-C), 139.3 (Ar-C), 134.6 (Ar-C), 134.3 (Ar-C), 130.3 (Ar-C), 128.2 (Ar-C), 127.3 (Ar-C), 127.2 (Ar-C).

### 2-Chloro-6-methylquinoline-3-carbaldehyde (2.3d)



Pale yellow solid. Yield (63%). M.p. 118–120 °C (*lit.*<sup>8</sup> 122–123 °C).  $^1\text{H-NMR}$  (600 MHz;  $\text{CDCl}_3$ ):  $\delta_{\text{H}}$  10.53 (1H, s,  $\text{CHO}$ ), 8.64 (1H, s, Ar-H), 7.95 (1H, d,  $J = 6.0$  Hz, Ar-H), 7.71–7.69 (2H, m, Ar-H), 2.55 (1H, s,  $\text{CH}_3$ ).  $^{13}\text{C-NMR}$  (150 MHz,  $\text{CDCl}_3$ ):  $\delta_{\text{C}}$  189.4 ( $\text{CHO}$ ), 149.4 (Ar-C), 148.4 (Ar-C), 139.7 (Ar-C), 138.5 (Ar-C), 136.1 (Ar-C), 128.5 (Ar-C), 128.4 (Ar-C), 126.7 (Ar-C), 126.4 (Ar-C), 21.7 ( $\text{CH}_3$ ).

## 2-Chloro-6-methoxyquinoline-3-carbaldehyde (2.3e)



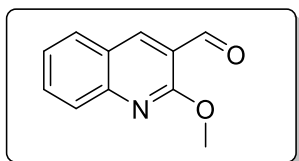
Orange-brown solid. Yield (88%). M.p. 144–146 °C (*lit.*<sup>9</sup> 146-147 °C).

<sup>1</sup>H-NMR (600 MHz; CDCl<sub>3</sub>): δ<sub>H</sub> 10.61 (1H, s, CHO), 8.71 (1H, s, Ar-H), 8.03 (1H, d, *J* = 8.9 Hz, Ar-H), 7.58 (1H, d, *J* = 9.1 Hz, Ar-H), 7.33 (1H, s, Ar-H), 4.02 (1H, s, OCH<sub>3</sub>). <sup>13</sup>C-NMR (150 MHz, CDCl<sub>3</sub>): δ<sub>C</sub> 189.6 (CHO), 159.0 (Ar-C), 147.8 (Ar-C), 146.0 (Ar-C), 138.8 (Ar-C), 130.1 (Ar-C), 128.0 (Ar-C), 126.7 (Ar-C), 126.6 (Ar-C), 106.6 (Ar-C), 55.9 (OCH<sub>3</sub>).

## 4.4 General Synthesis of 6-substitued 2-methoxyquinoline-3-carbaldehydes (2.4a-e)

To a solution of potassium hydroxide (1.78 mmol) in 50 mL of methanol was added 6-substitued-2-chloroquinoline-3-carbaldehyde (13.1 mmol). The mixture was heated cautiously at 70 °C for 3 hours. After completion of the reaction as guided by TLC, the mixture was then cooled and poured onto small crushed ice. The resultant precipitate was filtered, washed with cold water, dried and purified by column chromatography (Hexane/Ethyl acetate 8:2) to afford **2.4a-e**.

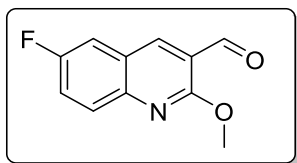
## 2-Methoxyquinoline-3-carbaldehyde (2.4a)



Pale yellow solid. Yield (40%). M.p. 104–106 °C (*lit.*<sup>10</sup> 112 - 114 °C).

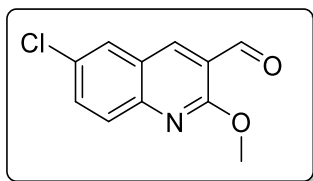
<sup>1</sup>H-NMR (300 MHz; CDCl<sub>3</sub>): δ<sub>H</sub> 10.46 (1H, s, CHO), 8.57 (1H, s, Ar-H), 7.88 – 7.82 (2H, m, Ar-H), 7.76 – 7.70 (1H, m, Ar-H), 7.45 – 7.40 (1H, m, Ar-H), 4.18 (3H, s, OCH<sub>3</sub>). <sup>13</sup>C-NMR (75 MHz, CDCl<sub>3</sub>): δ<sub>C</sub> 189.4 (CHO), 161.4 (Ar-C), 149.1 (Ar-C), 140.1 (Ar-C), 132.7 (Ar-C), 129.9 (Ar-C), 127.4 (Ar-C), 125.2 (Ar-C), 124.5 (Ar-C), 120.2 (Ar-C), 53.9 (OCH<sub>3</sub>).

### 6-Fluoro-2-methoxyquinoline-3-carbaldehyde (2.4b)



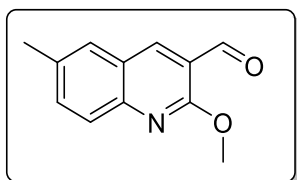
Brown-orange solid. Yield (22%). M.p. 116–118 °C.  $^1\text{H-NMR}$  (300 MHz;  $\text{CDCl}_3$ ):  $\delta_{\text{H}}$  10.46 (1H, s,  $\text{CHO}$ ), 8.50 (1H, s, Ar-H), 7.84 (1H, dd,  $J = 9.0, 5.1$ , Ar-H), 7.52 – 7.43 (2H, m, Ar-H), 4.16 (3H, s,  $\text{OCH}_3$ ).  $^{13}\text{C-NMR}$  (75 MHz,  $\text{CDCl}_3$ ):  $\delta_{\text{C}}$  189.2 ( $\text{CHO}$ ), 160.9 (Ar-C-F), 157.8 (Ar-C-F), 146.0 (Ar-C), 139.2 (Ar-C), 129.6 (Ar-C), 124.9 (Ar-C), 122.5 (Ar-C), 122.2 (Ar-C), 120.7 (Ar-C), 112.7 (Ar-C), 54.0 ( $\text{OCH}_3$ ).

### 6-Chloro-2-methoxyquinoline-3-carbaldehyde (2.4c)



Orange solid. Yield (34%). M.p. 139–140 °C (*lit.*<sup>10</sup> 145- 147 °C).  $^1\text{H}$  NMR (300 MHz;  $\text{CDCl}_3$ ):  $\delta_{\text{H}}$  10.45 (1H, s,  $\text{CHO}$ ), 8.48 (1H, s, Ar-H), 7.82 – 7.79 (2H, m, Ar-H), 7.65 (1H, dd,  $J = 6.0, 3.0$  Hz, Ar-H), 4.18 (3H, s,  $\text{OCH}_3$ ).  $^{13}\text{C-NMR}$  (75 MHz,  $\text{CDCl}_3$ ):  $\delta_{\text{C}}$  189.1 ( $\text{CHO}$ ), 161.5 (Ar-C), 147.4 (Ar-C), 139.0 (Ar-C), 133.3 (Ar-C), 130.6 (Ar-C), 128.9 (Ar-C), 128.3 (Ar-C), 125.1 (Ar-C), 120.7 (Ar-C), 54.2 ( $\text{OCH}_3$ ).

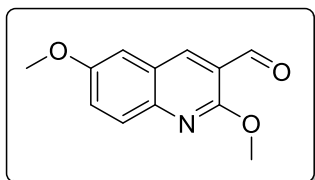
### 2-Methoxy-6-methylquinoline-3-carbaldehyde (2.4d)



White needle-like solid. Yield (54%). M.p. 90 – 92 °C (*lit.*<sup>10</sup> 94-96 °C).  $^1\text{H}$  NMR (600 MHz;  $\text{CDCl}_3$ ):  $\delta_{\text{H}}$  10.45 (1H, s,  $\text{CHO}$ ), 8.49 (1H, s, Ar-H), 7.76 (1H, d,  $J = 6.0$  Hz, Ar-H), 7.59 (1H, s, Ar-H), 7.57 – 7.55 (1H, m, Ar-H) 4.17 (3H, s,  $\text{OCH}_3$ ), 2.49 (3H, s,  $\text{CH}_3$ ).  $^{13}\text{C-NMR}$  (150 MHz,  $\text{CDCl}_3$ ):  $\delta_{\text{C}}$  189.6 ( $\text{CHO}$ ), 161.0 (Ar-C), 147.4 (Ar-C), 139.6 (Ar-

C), 134.9 (Ar-C), 134.9 (Ar-C), 128.7 (Ar-C), 127.0 (Ar-C), 124.5 (Ar-C), 120.0 (Ar-C), 53.9 (OCH<sub>3</sub>), 21.4 (CH<sub>3</sub>).

### 2,6-Dimethoxyquinoline-3-carbaldehyde (2.4e)

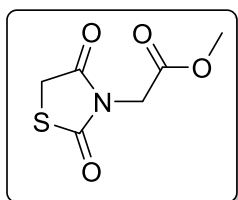


Pale yellow solid. Yield (60%). M.p. 119–121 °C (*lit.*<sup>11</sup> 122-124 °C).

<sup>1</sup>H-NMR (400 MHz; CDCl<sub>3</sub>): δ<sub>H</sub> 10.45 (1H, s, CHO), 8.48 (1H, s, Ar-H), 7.78 (1H, d, *J* = 8.0 Hz, Ar-H), 7.39 (1H, dd, *J* = 8.0, 4.0 Hz, Ar-H), 7.11 (1H, d, *J* = 4.0 Hz, Ar-H), 4.15 (s, 3H, OCH<sub>3</sub>), 3.90 (s, 3H, OCH<sub>3</sub>). <sup>13</sup>C-NMR (100 MHz, CDCl<sub>3</sub>): δ<sub>C</sub> 189.6 (CHO), 160.2 (Ar-C), 156.8 (Ar-C), 144.7 (Ar-C), 138.8 (Ar-C), 128.6 (Ar-C), 125.1 (Ar-C), 125.0 (Ar-C), 120.1 (Ar-C), 107.4 (Ar-C), 55.7 (OCH<sub>3</sub>), 53.9 (OCH<sub>3</sub>).

### 4.5 Synthesis of methyl 2-(2,4-dioxothiazolidin-3-yl)acetate, 2.10<sup>12</sup>

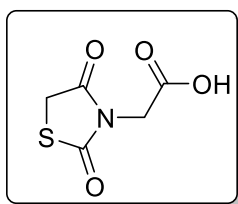
A mixture of 2,4-thiazolidinedione (10 mmol), methyl bromoacetate (20 mmol), K<sub>2</sub>CO<sub>3</sub> (20 mmol,) in acetone (30 mL) was refluxed for 24 hours. After completion of the reaction as indicated by TLC, the solvent was evaporated, followed by the addition of H<sub>2</sub>O (20 mL) and extraction with DCM (20 mL). The organic layer was then washed with 5% HCl solution, dried over MgSO<sub>4</sub>, concentrated *in vacuo* and purified by silica gel column chromatography using 70% ethyl acetate-hexane to afford compound **2.10** as yellow liquid.



Yield (48%). <sup>1</sup>H-NMR (400 MHz, CDCl<sub>3</sub>): δ<sub>H</sub> 4.36 (2H, s, CH<sub>2</sub>), 4.04 (2H, s, CH<sub>2</sub>), 3.77 (3H, s, CH<sub>3</sub>).

#### 4.6 Synthesis of 2-(2,4-dioxothiazolidin-3-yl)acetic acid<sup>12</sup> (2.11)

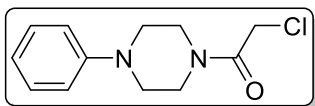
A mixture of **6** (900 mg), 48% HBr (10 mL) and glacial acetic acid (17 mL) in a round bottom flask was refluxed for 8 hours. Upon cooling, water (10 mL) was added and reaction mass extracted with ethyl acetate (50 mL × 3). The combined organic layer was dried over MgSO<sub>4</sub>, filtered and concentrated *in vacuo* to give 2-(2,4-dioxo-1,3-thiazolidin-3-yl)acetic acid **2.11** as a pale white solid.



Pale white solid. Yield (52%). M.p. 140–142 °C (*lit*<sup>12</sup>. 143 °C). FT-IR ( $\nu_{\max}/\text{cm}^{-1}$ ): 3105 (OH), 2947 (CH<sub>2</sub>), 1760 (C=O), 1730 (C=O), 1653 (C=O). <sup>1</sup>H-NMR (300 MHz, DMSO-*d*<sub>6</sub>):  $\delta_{\text{H}}$  4.32 (2H, s, CH<sub>2</sub>), 4.20 (2H, s, CH<sub>2</sub>). <sup>13</sup>C-NMR (75 MHz, DMSO-*d*<sub>6</sub>):  $\delta_{\text{C}}$  171.8 (C=O), 171.4 (C=O), 168.0 (C=O), 42.0 (CH<sub>2</sub>), 33.96 (CH<sub>2</sub>).

#### 4.7 Synthesis of 2-chloro-1-(4-phenylpiperazin-1-yl)ethan-1-one<sup>12</sup> (2.13)

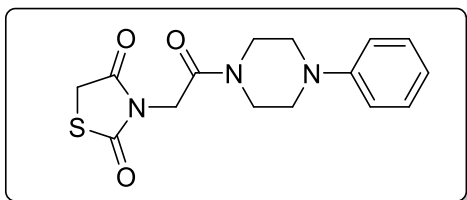
1-(Phenyl)-piperazine (12.3 mmol) was dissolved in DCM (60 mL) followed by addition of triethylamine (2.2 mL). The reaction mixture was then cooled to 0 °C. Subsequently, chloroacetyl chloride (10.6 mmol) was added dropwise at 0 °C, and the reaction mixture was allowed to warm up to room temperature and stirred for 1 hour. Thereafter, a saturated sodium bicarbonate solution (60 mL) was added and stirred for 15 minutes at room temperature. The organic layer was then separated and washed with brine, dried over magnesium sulphate, filtered and concentrated under reduced pressure to give clear/white residue. The concentrate was then purified by silica gel column chromatography using 7:3 Hexane:Ethyl acetate to yield compound **2.13** as a white solid.



White solid. Yield (52%). M.p. 77–79 °C (*lit.*<sup>12</sup> 77°C). <sup>1</sup>H-NMR (300 MHz, CDCl<sub>3</sub>): δ<sub>H</sub> 7.24 – 7.20 (2H, m, Ar-H), 6.89 – 6.84 (3H, m, Ar-H), 4.05 (2H, s, CH<sub>2</sub>Cl), 3.75 – 3.61 (4H, m, CH<sub>2</sub>), 3.20 – 3.11 (4H, m, CH<sub>2</sub>). <sup>13</sup>C-NMR (75 MHz, CDCl<sub>3</sub>): δ<sub>C</sub> 165.3 (C=O), 150.9 (Ar-C), 129.4 (Ar-C × 2), 120.9 (Ar-C), 116.9 (Ar-C × 2), 49.8 (CH<sub>2</sub>), 49.4 (CH<sub>2</sub>), 46.4 (CH<sub>2</sub>), 42.3 (CH<sub>2</sub>), 40.9 (CH<sub>2</sub>).

#### 4.8 Synthesis of 3-(2-oxo-2-(4-phenylpiperazin-1-yl)ethyl)thiazolidine-2,4-dione<sup>12</sup> (**2.14**)

A reaction mixture of **2.13** (41.8 mmol), 2,4-thiazolidinedione (2.0 equiv.), and K<sub>2</sub>CO<sub>3</sub> (2.0 equiv.) in acetone (130 mL) was heated at 65 °C for 24 hours under N<sub>2</sub> atmosphere. The reaction progress was monitored by TLC, and upon completion the reaction product was cooled to room temperature, filtered, and the filtrate concentrated *in vacuo* to obtain compound **2.14** as white solid.

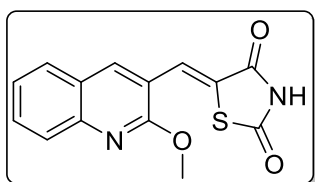


White Solid. Yield (50%). M.p. 174–176 °C (*lit.*<sup>12</sup> 175 °C). <sup>1</sup>H-NMR (300 MHz, CDCl<sub>3</sub>): δ<sub>H</sub> 7.31 – 7.26 (2H, m, Ar-H), 6.94 – 6.89 (3H, m, Ar-H), 4.45 (2H, s, CH<sub>2</sub>), 4.04 (-CH<sub>2</sub>), 3.77 – 3.61 (4H, m, CH<sub>2</sub>), 3.26 – 3.16 (4H, m, CH<sub>2</sub>). <sup>13</sup>C-NMR (75 MHz, CDCl<sub>3</sub>): δ<sub>C</sub> 171.7 (C=O), 171.3 (C=O), 162.9 (C=O), 150.9 (Ar-C), 129.4 (Ar-C × 2), 120.9 (Ar-C), 116.9 (Ar-C × 2), 49.6 (CH<sub>2</sub>), 49.4 (CH<sub>2</sub>), 44.9 (CH<sub>2</sub>), 42.4 (CH<sub>2</sub>), 42.4 (CH<sub>2</sub>), 34.0 (CH<sub>2</sub>).

#### 4.9 General synthesis of quinoline-thiozolidinedione derivatives (2.6a-d)

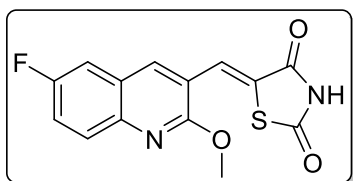
2,4-Thiazolidinedione (1.175 mmol) was dissolved in toluene (8 mL) followed by addition of piperidine (1.5 eq) and 2-3 drops of acetic acid. After adding an appropriate 2-methoxyquinoline-3-carbaldehyde (1.068 mmol) the reaction mixture allowed to reflux for 4–6 hours. The TLC confirmed the completion of the reaction, and the reaction mixture was cooled to room temperature resulting in the formation of the precipitate, which was filtered by vacuum filtration. The solid obtained was further purified by recrystallization using ethanol and washed with ice cold diethyl ether to obtain **2.6a-d**.

##### (Z)-5-((2-Methoxyquinolin-3-yl)methylene)thiazolidine-2,4-dione- 2.6a



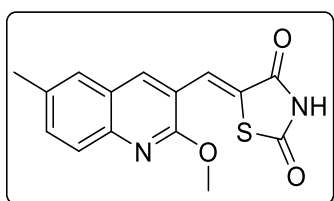
Yellow Solid. Yield (41%). M.p. 240–242 °C. FT-IR ( $\nu_{\max}/\text{cm}^{-1}$ ): 2994 (C-H), 1741 (C=O), 1687 (C=O).  $^1\text{H-NMR}$  (600 MHz,  $\text{DMSO-}d_6$ ):  $\delta_{\text{H}}$  12.69 (1H, s, CONH), 8.29 (1H, s, Ar-H), 8.02 (1H, d,  $J = 7.80$  Hz, Ar-H), 7.90 (1H, s, C=CH), 7.78 (1H, d,  $J = 7.8$  Hz, Ar-H), 7.73 (1H, t,  $J = 7.5$  Hz, Ar-H), 7.48 (1H, t,  $J = 6.9$  Hz, Ar-H), 4.06 (3H, s, OCH<sub>3</sub>).  $^{13}\text{C-NMR}$  (150 MHz,  $\text{DMSO-}d_6$ ):  $\delta_{\text{C}}$  167.8 (C=O), 167.2 (C=O), 158.9 (Ar-C), 145.9 (Ar-C), 138.2 (Ar-C), 131.5 (Ar-C), 128.8 (Ar-C), 126.6 (Ar-C), 126.5 (Ar-C), 125.0 (Ar-C), 124.5 (Ar-C), 124.4 (Ar-C), 118.1 (Ar-C), 53.9 (OCH<sub>3</sub>).  $m/z$  (ESI) calcd for  $\text{C}_{14}\text{H}_{10}\text{N}_2\text{O}_3\text{S}$ : 286.0412. Found 287.0488  $[\text{M}+\text{H}]^+$ .

**(Z)-5-((6-Fluoro-2-methoxyquinolin-3-yl)methylene)thiazolidine-2,4-dione – 2.6b**



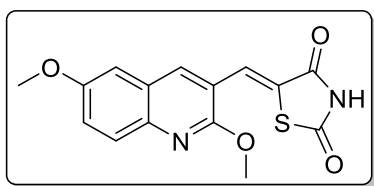
Brown solid. Yield (20%). M.p. 256–258 °C. FT-IR ( $\nu_{\max}/\text{cm}^{-1}$ ): 3104 (N-H), 1744 (C=O), 1687 (C=O).  $^1\text{H-NMR}$  (300 MHz,  $\text{DMSO-}d_6$ ):  $\delta_{\text{H}}$  12.32 (1H, s, CONH), 8.31 (1H, s, Ar-H), 7.90 (1H, dd,  $J = 9.3, 3.0$  Hz, Ar-H), 7.87 (1H, s, -C=CH), 7.83 (1H, dd,  $J = 9.0, 5.3$  Hz, Ar-H), 7.62 (1H, td,  $J = 9.0, 3.0$  Hz, Ar-H), 4.07 (3H, s, OCH<sub>3</sub>).  $^{13}\text{C-NMR}$  (75 MHz,  $\text{DMSO-}d_6$ ):  $\delta_{\text{C}}$  168.6 (C=O), 159.1 (C=O), 157.6 (Ar-C), 143.2 (Ar-C), 137.8 (Ar-C), 129.4 (Ar-C), 128.5 (Ar-C), 125.4 (Ar-C), 124.0 (Ar-C), 121.3 (Ar-C), 120.9 (Ar-C), 119.6 (Ar-C), 112.8 (Ar-C), 54.5 (OCH<sub>3</sub>).  $m/z$  (ESI) calcd for  $\text{C}_{14}\text{H}_9\text{FN}_2\text{O}_3\text{S}$ : 304.0318. Found 305.0392  $[\text{M}+\text{H}]^+$ .

**(Z)-5-((2-Methoxy-6-methylquinolin-3-yl)methylene)thiazolidine-2,4-dione- 2.6c**



Yellow solid. Yield (49%). M.p. 266–268 °C. FT-IR ( $\nu_{\max}/\text{cm}^{-1}$ ): 3012 (N-H), 1738 (C=O), 1684 (C=O), 1587 (C=O).  $^1\text{H-NMR}$  (300 MHz,  $\text{DMSO-}d_6$ ):  $\delta_{\text{H}}$  12.06 (1H, s, CONH), 8.18 (1H, s, Ar-H), 7.88 (1H, s, C=CH), 7.78 (1H, s, Ar-H), 7.68 (1H, d,  $J = 8.7$  Hz, Ar-H), 7.56 (1H, dd,  $J = 8.4, 1.8$  Hz, Ar-H), 4.05 (3H, s, OCH<sub>3</sub>), 2.45 (3H, s, CH<sub>3</sub>).  $^{13}\text{C-NMR}$  (75 MHz,  $\text{DMSO-}d_6$ ):  $\delta_{\text{C}}$  168.5 (C=O), 168.0 (C=O), 159.0 (Ar-C), 144.7 (Ar-C), 138.1 (Ar-C), 134.8 (Ar-C), 133.9 (Ar-C), 128.1 (Ar-C), 127.1 (Ar-C), 126.8 (Ar-C), 125.0 (Ar-C), 124.8 (Ar-C), 118.4 (Ar-C), 54.8 (OCH<sub>3</sub>), 21.3 (CH<sub>3</sub>).  $m/z$  (ESI) calcd for  $\text{C}_{15}\text{H}_{12}\text{N}_2\text{O}_3\text{S}$ : 300.0569. Found 301.0652  $[\text{M}+\text{H}]^+$ .

**(Z)-5-((2,6-Dimethoxyquinolin-3-yl)methylene)thiazolidine-2,4-dione- 2.6d**

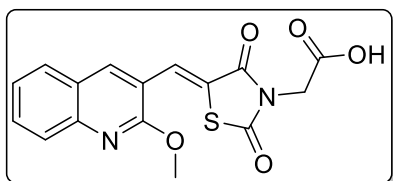


Orange solid. Yield (52%). M.p. 280–282 °C. FT-IR ( $\nu_{\max}/\text{cm}^{-1}$ ): 3101 (N-H), 1747 (C=O), 1688 (C=O).  $^1\text{H-NMR}$  (400 MHz,  $\text{DMSO-}d_6$ ):  $\delta_{\text{H}}$  12.73 (1H, s, CONH), 8.18 (1H, s, Ar-H), 7.87 (1H, s, Ar-H), 7.68 (1H, d,  $J = 9.0$  Hz, Ar-H), 7.49 (1H, s, C=CH), 7.35 (1H, d,  $J = 9.0$  Hz, Ar-H), 4.03 (3H, s, OCH<sub>3</sub>), 3.86 (3H, s, OCH<sub>3</sub>).  $^{13}\text{C NMR}$  (100 MHz,  $\text{DMSO-}d_6$ ):  $\delta_{\text{C}}$  168.6 (C=O), 162.1 (C=O), 158.1 (Ar-C), 156.6 (Ar-C), 141.8 (Ar-C), 137.5 (Ar-C), 128.3 (Ar-C), 127.5 (Ar-C), 125.7 (Ar-C), 124.6 (Ar-C), 123.6 (Ar-C), 120.8 (Ar-C), 118.5 (Ar-C), 107.8 (Ar-C), 56.0 (OCH<sub>3</sub>), 54.2 (OCH<sub>3</sub>).  $m/z$  (ESI) calcd for  $\text{C}_{15}\text{H}_{12}\text{N}_2\text{O}_4\text{S}$ : 316.0518, Found 317.0587  $[\text{M}+\text{H}]^+$ .

**4.10 General synthesis of quinoline-thiazolidinedione acid derivatives (2.7a-d)**

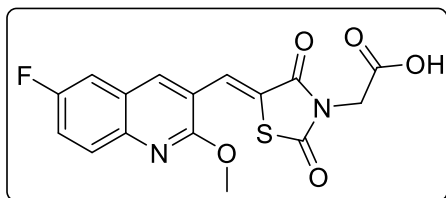
2-(2,4-dioxothiazolidin-3-yl)acetic acid (1.175 mmol) was dissolved in toluene (8 mL) followed by addition of piperidine (1.5 eq) and 2-3 drops of acetic acid. An appropriate 2-methoxyquinoline-3-carbaldehyde (1.068 mmol) was added to the reaction mixture, which then was allowed to reflux for 4 – 6 hours. The reaction progress was monitored by TLC and when the reaction had reached completion, the reaction mixture was cooled to room temperature and the formed precipitate was filtered and washed with diethyl ether. Recrystallization of the solid obtained using ethanol and was washed with diethyl ether gave compounds **2.7a-d** in moderate yields.

**(Z)-2-(5-((2-Methoxyquinolin-3-yl)methylene)-2,4-dioxothiazolidin-3-yl)acetic acid- 2.7a**



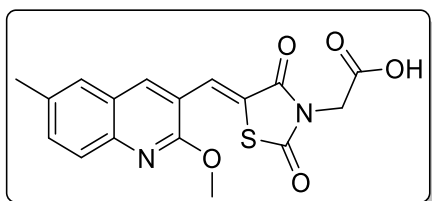
Yellow solid. Yield (29 %). M.p. 176–178 °C. FT-IR ( $\nu_{\max}/\text{cm}^{-1}$ ): 3407 (OH), 2951 (C-H), 1731 (C=O), 1681 (C=O), 1590 (C=O).  $^1\text{H-NMR}$  (400 MHz, DMSO- $d_6$ ):  $\delta_{\text{H}}$  9.02 (1H, s, COOH), 8.36 (1H, s, Ar-H), 8.03 (1H, d,  $J = 8.0$  Hz, Ar-H), 8.01 (1H, s, C=CH), 7.79 – 7.72 (2H, m, Ar-H), 7.49 (1H, t,  $J = 7.3$  Hz, Ar-H), 4.22 (2H, s, CH<sub>2</sub>), 4.07 (3H, s, OCH<sub>3</sub>).  $^{13}\text{C NMR}$  (100 MHz, DMSO- $d_6$ ):  $\delta_{\text{C}}$  168.4 (C=O), 167.4 (C=O), 165.5 (C=O), 159.3 (Ar-C), 146.5 (Ar-C), 139.3 (Ar-C), 132.1 (Ar-C), 129.4 (Ar-C), 127.0 (Ar-C), 126.8 (Ar-C), 125.5 (Ar-C), 124.9 (Ar-C), 124.6 (Ar-C), 118.3 (Ar-C), 54.4 (OCH<sub>3</sub>), 44.0 (CH<sub>2</sub>).  $m/z$  (ESI) calcd for C<sub>16</sub>H<sub>12</sub>N<sub>2</sub>O<sub>5</sub>S: 344.0467. Found 345.0547 [M+H]<sup>+</sup>.

**(Z)-2-(5-((6-Fluoro-2-methoxyquinolin-3-yl)methylene)-2,4-dioxothiazolidin-3-yl)acetic acid- 2.7b**



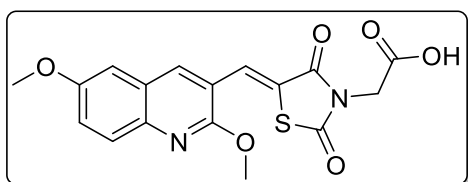
Pale brown solid. Yield (46%). M.p. 216–218 °C. FT-IR ( $\nu_{\max}/\text{cm}^{-1}$ ): 3040 (OH), 2944 (C-H), 1752 (C=O), 1716 (C=O), 1675 (C=O).  $^1\text{H-NMR}$  (300 MHz, DMSO- $d_6$ ):  $\delta_{\text{H}}$  8.39 (1H, s, Ar-H), 8.01 (1H, s, C=CH), 7.91 (1H, dd,  $J = 9.4, 2.9$  Hz), 7.86 – 7.77 (1H, m, Ar-H), 7.67 – 7.60 (1H, m, Ar-H), 4.27 (2H, s, CH<sub>2</sub>), 4.08 (3H, s, OCH<sub>3</sub>).  $^{13}\text{C-NMR}$  (75 MHz, DMSO- $d_6$ ):  $\delta_{\text{C}}$  171.8 (C=O), 171.5 (C=O), 168.1 (C=O), 167.9 (Ar-C), 166.9 (Ar-C), 165.1 (Ar-C), 158.6 (Ar-C), 157.1 (Ar-C), 143.0 (Ar-C), 138.1 (Ar-C), 128.9 (Ar-C), 125.8 (Ar-C), 125.0 (Ar-C), 118.9 (Ar-C), 112.1 (Ar-C), 54.0 (OCH<sub>3</sub>), 43.5 (CH<sub>2</sub>).  $m/z$  (ESI) calcd for C<sub>16</sub>H<sub>11</sub>FN<sub>2</sub>O<sub>5</sub>S: 362.0373. Found C<sub>16</sub>H<sub>12</sub>FN<sub>2</sub>O<sub>5</sub>S: 363.0442 [M+H]<sup>+</sup>.

**(Z)-2-(5-((2-Methoxy-6-methylquinolin-3-yl)methylene)-2,4-dioxothiazolidin-3-yl)acetic acid- 2.7c**



Yellow solid. Yield (39%). M.p. 202–204 °C. FT-IR ( $\nu_{\max}/\text{cm}^{-1}$ ): 3352 (OH), 2946 (C-H), 1735 (C=O), 1677 (C=O), 1592 (C=O).  $^1\text{H-NMR}$  (600 MHz,  $\text{DMSO-}d_6$ ):  $\delta_{\text{H}}$  8.80 (1H, s, COOH), 8.29 (1H, s, Ar-H), 8.02 (1H, s, C=CH), 7.82 (1H, s, Ar-H), 7.72 – 7.65 (1H, m, Ar-H), 7.59 (1H, d,  $J = 8.4$  Hz, Ar-H), 4.27 (2H, s, CH<sub>2</sub>), 4.06 (3H, s, OCH<sub>3</sub>), 2.45 (3H, s, CH<sub>3</sub>).  $^{13}\text{C-NMR}$  (150 MHz,  $\text{DMSO-}d_6$ ):  $\delta_{\text{C}}$  167.2 (C=O), 166.0 (C=O), 165.3 (C=O), 144.5 (Ar-C), 138.4 (Ar-C), 134.5 (Ar-C), 133.8 (Ar-C), 131.0 (Ar-C), 127.8 (Ar-C), 126.4 (Ar-C), 124.5 (Ar-C), 123.7 (Ar-C), 117.9 (Ar-C), 113.7 (Ar-C), 53.9 (OCH<sub>3</sub>), 43.6 (-CH<sub>2</sub>), 22.3 (-CH<sub>3</sub>).  $m/z$  (ESI) calcd for  $\text{C}_{17}\text{H}_{14}\text{N}_2\text{O}_5\text{S}$ : 358.0623. Found 359.0699 [M+H]<sup>+</sup>.

**(Z)-2-(5-((2,6-Dimethoxyquinolin-3-yl)methylene)-2,4-dioxothiazolidin-3-yl)acetic acid- 2.7d**



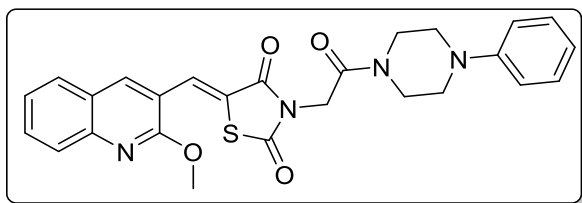
Orange solid. Yield (36%). M.p. 172-174 °C. FT-IR ( $\nu_{\max}/\text{cm}^{-1}$ ): 3406 (OH), 2954 (C-H), 1738 (C=O), 1684 (C=O), 1588 (C=O).  $^1\text{H-NMR}$  (400 MHz,  $\text{DMSO-}d_6$ ):  $\delta_{\text{H}}$  8.28 (1H, s, Ar-H), 8.02 (1H, s, Ar-H), 7.72 – 7.65 (1H, m, Ar-H), 7.52 (1H, s, C=CH), 7.37 (1H, d,  $J = 9.0$  Hz, Ar-H), 4.28 (2H, s, CH<sub>2</sub>), 4.04 (3H, s, OCH<sub>3</sub>), 3.87 (3H, s, OCH<sub>3</sub>).  $^{13}\text{C-NMR}$  (100 MHz,  $\text{DMSO-}d_6$ ):  $\delta_{\text{C}}$  168.4 (C=O), 167.4 (C=O), 165.5 (C=O), 158.0 (Ar-C), 156.7 (Ar-C), 142.0 (Ar-C), 138.2 (Ar-C), 128.3 (Ar-C), 127.0 (Ar-C), 125.7 (Ar-C), 124.2 (Ar-C), 123.8 (Ar-C), 118.2 (Ar-C), 107.9 (Ar-C), 56.0 (-OCH<sub>3</sub>), 54.2 (-OCH<sub>3</sub>),

44.0 ( $-\underline{\text{CH}_2}$ ).  $m/z$  (ESI) calcd for  $\text{C}_{17}\text{H}_{14}\text{N}_2\text{O}_6\text{S}$ : 374.0573. Found  $\text{C}_{17}\text{H}_{15}\text{N}_2\text{O}_6\text{S}$ : 375.0647  
[M+H]<sup>+</sup>

#### 4.11 General synthesis of thiazolidinedione-phenyl piperazine derivatives (2.8a-e)

To a mixture of 3-(2-oxo-2-(4-phenylpiperazin-1-yl)ethyl)thiazolidine-2,4-dione (0.5 mmol) and 2-methoxyquinoline-3-carbaldehyde (0.55 mmol) in ethanol (4 mL) was added a catalytic amount of piperidine. The reaction mixture was allowed to reflux until complete conversion of starting materials as observed by TLC. After cooling, the precipitate was filtered, washed and recrystallized in ethanol to obtain compounds **2.8a-e**.

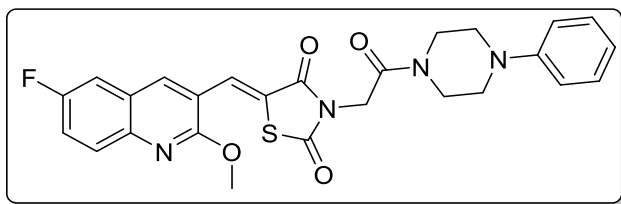
#### (Z)-5-((2-Methoxyquinolin-3-yl)methylene)-3-(2-oxo-2-(4-phenylpiperazin-1-yl)ethyl)thiazolidine-2,4-dione (2.8a)



Yellow solid. Yield (40%). M.p. 212–214 °C.

<sup>1</sup>H-NMR (400 MHz, DMSO-*d*<sub>6</sub>): FT-IR ( $\nu_{\text{max}}/\text{cm}^{-1}$ ): 2891 (C-H), 1742 (C=O), 1688 (C=O), 1588 (C=O).  $\delta_{\text{H}}$  8.42 (1H, s, Ar-H), 8.07 (1H, s, Ar-H), 8.06 (1H, s, C=CH), 7.85 – 7.72 (2H, m, Ar-H), 7.51 (1H, t,  $J = 7.4$  Hz, Ar-H), 7.24 (2H, t,  $J = 8.0$  Hz, Ar-H), 6.98 (2H, d,  $J = 8.0$  Hz, Ar-H), 6.83 (1H, t,  $J = 7.3$  Hz, Ar-H), 4.70 (2H, s, CH<sub>2</sub>), 4.10 (3H, s, OCH<sub>3</sub>), 3.71 – 3.60 (4H, m, CH<sub>2</sub>), 3.32 – 3.12 (4H, m, CH<sub>2</sub>). <sup>13</sup>C-NMR (100 MHz, DMSO-*d*<sub>6</sub>):  $\delta_{\text{C}}$  167.9 (C=O), 165.6 (C=O), 163.7 (C=O), 159.3 (Ar-C), 151.2 (Ar-C), 146.6 (Ar-C), 139.5 (Ar-C), 132.2 (Ar-C), 129.5 (Ar-C × 2), 129.4 (Ar-C), 127.2 (Ar-C), 127.0 (Ar-C), 125.6 (Ar-C), 125.0 (Ar-C), 124.5 (Ar-C), 119.9 (Ar-C), 118.3 (Ar-C), 116.5 (Ar-C × 2), 54.4 (OCH<sub>3</sub>), 49.1 (CH<sub>2</sub>), 48.7 (CH<sub>2</sub>), 44.5 (CH<sub>2</sub>), 43.2 (CH<sub>2</sub>), 42.1 (CH<sub>2</sub>). HRMS  $m/z$  (ESI) calcd for  $\text{C}_{26}\text{H}_{24}\text{N}_4\text{O}_4\text{S}$ : 488.1518. Found 489.1596 [M+H]<sup>+</sup>.

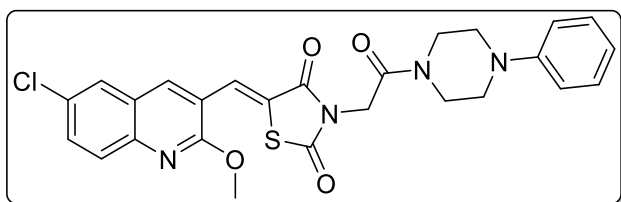
**(Z)-5-((6-Fluoro-2-methoxyquinolin-3-yl)methylene)-3-(2-oxo-2-(4-phenylpiperazin-1-yl)ethyl)thiazolidine-2,4-dione (2.8b)**



Yellow solid. Yield (22%). M.p. 250–252

°C. FT-IR ( $\nu_{\max}/\text{cm}^{-1}$ ): 2839 (C-H), 1742 (C=O), 1669 (C=O), 1596 (C=O).  $^1\text{H-NMR}$  (300 MHz,  $\text{CDCl}_3$ ):  $\delta_{\text{H}}$  8.23 (1H, s, Ar-H), 8.05 (1H, s, C=CH), 7.82 (1H, dd,  $J = 9.0, 3.0$  Hz, Ar-H), 7.44 (2H, t,  $J = 9.0$  Hz, Ar-H), 7.31 (2H, t,  $J = 7.5$  Hz), 6.96 (3H, d,  $J = 9.0$  Hz, Ar-H), 4.62 (2H, s, CH<sub>2</sub>), 4.12 (3H, s, OCH<sub>3</sub>), 3.80 (2H, br, CH<sub>2</sub>), 3.69 (2H, br-s, CH<sub>2</sub>), 3.29 (2H, br, CH<sub>2</sub>), 3.21 (2H, br, CH<sub>2</sub>).  $^{13}\text{C-NMR}$  (75 MHz,  $\text{CDCl}_3$ ):  $\delta_{\text{C}}$  167.7 (C=O), 165.7 (C=O), 163.0 (C=O), 150.8 (Ar-C), 147.7 (Ar-C), 143.9 (Ar-C), 137.8 (Ar-C), 129.5 (Ar-C × 2), 129.3 (Ar-C), 128.2 (Ar-C), 124.6 (Ar-C), 121.2 (Ar-C), 120.8 (Ar-C), 119.7 (Ar-C), 119.1 (Ar-C), 117.1 (Ar-C × 2), 111.9 (Ar-C), 111.6 (Ar-C), 54.1 (OCH<sub>3</sub>), 49.7 (CH<sub>2</sub>), 49.5 (CH<sub>2</sub>), 44.9 (CH<sub>2</sub>), 42.6 (CH<sub>2</sub>), 42.4 (CH<sub>2</sub>).  $m/z$  (ESI) calcd for  $\text{C}_{26}\text{H}_{23}\text{FN}_4\text{O}_4\text{S}$ : 506.1524. Found 507.1508 [M+H]<sup>+</sup>.

**(Z)-5-((6-Chloro-2-methoxyquinolin-3-yl)methylene)-3-(2-oxo-2-(4-phenylpiperazin-1-yl)ethyl)thiazolidine-2,4-dione (2.8c)**

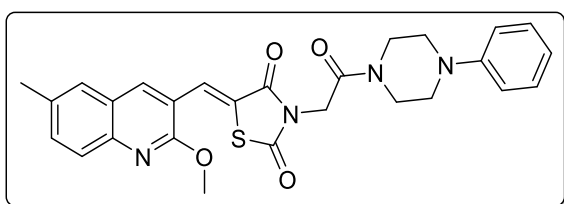


Yellow solid. Yield (34%). M.p. 264–266

°C. FT-IR ( $\nu_{\max}/\text{cm}^{-1}$ ): 2938 (C-H), 1742 (C=O), 1669 (C=O), 1592 (C=O).  $^1\text{H-NMR}$  (400 MHz,  $\text{CDCl}_3$ ):  $\delta_{\text{H}}$  8.22 (1H, s, Ar-H), 8.02 (1H, s, C=CH), 7.77 (2H, d,  $J = 8.9$  Hz, Ar-H), 7.61 (1H, d,  $J = 8.8$  Hz, Ar-H), 7.34 – 7.30 (2H, m, Ar-H), 7.02 – 6.98 (3H, m, Ar-H), 4.62 (2H, s, CH<sub>2</sub>), 4.13 (3H, s, OCH<sub>3</sub>), 3.84 (2H, br, CH<sub>2</sub>), 3.73 (2H, br, CH<sub>2</sub>), 3.31 (2H, br, CH<sub>2</sub>), 3.23

(2H, br,  $\underline{\text{CH}_2}$ ).  $^{13}\text{C}$ -NMR (100 MHz,  $\text{CDCl}_3$ ):  $\delta_{\text{C}}$  165.7 ( $\underline{\text{C=O}}$ ), 163.0 ( $\underline{\text{C=O}}$ ), 159.8 ( $\underline{\text{C=O}}$ ), 145.5 (Ar-C), 137.5 (Ar-C), 132.4 (Ar-C), 132.0 (Ar-C), 129.6 (Ar-C  $\times$  2), 128.8 (Ar-C), 128.1 (Ar-C), 127.0 (Ar-C  $\times$  2), 124.8 (Ar-C), 122.0 (Ar-C), 119.8 (Ar-C), 117.4 (Ar-C), 117.3 (Ar-C), 108.8 (Ar-C), 102.5 (Ar-C), 54.2 ( $\underline{\text{OCH}_3}$ ), 44.8 ( $\underline{\text{CH}_2}$ ), 42.5 ( $\underline{\text{CH}_2}$ ), 42.3 ( $\underline{\text{CH}_2}$ ), 40.1 ( $\underline{\text{CH}_2}$ ), 37.5 ( $\underline{\text{CH}_2}$ ).  $m/z$  (ESI) calcd for  $\text{C}_{26}\text{H}_{23}\text{ClN}_4\text{O}_4\text{S}$ : 523.1129. Found 523.1202  $[\text{M}+\text{H}]^+$ .

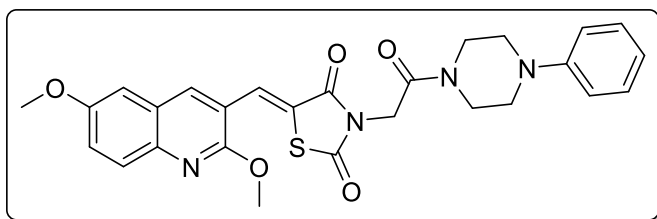
**(Z)-5-((2-Methoxy-6-methylquinolin-3-yl)methylene)-3-(2-oxo-2-(4-phenylpiperazin-1-yl)ethyl)thiazolidine-2,4-dione (2.8d)**



Yellow solid. Yield (16%). M.p. 242–244 °C. FT-

IR ( $\nu_{\text{max}}/\text{cm}^{-1}$ ): 2900 (C-H), 1742 (C=O), 1669 (C=O), 1588 (C=O).  $^1\text{H}$ -NMR (400 MHz,  $\text{CDCl}_3$ ):  $\delta_{\text{H}}$  8.25 (1H, s, Ar-H), 8.03 (1H, s, C= $\underline{\text{CH}}$ ), 7.43 (1H, d,  $J = 8.0$  Hz, Ar-H), 7.55 – 7.50 (2H, m, Ar-H), 7.30 (2H, d,  $J = 8.0$  Hz, Ar-H), 6.96 – 6.91 (3H, m, Ar-H), 4.61 (2H, s,  $\underline{\text{CH}_2}$ ), 4.12 (3H, s,  $\underline{\text{OCH}_3}$ ), 3.81 – 3.67 (4H, m,  $-\underline{\text{CH}_2}$ ), 3.29 – 3.19 (4H, m,  $\underline{\text{CH}_2}$ ), 2.50 (3H, s,  $\underline{\text{CH}_3}$ ).  $^{13}\text{C}$ -NMR (100 MHz,  $\text{CDCl}_3$ ):  $\delta_{\text{C}}$  168.0 ( $\underline{\text{C=O}}$ ), 165.9 ( $\underline{\text{C=O}}$ ), 163.1 ( $\underline{\text{C=O}}$ ), 159.3 (Ar-C), 150.9 (Ar-C), 145.5 (Ar-C), 138.2 (Ar-C), 134.8 (Ar-C), 133.6 (Ar-C), 129.4 (Ar-C  $\times$  2), 128.9 (Ar-C), 127.5 (Ar-C), 127.0 (Ar-C), 124.7 (Ar-C), 123.6 (Ar-C), 121.0 (Ar-C), 118.6 (Ar-C), 117.0 (Ar-C  $\times$  2), 53.9 ( $\underline{\text{OCH}_3}$ ), 49.7 ( $\underline{\text{CH}_2}$ ), 49.5 ( $\underline{\text{CH}_2}$ ), 45.0 ( $\underline{\text{CH}_2}$ ), 42.5 ( $\underline{\text{CH}_2}$ ), 42.4 ( $\underline{\text{CH}_2}$ ), 21.4 ( $\underline{\text{CH}_3}$ ).  $m/z$  (ESI) calcd for  $\text{C}_{27}\text{H}_{26}\text{N}_4\text{O}_4\text{S}$ : 502.1675. Found 503.1752  $[\text{M}+\text{H}]^+$ .

**(Z)-5-((2,6-Dimethoxyquinolin-3-yl)methylene)-3-(2-oxo-2-(4-phenylpiperazin-1-yl)ethyl)thiazolidine-2,4-dione (2.8e)**



Yellow solid. Yield (27%). M.p. 236–238

°C). FT-IR ( $\nu_{\max}/\text{cm}^{-1}$ ): 2834 (C-H), 1738 (C=O), 1669 (C=O), 1596 (C=O).  $^1\text{H-NMR}$  (400 MHz,  $\text{CDCl}_3$ ):  $\delta_{\text{H}}$  8.44 (1H, s, Ar-H), 8.21 (1H, s, C=CH), 7.93 (1H, dd,  $J = 8.0, 4.0$  Hz, Ar-H), 7.53 – 7.44 (4H, m, Ar-H), 7.13 (3H, s, Ar-H), 4.80 (2H, s, CH<sub>2</sub>), 4.29 (3H, s, OCH<sub>3</sub>), 4.12 (3H, s, OCH<sub>3</sub>), 3.98 (2H, br, CH<sub>2</sub>), 3.87 (2H, br, CH<sub>2</sub>), 3.47 (2H, br, CH<sub>2</sub>), 3.39 (2H, br, CH<sub>2</sub>).  $^{13}\text{C-NMR}$  (100 MHz,  $\text{CDCl}_3$ ):  $\delta_{\text{C}}$  167.9 (C=O), 165.8 (C=O), 163.1 (C=O), 158.4 (Ar-C), 156.8 (Ar-C), 150.9 (Ar-C), 142.7 (Ar-C), 137.6 (Ar-C), 129.4 (Ar-C × 2), 128.9 (Ar-C), 128.6 (Ar-C), 125.3 (Ar-C), 123.7 (Ar-C), 123.6 (Ar-C), 121.0 (Ar-C), 118.7 (Ar-C), 117.0 (Ar-C), 106.5 (Ar-C), 55.8 (OCH<sub>3</sub>), 53.9 (OCH<sub>3</sub>), 49.7 (CH<sub>2</sub>), 49.5 (CH<sub>2</sub>), 45.0 (CH<sub>2</sub>), 42.5 (CH<sub>2</sub>), 42.4 (CH<sub>2</sub>).  $m/z$  (ESI) calcd for  $\text{C}_{27}\text{H}_{26}\text{N}_4\text{O}_5\text{S}$ : 518.1624. Found 519.1696  $[\text{M}+\text{H}]^+$ .

## 4.12 Biological procedures

### 4.12.1 *In vitro* anti-*Plasmodium falciparum* (procedure adapted from <sup>18</sup>)

Activity was determined against chloroquine-resistant isolate of human malaria (*P. falciparum* Dd2). Parasites were maintained in continuous culture using a modified method of Trager and Jensen<sup>13</sup>. Growth medium was supplemented with Albumax II (Gibco), a bovine serum albumin preparation, instead of human serum. Cultures did not exceed 4% haematocrit and parasitemia was diluted to 1% when the cultures were in the trophozoite stage. The compounds were tested in triplicate on at least three occasions *in vitro* against the human malaria parasite. Compounds were prepared to 0.02 g ml<sup>-1</sup> stock solutions in dimethyl sulfoxide and sonicated

for 10 min to enhance solubility. Compounds that did not dissolve completely were tested as a suspension. Stock solutions were stored at  $-20^{\circ}\text{C}$ . Dilutions to the desired starting concentration of each compound were prepared in complete medium immediately prior to use on each occasion.

#### **4.12.2 *In vitro* anti-tubercular activity (procedure adapted from <sup>19</sup>)**

The minimum inhibitory concentration (MIC) was determined using the standard broth micro dilution method, where a 10 mL culture of *Mycobacterium tuberculosis* pMSp12:GFP<sup>14</sup>, was grown to an optical density (OD<sub>600</sub>) of 0.6–0.7. The media used were: (i) Gaste-Fe (glycerol-alanine-salts) medium pH 6.6, supplemented with 0.05% Tween-80 and 1% Glycerol, and (ii) 7H9 supplemented with 10% Albumin Dextrose Catalase supplement (ADC), 0.05% Tween-80<sup>15,16</sup>. Cultures grown in Gaste-Fe were diluted 1:100, and cultures grown in 7H9 ADC were diluted 1:500, prior to inoculation of the MIC assay. The compounds to be tested are reconstituted to a concentration of 10 mM in DMSO. Two-fold serial dilutions of the test compound are prepared across a 96-well micro titre plate, after which, 50  $\mu\text{L}$  of the diluted *M. tuberculosis* cultures were added to each well in the serial dilution. The plate layout was a modification of the method previously described<sup>17</sup>. Assay controls used were a minimum growth control (Rifampicin at  $2 \times \text{MIC}$ ), and a maximum growth control (5% DMSO). The micro titre plates were sealed in a secondary container and incubated at  $37^{\circ}\text{C}$  with 5%  $\text{CO}_2$  and humidification. Relative fluorescence (excitation 485 nM; emission 520 nM) was measured using a plate reader (FLUOstar OPTIMA, BMG LABTECH, Ortenberg, Germany), at day 7 and day 14. The raw fluorescence data were archived and analyzed using the CDD Vault from Collaborative Drug Discovery, in which, data were normalized to the minimum and maximum inhibition controls to generate a dose response curve (% inhibition), using the Levenberg-Marquardt (Burlingame, CA, USA [www.collaborativedrug.com](http://www.collaborativedrug.com)) damped least

squares method, from which the MIC90 was calculated. The lowest concentration of drug that inhibits growth of more than 90% of the bacterial population was considered the MIC90.

#### **4.12.3 *In vitro* cytotoxicity (procedure adapted from <sup>18</sup>).**

HeLa cells (Cellonex) were cultured in Dulbecco's modified Eagle medium (Lonza) supplemented with 10% foetal calf serum and antibiotics (penicillin/streptomycin/amphotericin B) at 37 °C in a 5% CO<sub>2</sub> incubator. Cells were plated in 96-well plates at a cell density of  $2 \times 10^4$  cells per well and grown overnight. Serial dilutions of test compounds were incubated with the cells for an additional 24 h, and cell viability in the wells assessed by adding 20  $\mu$ l of 0.54 mM resazurin in PBS for an additional 2–4 h. Fluorescence readings (excitation 560 nm, emission 590 nm) obtained for the individual wells were converted to percentage cell viability relative to the average readings obtained from untreated control wells.

#### 4.13 REFERENCES

1. Boudebouz, I., Arrous, S., Bakibaev, A., Hoang, P., and Malkov, V., *Int. J. ChemTech Res.*, **2018**, 11, 301–315.
2. Thakkar, D. V., and Mehta, R. S., *J. Chem. Pharm. Res.*, **2017**, 9, 46–54.
3. Pearson, D. E., Carter, K. N., and Greer, C. M., *J. Am. Chem. Soc.*, **1953**, 75, 5905–5908.
4. Liu, H., Wang, X., and Gu, Y., *Org. Biomol. Chem.*, **2011**, 9, 1614–1620.
5. 4'-Nitroacetanilide CAS 104-04-1 | 820880. Available at: [http://www.merckmillipore.com/ZA/en/product/4-Nitroacetanilide,MDA\\_CHEM-820880?RedirectedFrom=http%3A%2F%2Fwww.merckmillipore.com%2Fchemicals%2FMDA\\_CHEM-820880%2Fp\\_uuid&ReferrerURL=http%3A%2F%2Fwww.chemspider.com%2FChemical-Structure.7407.html](http://www.merckmillipore.com/ZA/en/product/4-Nitroacetanilide,MDA_CHEM-820880?RedirectedFrom=http%3A%2F%2Fwww.merckmillipore.com%2Fchemicals%2FMDA_CHEM-820880%2Fp_uuid&ReferrerURL=http%3A%2F%2Fwww.chemspider.com%2FChemical-Structure.7407.html). (Accessed: 6th March 2019)
6. Devi, I., Baruah, B., and Bhuyan, P., *Synlett.*, **2006**, 16, 2593–2596.
7. Meth-Cohn, O., Narine, B., and Tarnowski, B., *Tetrahedron Lett.*, **1979**, 20, 3111–3114.
8. Subashini, R., Mohana Roopan, S., and Nawaz Khan, F., *J. Chil. Chem. Soc.*, **2010**, 55, 317–319.
9. Tóth, J., Blaskó, G., Dancsó, A., Tőke, L. & Nyerges, M., *Synth. Commun.*, **2006**, 36, 3581–3589.
10. Joshi, S. D., More, U. A., Parkale, D., Aminabhavi, T. M., Gadad, A. K., Nadagouda, M. N., and Jawarkar, R., *Med. Chem. Res.*, **2015**, 24, 3892–3911.
11. Rajeev, P. V., and Rajendran, S. P., *Synth. Commun.*, **2010**, 40, 2837–2843.
12. Sharma, R. K., Younis, Y., Mugumbate, G., Njoroge, M., Gut, J., Rosenthal, P. J., and Chibale, K. *Eur. J. Med. Chem.*, **2015**, 90, 507–518.
13. Trager, W., and Jensen, J. B., *Science*, **1976**, 55, 439.

14. Abrahams, G.L., Kumar, A., Savvi, S., Hung, A.W., Wen, S., Abell, C., Barry, C.E., 3<sup>rd</sup>, Sherman, D.R., Boshoff, H.I., and Mizrahi, V., *Chem. Biol.* **2012**, 19, 844–854.
15. De Voss, J.J., Rutter, K., Schroeder, B.G., Su, H., Zhu, Y., and Barry III, C.E., *Proc. Nat. Acad. Sci. USA*, **2000**, 97, 1252–1257.
16. Franzblau, S.G., DeGroot, M.A., Cho, S.H., Andries, K., Nuermberger, E., Orme, I.M., Mdluli, K., Angulo-Barturen, I., Dick, T., Dartois, V., Lenaerts, A. J., *Tuberculosis*, **2012**, 92, 453–488.
17. Ollinger, J., Bailey, A., Moraski, C., Casey, A., Florio, S., Alling, T., Miller, J., and Parish, T., *PLoS ONE*, **2013**, 8, e60531.
18. Oderinlo, O. O., Tukulula, M., Isaacs, M., Hoppe, H. C., Taylor, D., Smith, V. J., Khanye, S. D., *Appl. Organomet. Chem.*, **2018**, 32, e4385.
19. Gumbo, M., Beteck, R. M., Mandizvo, T., Seldon, R., Warner, D. F., Hoppe, H. C., Isaacs, M., Laming, D., Tam, C. C., Cheng, L. W., Liu, N., Land, K. M., Khanye, S. D., *Molecules*, **2018**, 23, 2038.